Yale University
EliScholar – A Digital Platform for Scholarly Publishing at Yale

Yale Medicine Thesis Digital Library | School of Medicine

January 2015

T Cell Calcium Flux And Clonal Proliferation Report On Antigen-Specific Myeloid Cell Encounters

Nour Kibbi
Yale School of Medicine, nour.ag.kibbi@gmail.com

Follow this and additional works at: http://elischolar.library.yale.edu/ymtdl

Recommended Citation
Kibbi, Nour, "T Cell Calcium Flux And Clonal Proliferation Report On Antigen-Specific Myeloid Cell Encounters" (2015). *Yale Medicine Thesis Digital Library*. 1982.
http://elischolar.library.yale.edu/ymtdl/1982

This Open Access Thesis is brought to you for free and open access by the School of Medicine at EliScholar – A Digital Platform for Scholarly Publishing at Yale. It has been accepted for inclusion in Yale Medicine Thesis Digital Library by an authorized administrator of EliScholar – A Digital Platform for Scholarly Publishing at Yale. For more information, please contact elischolar@yale.edu.

المنارة للاستشارات
www.manaraa.com

T CELL CALCIUM FLUX AND CLONAL PROLIFERATION REPORT ON ANTIGEN-SPECIFIC MYELOID CELL ENCOUNTERS

A thesis presented by

Nour Kibbi

to the Office of Student Research

at the Yale School of Medicine

in partial fulfillment of the requirements for

Doctorate of Medicine (M.D.)

Yale School of Medicine

New Haven, Connecticut

March 2015

www.manaraa.com

ABSTRACT

Despite its clinical success, the mechanism underlying extracorporeal photopheresis (ECP) is not well understood, however, the plate-passage (PP) step appears integral to generating activated monocytes. In the first part of the project, we developed a functional assay to evaluate the efficacy of plate-passed myeloid cells (PPM) compared with freshly isolated, unstimulated monocytes (UM) and conventional dendritic cells derived from blood monocytes cultured with GM-CSF/IL4 (DC). Each of these three antigen presenting cell (APC) was co-cultured with purified, autologous CD8 cells, with or without CD4 cells. Cultures were carried out using melanoma antigen MART-1 "long peptide (LP)," a 25-amino acid peptide containing the binding sequences for the appropriate MHC class I and II, and for presentation to CD8+ and CD4+ cells. Results showed reliable expansions of freshly isolated naïve human T cells using the three types of APC, without any significant differences among the types, and the addition of CD4+ tended to enhance expansion of PPM and DC, but not UM. In the second part, we sought to develop a method for directly tracking early T cell responses during immunotherapy. Using calcium flux to indicate early T cell signaling, we focused mostly on the ovalbumin (OVA)-derived, SIINFEKL-specific transgenic mouse model (OT1). After a few protocol modifications, we were able to detect antigen-specific calcium flux (ASF) upon mixing naïve OT1 cells with SIINFEKL peptide-loaded DC compared with non-specific peptide counterparts. We could still detect ASF down to a peptide-loading concentration of ~10^{-3}uM and at a frequency of ~0.1% OT1 cells among wild-type (WT), non-responding cells. We next identified the activation requirements of early effector and memory OT1 cells from the spleen, lymph nodes, and peripheral blood after adoptive transfer into WT recipients immunized with OVA. At 1 week, OT1 cells from all 3 tissues had become activated, effector cells ($CD44^{hi}$ and $CD62^{lo}$), and while detectable, ASF in all three tissues was reduced compared with naïve cells. At 6 weeks, only the peripheral blood OT1 cells had generated a memory response ($CD127^{hi}$ $KLRG1^{lo}$), and ASF in all three tissues was further reduced. Herein, we have shown that ASF can be detected in naïve, and less so antigen-experienced and memory T cells in a single-antigen, transgenic system from which we hope to develop a multi-antigen tumor model.

www.manaraa.com

ACKNOWLEDGMENTS

Contributors to this research include:

Harib Ezaldein, B.E., Douglas Hanlon, Ph.D., Richard Edelson, M.D, Robert Tigelaar, M.D

Yale University Department of Dermatology

Enping Hong, B.E., Tarek Fahmy, Ph.D.

Yale University Department of Biomedical Engineering

Office of Student Research

Funding provided by:

Richard Gershon Fellowship, Office of Student Research, Yale University

www.manaraa.com

TABLE OF CONTENTS

www.manaraa.com

INTRODUCTION

The anti-tumor immune response

The interface between cancer and the immune system has been postulated at least for a few decades (1,2,3) but may date back to as early as 1863 when Virchow hypothesized that sites of chronic inflammation were susceptible to cancer (4). Since the 19th century, our understanding of the anti-tumor response continues to evolve, permitting us more than ever to develop drugs that generate effective therapeutic responses (5). Classically, an anti-tumor immune response begins with tumor cells in the tumor environment expressing a variety of tumor-associated antigens (TAAs) (**Figure 1**). In fact, TAAs may be mutated self-antigens (neoantigens resulting from somatic mutations)(6,7,8) or wild-type self-antigens which are over-expressed or selectively expressed by the tumor. TAAs act as a source of antigen for the infiltrating dendritic cells (DC) of the tumor bed. By various mechanisms, TAAs are taken up, processed and presented as peptides onto major histocompatibility complex (MHC) class I or II, in processes known as cross-presentation or presentation, respectively, or generally referred to as immunization. DC home to regional lymph nodes where they are able to make contacts with naïve, "virgin" CD8+ cytotoxic T cell precursors and CD4+ helper T cell precursors that express TCRs specific for peptide-MHC complex. If DC are in a matured state in which they express costimulatory molecules, they will transmit an activation signal to T cells to proliferate and differentiate. Once a T cell response is initiated, T cells then exit the lymph node and traffic back to the tumor microenvironment where they infiltrate and trigger tumor cell death by various death mechanisms. However, if DC receive no maturation stimulus, they may instead induce tolerance ("down-regulation") via T cell deletion, anergy or production of T regulatory (Treg) cells. In fact, a host of immunosuppressive defense mechanisms are produced by the tumor or other infiltrating myeloid cells that oppose T cell killing which otherwise would result in tumor shrinkage. Some of these mechanisms include upregulation of programmed death-ligand, (PD-L1/L2) on the cancer cell surface, release of prostaglandin E2 (PGE2), arginase and vascular endothelial growth factor (VEGF). Interestingly, compared with over- and selectively-expressed TAAs, analysis of T cell responses in melanoma showed that the most dominant and enduring responses were against neoantigens (9). This suggests that immunotherapies are most likely successful if they promote responses to neoantigens.

www.manaraa.com

In fact, different cancer immunotherapies target the different steps in the cascade just described to enhance production of anti-tumor T cells, which presumably function to destroy tumor cells. These therapies and their effect on anti-tumor T cells will be discussed next. For instance, therapies targeting the immunization step include DC- or peptide-based vaccines or exogenously administered activation signals such as those delivered via Toll-like Receptor (TLR). Peptides (such as 20-mers) have been used in vaccines against vulvar cancer in which they have been shown to promote T cell infiltrates (10). Cell-based therapies such as Provenge have shown variable and non-sustainable responses. In Provenge therapy, white blood cells are apheresed at weeks 0, 2, and 4 then cultured overnight in media containing a fusion protein from prostatic acid phosphatase (PAP) and granulocyte macrophage colony-stimulating factor (GMCSF) prior to reinfusion. Clinical results of a Phase III trial, unfortunately, showed little evidence of tumor shrinkage or delay in disease progression (11). In fact, by conventional clinical response criteria, known as Response Evaluation Criteria in Solid Tumors (RECIST; see Section, "Aim Two: Developing a method to evaluate anti-tumor responses"), only 1 in 341 patients exhibited a partial response. Although these numbers seemed bleak, the trial reported a 4.1 month improvement in median survival compared with placebo. Because of the limited options to treat advanced prostate cancer, the therapy was expedited for FDA approval. Additionally, biopsies of metastases after vaccination in some clinical trials revealed the presence of immune infiltrates in association with extensive edema, which often were followed by fibrosis (12). Since the tumor progressed in spite of such infiltrates, two conclusions were presented: 1) cells were of low avidity or subject to additional inhibition by endogenous tumor signals (13) and; 2) more powerful metrics were needed to evaluate clinical response.

Other methods target the T cell activation phase of the immune response. In one strategy, adoptive transfer of exogenously modified T cells modifies the T cell response. Typically these methods follow a lymphodepletion of the host, and in melanoma patients, this has shown incredible promise in expanding the tumor infiltrating lymphocyte (TIL) pool (14, 15). Lymphodepletion appears to be necessary to increase the efficacy of the treatment, possibly due to elimination of T cells and other homeostatic cytokines that might interfere with a response (16). A variant of adoptive cell transfer therapy is chimeric antigen receptor (CAR) therapy in which T cells are exogenously genetically modified to express an artificial tumor-specific TCR that is expanded and reinfused back into the patient. Results from CAR therapy have been promising

www.manaraa.com

in inducing T cell infiltrates, and indeed, objective clinical responses (17), but once again the field is faced with limited methods to track those clinical responses.

Lastly, and perhaps most promising are molecular-based therapies that counteract the tumor's immune suppressive defense mechanisms. These include molecules such as cytotoxic T-lymphocyte-associated protein-4 (CTLA-4), classically expressed on Treg cells, and programmed cell death 1 (PD-1) and PD-L1, expressed on the surface of T cells and tumor cells respectively. Melanoma-specific CD8 T cell responses have been reported in the case of ipilimumab, a CTLA-4 monoclonal antibody (18). Recent studies established a correlation between clinical responses to ipilimumab and elevated peripheral blood lymphocyte count (19), expression of T cell activation markers, inflammation in the microenvironment (20, 21), and an elevated frequency T cell receptor clones. Most recently, a study correlated the mutational burden of melanoma with duration of clinical therapy benefit from ipilimumab therapy (22), which suggested that highly mutated melanomas expressed more antigens and thus were more capable at triggering the host immune system. However, this hypothesis has been somewhat discredited as mutational burden was demonstrated not to be a sufficient predictor of therapeutic response. This again suggests that, without better markers of immune *function*, it will be difficult to evaluate clinical outcome relying solely on phenotypic characterization. Similarly, in a study evaluating the immune correlates of anti-PD-1 antibody therapy in various cancer types including melanoma and prostate cancer, 66% of patients whose tumors expressed PD-1 did not correlate with objective response (23). In short, determinants of therapeutic response may be more complex and a more direct assessment of T cell function may be needed to more accurately predict response to therapy.

Some histological features of the tumor environment may shed light on the interface between the immune system and the tumor. For instance, the association between improved survival and the presence of CD8+, Th1, and memory T cell infiltrates is well established in various cancer types (24, 25, 26). By contrast, the presence of mast cells has been a poor prognostic factor (27). In fact, the type, density and location of immune cells within the tumor bed may correlate with the clinical outcome, and these metrics have been proposed as an adjunctive prognostic measurement alongside the conventional TNM staging system (28). The major caveat behind relying on histological examination is that it does not incorporate function. In the example of Provenge, functional examination of T cells revealed two metrics that

www.manaraa.com

correlated with clinical response: delayed-type hypersensitivity (DTH) responses to recall antigens, and secretion of cytokines after non-specific stimulation (29). Unfortunately, in this study, the authors could not demonstrate tumor antigen-specific immunity: in other words, T cells from patients who received DC alone versus DC plus tumor antigen did not respond differently. Because the technique could not distinguish a tumor-specific response from an non-specific one, it was not generalizable. Although evidence for an important interface between the immune system and tumor is strong, therapy for cancer as well as T cell-mediated disorders still lacks validated methods for directly tracking T cell responses.

Extracorporeal photopheresis: an immunomodulatory therapy

In this section, I turn to an immunomodulatory therapy developed in the early 1980s by our group and discuss it as a lens for studying the field of cancer immunotherapy. Extracorporeal photopheresis (ECP) resulted in the cure of many patients with advanced, and at the time, terminal, cutaneous T-cell lymphoma (CTCL) (30, 31). CTCL is a clinically heterogenous disease of CD4+ skin-homing T cells (32). Early on, involvement in CTCL is confined to the skin with erythematous patches that evolve into scaling and poikiloderma (33), but as the disease advances, patches thicken to become plaque-like and involvement of peripheral blood increases (34). Moreover, erythroderma, a late manifestation of the disease, presents with near-complete skin involvement and varying amounts of scaling and pruritis.

During ECP, a patient's blood is apheresed, i.e., exposed to centrifugal forces, to separate the red blood cells from the rest of the blood (**Figure 2A**). Red blood cells are reinfused immediately back into the patient, while the patient's plasma and leukocytes are passed through a polystyrene plate under low flow conditions that recapitulate forces in the post-capillary venule. This first step is termed "plate passage." For some time during this plate passage procedure, leukocytes, constituting about 5% of the patient's total peripheral pool are exposed *ex vivo* to a photoactivated psoralen drug, 8-methoxy psoralen (8-MOP) in the presence of ultraviolet light type A (UVA), a combination therapy referred to as psoralen and UVA (PUVA). Because 8-MOP is inactive without UVA, the duration of activity of the drug is controlled by exposure to UVA (35).

Since its FDA approval, ECP has been effective in the treatment not only of CTCL but also of solid organ transplant rejection (SOTR) (36), graft-*versus*-host disease (GVHD) (37, 38), and autoimmune

www.manaraa.com

diseases such as progressive systemic sclerosis (39) and pemphigus vulgaris (36). SOTR and GVHD are life-threatening complications of organ transplantation and allogeneic hematopoietic stem cell transplantation (AHSCT), respectively (40). In SOTR, the host immune system attacks graft tissue resulting in graft rejection and potentially death. In AHSCT, host irradiation and chemotherapy is thought to create an inflammatory milieu, which activates clonal expansion of donor T cells against host antigen, promotes cytokine secretion, and expands the pool of natural killer (NKT) cells. Without GVHD, HSCT holds promise in the treatment of high-grade malignant hematologic disease, autoimmune disease, and immunologic deficiencies, including HIV (41). ECP has been used to treat rejection in heart (42, 43), kidney (44), and lung (45, 46) transplants. Moreover, randomized trials have demonstrated phototherapy's efficacy for the prevention of cardiac rejection (47, 48). In fact, after several cycles of ECP, transplant patients are often less dependent on broad immunosuppression (49). When used in the treatment of GVHD, ECP diminishes the graft-*versus*-leukemia effect, allowing the immune system to harness an effective response against leukemic cells (50). Lastly, similar to its effect in CTCL, when used in STOR and GVHD, ECP carries no carry life-long risks of infection, unlike conventional therapy with broad immunosuppression (51, 52).

At the end of the procedure, which normally lasts between 1 and 2 hours, the WBC and plasma are reinfused back into the patient. In the case of CTCL, the effect is to stimulate immune responses, and in SOTR and GVHD, the responses are downregulated. ECP's other major advantages are that it carries neither the risk of infection from immune suppression nor the toxic effects of chemotherapy. Such broad application is promising and simultaneously paradoxical, for how is a single therapy immunostimulatory (in the case of CTCL) and downregulatory (in the case of SOTR and GVHD), and in one case report, in the *same* patient (53)? Lastly, the main advantage of ECP compared with artificial DC therapies (11, 82, 83) is that, in ECP, physiologic conditions partner with the immune system to stimulate or regulate it, the way the immune system would in a healthy host.

Our lab has studied the mechanism underlying ECP using both human and mouse models. We hypothesize that central to the plate passage step is the interaction between adhered platelets and "rolling" monocytes (**Figure 2B**). Specifically, as platelets flow on the polystyrene surface, they adhere to the surface via fibrinogen receptors. Platelet adhesion under shear stress conditions is a well-recognized step in

www.manaraa.com

platelet activation, and we have shown in our model system, that this results in expression of activation molecules such P-selectin (54). This allows peripheral blood monocytes flowing over the plate to interact and adhere to the platelets (55). We have shown that without these flow conditions, such interactions are not possible (54). Platelets have been shown to have activating effects on monocytes that contact them (56, 57), and overall, plate passage appears to generate synchronized, activated monocytes expressing various DC differentiation markers (58).

To marry the paradoxical application of ECP in immunostimulation and downregulation, we have explored the second component of ECP: the effect of PUVA on DC. Our lab and others have shown, for instance, that 8-MOP and UVA upregulate expression of DC "suppression" genes thus favoring the generation of tolerogenic DC (59), and that PUVA plays a role in inhibiting graft rejection (60, 61). Therefore, we hypothesize PUVA's role in tolerogenesis is central to ECP's downregulatory effect. PUVA has the additional effect of preferentially inducing massive, slow apoptosis in the lymphocyte population (59, 62). We hypothesize that lymphocytes act as antigen sources for both tolerogenic and stimulatory DC. DC internalize these peptides, display them on class I or II major histocompatibility complex (MHC) molecules, and ultimately activate the adaptive immune system's CD8+ cytotoxic T cells or CD4+ helper T cells, respectively (63). Depending on the activation state of DC, the immune response is either stimulatory or downregulatory.

The advantages of ECP over other immune therapies are multiple: firstly, being a relatively "physiologic" therapy, requiring no addition of artificial cytokines, ECP has a great safety profile (64). This permits large-scale induction of antigen-presenting cells (APC) that are highly specific for dying pathogenic T cells. Additionally, since it's been approved for over three decades, there is accumulating clinical evidence supporting its efficacy in a variety of T cell mediated disorders (36, 39).

Since the introduction of ECP, next-generation modifications have been developed. In one, known as transimmunization, ECP is modified by an extra, overnight *ex vivo* incubation prior to reinfusion (65). The incubation step allows easier transfer of antigens (from apoptotic lymphocytes) to activated monocytes. Since ECP and its related therapy allow easy access to treated cells, it is an ideal model for designing a clinical tool for the purpose of immune monitoring.

www.manaraa.com

With this simplified introduction to immunotherapy (and with an emphasis on ECP), I turn to the focus of this project, which was two-fold: firstly, to establish a functional model that permits the evaluation and optimization of a laboratory model of ECP. Specifically, our first aim was to enhance our understanding of the process of generating *functional* myeloid APC via plate passage. Our second aim was to develop a method to more readily evaluate and quantitate immune responses during ECP, as well as other immune-based therapies. Although ECP has had promising success in the treatment of the various T cell disorders, responses remain variable. In fact, while complete responses certainly have been repeatedly observed, such patients remain a minority. In fact, the best responders to ECP were the patients with a short duration of disease, those without bulky lymphadenopathy or major internal organ involvement, patients with limited leukocytosis or leukemic burden and close to normal numbers of peripheral CD8+ T cells (66, 67, 68, 69). For this reason, ECP remains a promising therapy that merits closer inspection and optimization. Moreover, beyond CTCL, immunogenic cancers such as melanoma and renal cell carcinoma may stand to benefit from such a physiologic, immune-based therapy. As such, optimization of ECP as well as development of methods to evaluate the response would ideally allow a broader application of the therapy.

Aim One: Developing a laboratory model of ECP

In the first part of this project, our aim was to functionally evaluate plate-passed, myeloid APC against two other myeloid APC in order to optimize the laboratory plate-passage model. Specifically, we were interested in examining the role of CD4+ cells in the expansion of naïve CD8 cells from healthy human donors.

A naïve T cell, by definition is a circulating, mature T cell that has never encountered its specific (or cognate) peptide-MHC (70, 71). Naïve cells therefore circulate through the bloodstream and lymphoid organs for immunologic surveillance. Upon encountering an antigen, they undergo robust clonal expansion and differentiation into effector and memory cells (72). It is estimated that there are about 4,000-40,000 naïve circulating cells in a single clone, which is a frequency of about 10^{-6}-10^{-7} in the peripheral blood (73). One such antigen represented a relatively high frequency is the melanoma antigen recognized by T cells-1

www.manaraa.com

(MART-1), which was among the first human tumor antigens to be cloned (74, 75). The precursor frequency of naïve MART-1 specific cells has been estimated as high as 1 in 1000 naïve T cells (73).

MART-1 is expressed by melanocytes of the skin and retina (76), as well as in the majority of early stage melanosomes in melanoma tumors (77), but not other tumors. Although the protein function remains unknown, the MART-1 gene encodes a 118-amino acid polypeptide that acts a type III signal-anchor protein localized to the endoplasmic reticulum and *trans* Golgi network (78). This protein localization is clearly different from another melanocyte-specific polypeptide, tyrosinase, but it resembles that of gp100 (79). The uniqueness of MART-1 lies in its recognition by T lymphocytes in the context of a commonly encountered HLA haplotype, HLA-A*0201, making it an immunogenic peptide. In fact, it has been shown that MART-1 can be efficiently internalized and cross-presented by DC to T cells (80).

Since it is expressed in most melanocytic tumors and recognized by a common HLA haplotype, MART-1 has been used in several vaccination strategies. MART-1 peptide has been injected with adjuvant and/or pulsed on DC with modest clinical success (81, 82, 83). Often, responses to MART-1 are frequently assessed using tetramers, which are oligomers formed of multiple peptide-MHC class I complexes capable of binding to specific TCRs (84). MART-1 peptide has been used in 2 classical forms: as a long peptide (LP) spanning residues 16-40 and a short peptide (SP) spanning residues 26-35. It has been shown that LP is superior to SP in vaccination strategies, due to its preferential targeting of DC present in lymph nodes, and subsequent enhancement of antigen presentation *in vivo* (85). Additionally, cross-presentation and T cell expansion were found to be enhanced when the MART-1 peptide was modified at position 27 by replacing an alanine with a leucine residue. This anchor-optimized residue was shown to enhance MHC-peptide affinity by 2-3 log, in turn increasing the duration of T cell-DC contact, a critical step in T cell priming (86). It has also been proposed that this anchor residue may stabilize the TCR/MHC-peptide complex as a whole (87). Unfortunately, while the modified peptide improves cross-presentation, *in vitro* proliferation of naïve T cells is often not reproducible between experiments and within the same donor as % tetramer positive CD8+ cells range anywhere from 1% to 70% of the total CD8+ population (86). Clinically, peptide vaccinations resulted in expansions of specific T cells in 3-10% of patients, limiting the broad applicability of the MART peptide (88).

www.manaraa.com

Another important aspect of the MART system was the discovery of 2 novel MHC class II epitopes of MelanA/MART-1 in the region of the immunodominant 27-35 Class I epitope (89). From animal studies, we learned that concomitant activation of antigen-specific CD4 and CD8 cells boosted the effector function and maintained a longer-lasting memory population of CD8 cells (90, 91, 92). Bioley et al. were able to show that the modified MART-1_{A27L} LP was able to induce CD4 responses (89). The same group has also shown that MART-1 peptide vaccination showed *in vivo* reduction in FoxP3 expression levels in CD4 T cells, which suggested reduced regulatory T cell (Treg) activity, as well as restoration of peptide-specific proliferation and cytokine secretion (93). The authors had begun work on the role of CD4 cells in CD8 expansions, but these results remain unpublished. Another approach has been to TCR engineer CD4+CD25- T cells with transduced MHC Class I-restricted TCR for the MART epitope with some success (94).

In the first part of this project, we tested the functional APC capability of our plate-passed monocytes (PPM) by comparing them against untreated monocytes and conventional (GMCSF/IL4) DC. Because of its capacity to generate peptides capable of being bound by MHC Class I and II (and hence be recognized by both CD8+ and CD4+ cells), we used the MART-1_{A27L} LP system to study the role of CD4 cells in the expansion of naïve, human CD8 cells. We hoped to use such an assay to understand the mechanism underlying APC capability in ECP, and by modifying those conditions in vitro, we sought to optimize therapy.

Aim Two: Developing a method to evaluate immune responses

The second part of this project was directed toward developing a method to evaluate immune responses, which would be applicable in all immune-based therapies, whether anti-tumor or anti-graft, cell-based or molecular.

Improved methods to track T cell responses would enhance our understanding of the interface between cancer and the immune system. Indeed, I am convinced that such methods are *necessary* to replace conventional clinical response criteria which are problematic and inaccurate. Criteria such as RECIST and World Health Organization (WHO) are based on evaluation of tumor size and overall burden of disease (95). The problem with applying these measures in immunotherapy is patients may take longer to respond:

www.manaraa.com

in fact, responses to immunotherapy are on the order of weeks or months, as compared with conventional chemotherapy where responses are on the order of 6-8 weeks or approximately following 2 cycles of chemotherapy (96). In clinical trials, delayed response is often seen as delayed separation of Kaplan Meier curves which may be falsely interpreted as treatment failure (97). Particularly in studies comparing standard chemotherapy to immunotherapy, classical responses to chemotherapy will be apparent before any responses to immunotherapy can be measured. Delayed response lengthens the period for follow up which increases the probability of unexpected outcomes and leads to loss of statistical power (97, 98, 99). Additionally, certain response patterns to immunotherapy are not captured by conventional criteria. These include patients whose disease burden increases overall, whether by increase in size of existing lesions or emergence of new lesions prior to reduction in tumor burden. In fact, specifically for ipilimumab (CTLA-4 inhibitor), there are four patterns of response associated with favorable survival: 1) shrinkage in baseline lesions, without new lesions; 2) durable stable disease (in some patients followed by a slow, steady decline in total tumor burden); 3) response after an increase in total tumor burden; and 4) response in the presence of new lesions. Additionally up to 10% of patients who ultimately had a positive response to ipilimumab in two Phase II clinical trials followed response patterns 2, 3, and 4 and therefore were not captured by the clinical trial, which classified their disease as “progressive” or “stable” according to WHO criteria (100, 101). Modifications to RECIST have been proposed, such as, immune-related response criteria (irRC), however, these lack specificity for a therapeutic response (102, 103). Most clinical trials now use overall survival or progression-free survival as a primary outcome to evaluate therapeutic response, but this evaluation is also delayed, with mean response times in one trial of 2.1 months (104). That is a extensive period to be on a potentially highly toxic therapy such as ipilimumab without any knowledge of whether the patient is responding.

Since clinical criteria to evaluate immunotherapeutic response are insufficient, a number of methods evaluate T cell responses directly using peripheral blood have been developed (105). These include tetramers (discussed also in Aim One) (106), which do not report on any T cell functional capability. Alternatively, assays to evaluate T cell proliferation by staining with CFSE are influenced by the in vitro stimulation procedures, and therefore may not be an accurate measure of *in vivo* conditions. Other techniques such as enzyme-linked immunosorbent spot (ELISPOT) or flow cytometric assays detect

www.manaraa.com

cytokine levels in the peripheral blood. ELISPOT can be used to evaluate cytokine production levels, such as levels of IFNγ and TNFα, or expression levels of various surface markers. Some murine models have shown Th1 responses to be relevant in anti-tumor immunity (107), suggesting that IFNγ and TNFα cytokines are important in monitoring immune responses. However, such a strategy may not work if tumors have developed mutations in cytokine receptors that prevent receptor engagement, such as in human lung adenocarcinoma models (108) and prostate cancer cell lines (109). Furthermore, ELISPOT results did not correlate with disease-free survival in patients who underwent surgical resection of Stage II-IV melanomas then received a multi-peptide vaccine (81). The caveat to interpretation of this study is that subset analysis was not done so it remains unclear if stage of disease before resection contributed to disease-free survival or whether the technique was not standardized. Another study showed no correlation in Stage IV melanoma patients treated with a multi-peptide vaccine, even though the technique *was* standardized (110).

Though some have focused their efforts on standardizing these existing techniques and conducting large, prospective clinical trials, especially with ELISPOT (111, 112, 113, 114, 115), others have argued we should learn from the HIV field where techniques like ELISPOT have failed at measuring T cell responses against the virus. Rather than concentrate on harmonizing assays, we should be focused on developing new ones. In fact, the lack of monitoring tools has been suggested as one of nine critical hurdles in cancer immunotherapy (96). More recently, mRNA transcription of cytokines such as IFN-γ have been used to report on CD8+ responses following in vitro stimulation with peptide (antigen)-loaded, autologous peripheral blood mononuclear cells (PBMCs). Unfortunately, RT-PCR based methods are still expensive and time-consuming.

To address this clear gap in cancer immunotherapy, this project aims to develop a method that tracks early T cell signaling events. Such a tool would offer rapid clinical assessment and allow for early modification or discontinuation of therapy. Fortunately, understanding of the early signaling events in antigen-specific T cell activation continues to evolve. We now understand that an immunological synapse is formed by three dominant contacts (116): firstly, T cell receptor binds cognate peptide-MHC on the surface of a DC, which primarily controls the specificity of the immune response, and is often referred to as Signal 1. Secondly, adhesion molecules such lymphocyte function-associated antigen (LFA), CD2, and CD58 provide the energy needed to pull cells together allowing sustained antigen recognition and precise

www.manaraa.com

execution of effector functions, which has been shown to be necessary for tumor rejection (117). Thirdly, co-stimulatory and checkpoint receptors, known as Signal 2, alter the functional outcome of immunological synapse formation without having much signaling or adhesive activity.

Following the immunological synapse, a cascade of T cell phosphorylation events ensues that culminates in a supramolecular assembly that recruits phospholipase PLC-γ1, which becomes activated (118). Upon activation, PLC-γ1 hydrolyzes PtdIns(4,5)P_2 into diacylglycerol (DAG) and inositol-(1,4,5)-triphosphate (IP_3). IP_3 opens up calcium channels in the endoplasmic reticulum permitting release of calcium stores. This process triggers opening of store-operated calcium channels in the cytoplasmic membrane. As a result, several calcium-dependent signaling proteins and their target transcription factors are activated, including the phosphatase calcineurin and its targets: nuclear factor of activated T cells (NFATs), calcium-calmodulin-dependent kinase (CaMK), and nuclear factor kappa B (NFκB). By contrast, DAG activates GTPase Ras and kinase ERK, which in turn activate Ras-mitogen-activated protein kinase (MAPK) and protein kinase C (PKC) and a number of downstream transcription factors. These various signals are often integrated, such as with NFAT:Fos:Jun complex (119, 120). Integrated early signals drive the transcription of a large number of activation-associated genes and are important in cell proliferation and cytokine gene expression (121).

Calcium flux was first reported as a measure of lymphocyte activation nearly three decades ago (122). Methods to track calcium flux use fluorescent dyes that are detected by flow cytometry or confocal microscopy. In order for calcium flux to be used as an immune monitoring tool, several features must be present. Fundamentally, the method should detect responses that are antigen-specific. In other words, responses must be sensitive and specific for a T cell that has encountered cognate peptide-MHC. Moreover, to achieve true immunological monitoring, sufficient clinical responses must be recorded for correlations between *in vitro* and *in vivo* parameters to be made. Since all activated T cells will signal calcium early on, such a method would capture *all* activated T cells no matter the antigen specificity. It would capture all antigen types, including neoantigens and over-expressed self-antigens. Although such a tool would require staining the sample in a relatively laborious protocol, we hypothesized that if we developed a method that would be sensitive and specific to antigen-specific T cell responses, we could use label-free, non-tedious, existing technologies and elaborate new ones that would be significantly less tedious and would be

www.manaraa.com

compatible with a clinical test. To begin with, this project introduces a proof-of-principle concept using a transgenic mouse model (OT1) in which all T cells expressed TCR specific for the ovalbumin (OVA)-derived, SIINFEKL-peptide. Transgenic models have been invaluable for the understanding of basic concepts of T cell tumor biology (123, 124, 125), and we hoped to use the simplicity from such a model to prove the concept that early, antigen-specific T cell signals could be tracked.

STATEMENT OF PURPOSE

Firstly, to develop a functional assay to evaluate laboratory-produced, plate-passed myeloid cells

Secondly, to elaborate a method for directly tracking T cell responses during cancer immunotherapy

MATERIALS AND METHODS

Unless otherwise specified, all procedures were performed by the author.

Human donors

PBMC were obtained from healthy, HLA-A2 human donors, in accordance with the guidelines of the Yale Human Investigational Review Board, and informed consent obtained under protocol number 0301023636, Production of normal control allo-inhibitory dendritic cells. Typing of HLA-A2 (MHC Class I) was done using anti-HLA-A2 FITC mAb (BioLegend). When applicable, donors were also tested for two MHC Class II loci, HLA-DRB1 and HLA-DQB1, which are two MART-specific loci reported by Bioley et al (89). PBMC were obtained by Ficoll gradient centrifugation. When plasma was needed, whole blood was spun blood at 1000 RPM for 15 min prior to laying the Ficoll layer to separate plasma from PBMC and RBC, plasma layer was obtained, and the leftover cell-rich layer was brought up to the same volume and lain on a Ficoll column. Monocytes were purified from PBMC by negative selection using the Pan Monocyte Isolation Kit, human (by Miltenyi). Naïve CD4+ and CD8+ T cells were each purified from PBMC by negative selection, using Naïve CD4+ T cell isolation kit II and CD8+ T cell isolation kit, human, respectively. All purifications achieved >90% purity (data not shown).

APC preparation, including plate-passage

www.manaraa.com

Three different APC were prepared from human PBMC: conventional FastDC (FastDC), plate-passed monocytes (PPM), and unstimulated monocytes (UM). Two days prior to set up of functional assay (d-2), FastDC were prepared by culturing monocytes in the presence of 800IU/ml GMCSF and 1000IU/ml IL-4 to differentiate into DC over 2 days, as described by others. (126) On day 0, autologous donor monocytes were again negatively purified from PBMC using the same kit, and either left unstimulated (UM) or passed over a laboratory model of ECP (PPM). The ECP model was comprised of a polystyrene chamber measuring 4x2x0.029cm with a volume capacity of approximately 232 µl, engineered by the Fraunhofer Institute for Biomedical Engineering. The chamber has one entry and one exit port. The entry port is connected to a flow pump that can adjust for 2 variables: the rate of flow and the diameter of the syringe. The plate-passage is performed in a CO2-free incubator set at 37°C. To run the plate, 4ml of autologous platelet-containing plasma were spun at 900*g* for 15 min in order to deplete plasma of platelets and form platelet-poor plasma (PPP). 2 ml of PPP were mixed with 2ml of platelet-containing plasma to form a 1:1 diluted plasma that was loaded onto the plate at 2.92ml/hr. The plasma layer was left to coat the plate for 30min-1hour to allow platelet adhesion. Plasma was then washed at 2.92ml/hr with 6ml of RPMI media, and 8ml of 10e6/ml PBMC were run continually over the plate at 0.484ml/hr. Cells were then washed and collected using a low-volume, low-speed wash (at 0.484ml/hr), and a second high-volume-high-speed wash (at 14.8ml/hr) to remove any adherent monocytes. Throughout the plate-passage, another 8ml of 10e6/ml PBMC, constituting UM, were kept at 37°C. PBMC from both plate-passed and unstimulated groups, were then purified to monocytes.

MART functional assay

APC were co-cultured in 96-well round-bottomed plates, with autologous CD8+ cells in RPMI media supplemented with non-essential amino acids (100X, Sigma-Aldrich), sodium pyruvate (100X, Invitrogen), vitamin solution (100X, Invitrogen), 2-mercaptoethanol (100X, Invitrogen), and 10µM ciprofloxacin (Serologicals Proteins), and 5-10% human plasma. Cultures are set up at varying ratios of 1:5, 1:10, 1:20, and in some cases, 1:40, APC:T cells in the presence of 10uM $MART_{A27L}$ long-peptide. Negative controls were also set up by culturing T cells alone in the presence of peptide. Unless, otherwise noted, the CD8+ cell number was kept constant at 0.5e6/ml/well. When applicable, 0.5e6 autologous CD4+ cells were added

www.manaraa.com

at 1:1 CD4+:CD8+ cells, keeping the APC:CD8 cell or APC:total T cell ratios the same. Three days following co-culture, 12.5IU/ml IL-2 and 5ng/ml IL7 cytokines were added. Between d9 and d11 from co-culture, half of the media was changed, when needed, and IL2 and IL7 cytokines again supplemented. On d13, cells were harvested, washed and stained with 1:25 MART-1 PE-conjugated dextramer (Immudex) and, as a negative control, 1:25 gp100 APC-conjugated dextramer (Immudex). Cells were kept in the dark at 25^{o}C for 10min. Excess dextramer was removed by washing and cells were then surface stained with 1:50 anti-CD4 BV mAb (BioLegend), 1:50 anti-CD8 PE/Cy7 mAb (BioLegend), 1:75 anti-CD45RO Alexa Flour 488 mAb (BioLegend), then kept in the dark at 3^{o}C for 15min. Cells were washed and analyzed on 7-color Stratadigm. Before analyzing samples, 1:12 7AAD (BioLegend) was added at 1:12 on ice. 7AAD was added to exclude any apoptotic cells from the tetramer analysis.

Mice, reagents, and generation of bone-marrow derived DC (BMDC)

Wild-type B6-SJL CD45.1+ and OT-1 transgenic CD45.2+ mice were purchased from Taconic. Mice were between 7 and 10 weeks of age at the start of each experiment. All experimental procedures involving mice were performed with the approval of the Yale Animal Research Committee under the protocol number 2014-11620, “Murine Models for testing the bidirectional immunomodulatory actions of modified extracorporeal photochemistry”. All CD8+ cells were purified by negative selection using EasySep^{TM} Mouse CD8+ T cell Enrichment kit by STEMCELL. The protein ovalbumin (OVA) and the peptides H-2K^{b}-restricted OVA$_{257-264}$ (SIINFEKL) and the negative control peptide, EIINFEKL were purchased from Sigma-Aldrich. Lipopolysaccharide/OVA-containing nanoparticles (LPS/OVA-NP) were synthesized and used at10mg/ml [by Douglas Hanlon and Harib Ezaldein]. BMDC were generated from crushing of femur, tibia and fibula of a B6-SJL mouse using mortar and pestle. After filtering debris and washing mortar twice in RMPI media, filtered cells were washed, resuspended at 10-15e6/ml in T cell media supplemented with 20ng/ml, and cultured in 6-well plates. Cells were harvested between days 6 and 8 after culture, with approximately 60-70% recovery, and a purity of >85%, and subsequently used in antigen-presentation assays.

Adoptive transfer and vaccinations

www.manaraa.com

OT-1 CD45.2+ cells were obtained from crushing a spleen (SPL) from which 5e6 purified CD8+ cells were injected into each of the tail vein (i.v) and peritoneal cavity (i.p.) of a isoflurane-anesthetized B6-SJL CD45.1+ mouse, as shown in [done by Enping Hong] (**Figure 3A**). The mouse rested for 4 hours before the vaccinations. Vaccination of both B6-SJL CD45.1+ and OT-1 CD45.2+ mice with LPS/OVA-NP proceeded identically in all 7 sites, unless otherwise noted [done by Enping Hong]. 100ul was injected intraperitoneally, 40ul subcutaneously (s.c.) bilaterally at each base of the tail, 40ul s.c. bilaterally at each mid-thigh, and 40ul s.c. at each ventral chest area, for a total 3.4mg vaccination. To generate memory cells, B6-SJL CD45.1+ mice were rested for 7 days, then rechallenged with 3.4 mg dose of LPS/OVA-NP, as described previously [done by Enping Hong] (127). Vaccination was also attempted directly on OT1 mouse by injecting increasing quantities of LPS/OVA-NP. For peripheral blood (PBL) analysis, eye bleeds were performed of the R ophthalmic vein [done by Enping Hong]. For memory cell characterization, the following panels were used: CCR7 PerCP/Cy5.5, CD62L APC, KLRG1 AF488, CD127 PeCy7, CD44 AF700. For adoptive transfer experiments, the following antibodies were added: CD8 PE, CD45.2 eF450. For direct vaccination of transgenic OT1 mice, we used the following: TCRβ PE, CD8 eF450. All antibodies were from BioLegend.

Human cell line

The MART-1 tumor-reactive lymphocyte cell line called DMF5 was obtained as a gift from the National Cancer Institute (NCI). DMF5 is a cell-line cloned from the MART-specific tumor-infiltrating lymphocytes (TILs) of an HLA-0201 patient with melanoma. Compared to other clones from a pool of TILs from five patients, it was found to be the most avid against MART-1 expressing tumors *in vitro* (128). The authors then expanded in the presence of irradiated PBMC from healthy donors and high doses of IL-2, as described previously. Approximately 14 days from the start of an expansion, cells were frozen down in 4e6/ml aliquots. Staining using MART dextramer showed 30% of DMF5 cells expressed MART-specific TCR (data not shown).

Cell labeling and calcium flux assay

www.manaraa.com

As shown in **Figure 3B**, murine BMDC were loaded for 2 hours at 37°C with 1μg/ml LPS and either SIINFEKL or EIINFEKL peptide. For human experiments, FastDC were loaded with $MART_{A27L}$ short-peptide (SP) or gp100 SP, as a negative control. Unless noted, the peptide loading concentration was 10ug/ml. BMDC and FastDC were then washed from peptide and surface stained with 1:300 murine anti-CD11c FITC mAb (BioLegend) and 1:100 human anti-Cd11c FITC mAb (Biolegend), respectively. CD8+ (either OT1 or Dmf5) cells were loaded with 1μM Indo-1 AM by Life Technologies and kept at 37°C in the dark for 30 min. Indo-1 is a ratiometric indicator of free intracellular calcium that has been used by many authors to study the activation of lymphocytes (122, 129). It excites at 365 nm and emits at two different wavelengths depending on its bound state: at 485 nm (blue) for free Indo-1 and at 405nm (violet) for Indo-1 that is bound to calcium. The ratio of emission intensity of bound to free Indo-1 (i.e. Violet/Blue) represents the calcium content of the cell and is independent of the actual indo-1 concentration. Following Indo-labeling, OT1 CD8+ cells and DMF5 cells were stained with 1:100 murine anti-Cd8 PerCP-Cy5.5 mAb (Biolegend) and 1:100 human anti-CD8 PerCPCy5.5 mAb (Biolegend), respectively. Following staining, all cells were resuspended in calcium-chloride containing PBS: 1) APC (either BMDC or FastDC) were brought up in a constant volume of 150ul/ FACS tube while varying the cell number and concentration; 2) CD8+ cells were kept fixed at 1e6/ml, and 0.4e6 cells were added to FACS tubes, which were separate from the APC tubes. For the positive control, anti-CD3 antibodies, human and mouse, from eBioscience was used.

For flow cytometric analysis, an APC tube and its respective CD8+ T cell tube were pre-warmed for 2-3min, after which APC were added to T cell tube and mixed by pipetting. The sample was walked over to the centrifuge, spun at 1650 RPM for 20s, then the pellet was walked back to the cytometer, as described by others (130), vortexed and flicked to resuspend the pellet. The sample was then run for 7 min on the LSRII cytometer. Data were analyzed using FlowJo version 9.6.4; calcium plots were represented as kinetic curves, which graph the median value of the ratios of Indo-1 Violet/Blue collected for all events in one second. To quantify differences in T cell responses to antigen-specific and non-specific stimuli, the following parameters were tabulated: mean and peak Ratio of Indo Violet/Blue, area under the curve (AUC), slope of the curve and its oscillatory frequency (OF). The OF was calculated as the number of conjugate events per second.

www.manaraa.com

RESULTS

PPM functionally stimulate clonal expansion of MART-specific naïve T cells

Three different types of APC were prepared; for a detailed explanation, see Materials and Methods. 1) Conventional FastDC (FastDC) were generated by culturing purified monocytes over two days in the presence of GM-CSF and IL-4. 2) Plate-passed monocytes (PPM) were generated by passing PBMC through an IBMT chamber that was coated with autologous plasma/platelets. 3) Unstimulated monocytes (UM) were untreated but left to sit at 37^{o}C as a negative control during the time that the PPM were being prepared. No phenotypic characterization was done on the various types of APC. However, work done by others in our laboratory had shown plate-passage capable of generating functional APC that were differentiating along the DC pathway (55, 58).

To evaluate the functional capabilities of the three APC, each APC (purified by magnetic bead negative selection; *see* Materials and Methods) was co-cultured with autologous CD8+ cells at 4 DC:T cell ratios: 1:5, 1:10, 1:20, and 1:40, keeping the CD8+ cell number fixed, and in the presence of 10 μM $MART_{A27L}$ LP (**Figure 4A**). LP was chosen instead of the form-fitting, 10-mer SP used by others (131). In all six of donors tested, none of the DC:T cell ratios showed any superiority in expanding naïve T cells (results not shown). When all ratios were matched across all 3 APC types and concatenated, as shown in **Figure 4B**, the average tetramer+ expansion of CD8 cells co-cultured with each of the three APC types was the following: 10.86 % from FastDC (range=1.73-40.6, SD=11.56, n=6), 9.78% from UM (range=2.32-21.9, SD=5.87, n=8), and 7.3 % from PPM (range=1.71-17.4, SD=5.07, n=8). Differences among APC types were not significantly different. Negative controls were also set up using autologous CD8 cells only cultured in the presence of LP: those expansions averaged 1.1% (range=0.16-2.12; SD=0.75, n=8). Further, when possible, duplicates were set up. **Figure 4C** shows the coefficient of variance (COV) for the 6 experiments ranged from 23.5 to 53%. This is higher than the COV reported by Wolfl and Greenberg (131): for more, see *Discussion*.

CD4 cells may assist in CD8 proliferation

In donors that tested positive for a MART-specific MHC class II, CD4+ cells were added to the co-culture to evaluate whether helper T cells would potentiate the proliferative response of MART-specific clones

www.manaraa.com

(**Figure 5**). CD8 expansions stayed the same or decreased: for conventional FastDC, 3.9%, SD 1.64, with CD4 addition, 6.9%, SD 3.7; for UM, 9.7%, SD 6.8, with CD4 addition, 7%, SD 3.6; for PPM, 5%, SD 4.7, with CD4 addition, 7%, SD 4.8. Negative controls, set up with CD8 only, expanded to only 1.4%, SD 1.4, and with CD4 addition, 1.6%, SD 1.61. Thus with the addition of CD4 cells into the co-culture, CD8 expansions using FastDC and PPM increased, though the numbers did not attain statistical significance, whereas CD8 expansions using UM decreased.

Antigen-specific flux (ASF) cannot be detected without gating a population of interest

The second part of the project was to develop a proof-of-principle immunologic assay using calcium flux and show that early T signal signaling could report antigen-specific responses. We used Indo-1 AM, a dual wavelength calcium detection dye that is excited at 340 nm (in the UV range) and emits differentially at 475 nm when bound to calcium (Indo-Blue), and at 405 nm when free from calcium (Indo-Violet). Results are therefore reported as a ratio of calcium-bound (Indo-Violet)/ calcium-free (Indo-Blue). The advantages of using Indo-1 AM in this setting are multifold. Firstly, because Indo-1 is a ratiometric dye, it allows comparisons between samples and different experiments. Secondly, it is well-suited for flow cytometry detection. However, the limitations of Indo-1 include a small dynamic range, that is, the difference in intensity between baseline and activation may be small, which could present a problem when evaluating subtle differences. We also tried another calcium dye (Fluo-4AM), which is a single-wavelength dye, but achieved greater sensitivity with Indo-1AM (data not shown). Because of the complexity of a multi-antigen tumor model, we focused initially on the ovalbumin (OVA)-derived, SIINFEKL-specific transgenic mouse model (OT1). Naïve OT1 CD8+ T cells were labeled with Indo-1 AM then mixed with SIINFEKL (specific)- or EIINFEKL (non-specific) peptide-loaded DC. By flow cytometry, we could not detect antigen-specific calcium flux (ACF) in OT1 cells (**Figure 6A**). We reasoned that the absence of antigen-specific flux in the peptide-loaded DC groups may have been because the probability of DC-T cell encounter was low under the specific mixing conditions employed. To increase that probability, we mixed and then pelleted DC and T cells to facilitate immunological synapse formation. We also surface-labeled DC and T cells with anti-CD11c(FITC) and anti-CD8(PerCP/Cy5.5) antibodies respectively, which allowed gating on CD8+ CD11c+ conjugates. Conjugates represented T cells that had made stable contacts with

www.manaraa.com

DC. For more, *see* Materials and Methods. **Figure 6B** shows the conjugate gating strategy and a representative plot of conjugate % as the ratio of DC: T cell changes. Overall, by decreasing the ratio of DC:T cells through varying the DC number and concentration, ASC formation decreased.

Results pooled from 4 experiments reproduced these antigen-specific differences (**Figure 6C**). Comparing the 3 DC:T cell ratios tested: at the 3:1, 5:1, 10:1 ratios, ASC formed in 17% (STD=14.5), 33.5% (STD=15.8), and 48.4% of CD8+ cells (STD=12.5), respectively. At 3:1, 5:1, and 10:1 ratios, non-antigen specific conjugates (NASC) formed in 3% (STD=3.78), 8.49% (STD=4.73), and 14.5% of CD8+ cells (STD=11.4). These differences between ASC and NASC became more significant as the ratio of DC:T cell increased, which may have been due to reduced T cell competition to contact DC.

We were also able to show ASC formation in the human DMF5 cell line using MART SP- (specific peptide) or gp100 SP- (nonspecific peptide) loaded FastDC (**Figure 6D**). At the 3:1, 5:1, 10:1 ratios, ASC formed in 25.4% (STD=17), 36.6% (STD=11.7), and 42.6% of CD8+ cells (STD=12.3), respectively. At 3:1, 5:1, and 10:1 ratios, NASC formed in 11.9% (STD=3.1), 28% (STD=10.6), and 29.3% of CD8+ cells (STD=4.9). We concluded that the DMF5 cell line exhibited higher background levels of NASC, compared with OT1 cells. We hypothesized that this may be due to the presence of IL2 cytokine in the expansion media of the DMF5 resulting in non-specific background stimulation, or to the fact that this highly activated T cell line is sticky. Because differences in flux between ASC And NASC were maximized at the 5:1 ratio, the remainder of experiments in the OT1 system utilized this middle ratio. By contrast, DMF5 were used at 10:1 ratio where differences between ASC and NASC were maximized (data not shown).

ASF has a lower limit of detection

We were initially surprised to find that as ASC formation decreased, so did ASF (**Figure 7A**). The amplitude of flux in ASC and NASC increased as the DC:T cell ratios increased, as did the oscillatory frequency. However, upon further reflection, this result should probably not have been surprising, as increased ratios resulted in increased conjugate formation, with TCR contacting more available peptide-MHC (pMHC) complexes. Moreover, when the sample was vortexed "vigorously," following the pelleting step, ASC disappeared and no ASF was detectable.

www.manaraa.com

To determine the sensitivity of our system, we next titrated the peptide loading concentration. We showed that the peptide-loading concentration could be titrated down to the order of ~10^{-3}uM in the OT1 (**Figure 7B**) and DMF5 systems (**Figure 7C**). We also mixed responding cells (OT1 or DMF5) with wild-type (WT; non-responding cells), and showed that ASF disappeared when the proportion of antigen-specific cells in the mixture reached ~0.1% OT1 cells (**Figure 7D**) and around 1% of DMF5 cells (**Figure 7E**).

In vitro antigen-experienced T cells have a higher activation threshold than naïve cells

Next, we sought to compare the activation threshold of naïve cells with *in vitro* pre-activated counterparts. For pre-activation in the OT1 system, purified CD8+ OT1 cells were cultured with BMDC at a 10:1 ratio of T:DC in the presence of human IL2/IL7 (see *Materials and Methods* for concentrations). In the DMF5 pre-activation set-up, 3e6 DMF5 were cultured in the presence of 0.6e6 FastDC in the presence of classic maturation cocktail (TNFα, IL1β, IL6, PGE2; see *Materials and Methods* for concentrations) and either 10 μg/ml MART SP or gp100 SP. Forty hours later, non-adhered cells representing DMF5 were collected and used in calcium flux experiments. In all both T cell types (OT1 and DMF5), results suggested that pre-activated cells were less able to flux calcium as efficiently as freshly harvested OT1 (**Figure 8A, B**) and DMF5 (**Figure 8C, D**) cells. Additionally, somewhat surprisingly, DMF5 pre-activated using gp100 (a non-specific source of peptide), had *restored* ability to flux calcium compared to specifically pre-activated DMF5 (**8D; bottom rows**).

To examine the activation potential of naïve, human T cells, 7 day co-cultures were set up using FastDC from an HLA-A2+ donor and autologous naïve cells T in the presence of IL2, IL7, and either specific (S) peptide, i.e. MART-1 SP, or non-specific (NS) peptide, i.e. gp100 SP. On day 7, cells were harvested and tetramer stained. (S) T cells expanded to approximately 9% of the CD8 pool, whereas (NS) T cells did not (**Figure 9A**). By calcium flux, (S) T cells demonstrate ASC formation and ASF compared with (NS) T cells. Intriguingly, when (S) T cells are diluted with (NS) T cells at a 50% (1:1 ratio) dilution rate, ASC and ASF are not significantly altered (**Figure 9B**). In conclusion the *in vitro* naïve T cell expansion suggested that (NS) T cells were less able to activate calcium flux than (S) T cells. This contrasts with DMF5 data shown in Figure 9D. This could be on account of the fact that DMF5 cells are expanded in the presence of large amounts of IL2 cytokine, resulting in non-specific activation. It's possible that specifically pre-

www.manaraa.com

activated DMF5 become exhausted from the combination of both specific and non-specific stimulation. Since cytokine is added to the naïve T cell culture on day 3, exhaustion is less likely to occur as the expansion proceeds slowly. Because *in vitro* culture conditions may well not be particularly physiologically relevant, we next sought an *in vivo* activation model in the OT1 system.

T cell activation in antigen-experienced T cells *in vivo* differ depending on host

To generate *in vivo* antigen-experienced cells, two WT B6 SJL mice on a CD45.1+ background were vaccinated with 3.4 mg LPS/OVA nanoparticles (Vax WT). Because of this genetic background, wild-type cells could be labeled with CD45.1 fluorescent antibody that would distinguish wild-type cells from OT1 adoptively transferred cells, which were on a CD45.2+ background. Four hours later, one mouse received an adoptive transfer of 5e6 CD45.2+ CD8+ OT1 cells (Vax+AT WT), while the other did not. In doing so, we sought to compare the AT population to the endogenous SIINFEKL-specific T cell population in the WT mouse. One week later, splenic SIINFEKL-tetramer positive cells had expanded to 1.5% in the vaccinated WT mouse and to 4.4% in the WT+AT mouse (of the total CD8+ population). As positive control, naïve OT1 CD8+ splenocytes were 100% SIINFEKL tetramer positive (**Figure 10A**). Since activated T cells express CD44, we compared CD44 intensity in the tetramer+ and tetramer- populations, and found CD44 activation in the tetramer+ population in the vaccinated mice, but not the tetramer- population, and less so in naïve OT1 cells. There was no difference in activation between Vax WT and Vax+AT WT.

To compare calcium flux among the different groups, we diluted naïve OT1 cells from 100% to 4% in a WT non-responding population, then to 1% and 0.5% (**Figure 10B**). This permitted us to do side-by-side comparisons with the Vax+AT WT (at 4%, then diluted to 1%, 0.5%), and Vax WT (at 1%, then diluted to 0.5%). As with the *in vitro* pre-activated system, we saw decreased activation at 4% in the Vax+AT WT as compared with naïve animal. ASC were also lower in that animal (5% compared with 12% in naïve OT1). Surprisingly, at 1%, Vax WT ASF was *higher* than in naïve OT1 and Vax+AT WT, which suggested that *endogenous* antigen-specific cells might behave somewhat differently than AT transgenic cells. At 0.5%, ASF was similar in naïve OT1 and Vax WT, and lowest in Vax+AT WT.

www.manaraa.com

To further investigate the impact of host environment on the activation of T cells, we sought to compare naïve OT1 cells and Vax+AT WT cells (same conditions as above) to a *directly vaccinated* OT1 mouse (Vax OT1). Because we were not sure if cytokine storm would ensue when naïve OT1 cells encountered antigen for the first time, we chose to vaccinate the animal at $1/20^{th}$ of the dose, i.e. 0.17mg. Vax+AT WT mice expanded AT tetramer-positive population to 5.85% of total CD8+ cells. Phenotypic characterization of Vax+AT WT peripheral blood (PBL) showed shedding of CD62L after 1 week and increase in CD44 expression (**Figure 11A**), compared with naïve OT1 mouse. By contrast, phenotypic characterization of PBL from Vax OT1 showed no changes in CD44 and CD62L, so the mouse was vaccinated at $1/10^{th}$ the dose (0.34 mg) one week later, again without any increased expression of activation or memory markers (data not shown). Two weeks from the first dose, the OT1 mouse was vaccinated a third time at the full 3.4 mg dose, and still no activation response was measurable. Functional analysis of CD8+ cells from spleens (SPL) by calcium flux of all three T cell types revealed decreased activation levels in Vax OT1 as compared with naïve OT1 cells and AT cells from Vax+AT WT host (**Figure 11B**). ASF disappeared at 0.1% in naïve OT1 and at 1% in Vax+AT WT and Vax+OT1 hosts. Of note, the first lymph node purification from Vax+AT WT mice was unsuccessful, but see also below.

In vivo antigen-experienced AT T cells in the LN have greatest expansion potential

Since the spleen is not a secondary lymphoid organ, it is not a classic organ for the initiation of CD8+ T cell responses. The lymph node (LN), being a secondary lymphoid organ was a logical site to examine. We chose the AT+Vax WT mouse as our antigen-experienced model because we had seen greatest expansions in that mouse (see previous discussion) compared with Vax WT mouse, and with Vax OT1 mouse which showed no phenotypic change from naïve OT1. We next reattempted obtaining LN CD8+ cells from a Vax+AT WT mouse as well as PBL and SPL for comparison (**Figure 12A**). One week post-vaccination, cells from LN, SPL, and PBL were characterized by phenotype and found to be CD44+ and CD62L-, consistent with an activated population. Subsequently, LN and SPL CD8+ cells were purified but PBL was not since numbers were limiting. Upon purification, LN tetramer+ cells were enriched to 7% of total CD8+ population, and splenocytes to 3.5%. PBL tetramer+ cells comprised 5% of total PBL cells. Functional analysis revealed ASF in LN population at 1 μM and 0.1 μM peptide loading concentrations (**Figure 12B**).

www.manaraa.com

ASF could not be detected in PBL or SPL. This could partially be the result of lower starting %tetramer+ cells in the latter compartments, but could also reflect differences in the level of activation of CD8+ cells in those compartments, with LN cells being best poised to initiate T cell signaling upon encounter with cognate pMHC.

In vivo memory AT T cells have different phenotypes depending on the compartment

We next sought to identify the activation requirements of *memory* cells by examining the phenotype and functional potential of OT1 cells 6 weeks after adoptive transfer into WT recipients and immunization with OVA. During antigen-driven expansion, CD8 cells rapidly proliferate and differentiate into early effector cells (EEC), which are low in expression for CD127 and KLRG1. Following expansion, the majority of effector cells, known as short-lived effector cells (SLEC) and characterized by $CD127^{lo}$, $KLRG1^{hi}$ phenotype die in huge numbers via apoptosis (132, 133, 134). This is termed the contraction phase of the immune response, in which surviving cells are known as memory precursor effector cells (MPECs) and express $CD127^{hi}$, $KLRG1^{lo}$. MPECs then eventually differentiate into one of two populations: central memory cells (T_{CM}), which are CCR7+ $CD62L^{hi}$ are poised to drive cell division and promote survival (135, 136). By contrast, effector memory cells (T_{EM}), defined as CCR7-, $CD62L^{lo}$, demonstrate increased effector function (136). In one study it was shown that T_{CM} conferred superior antitumor immunity compared with T_{EM} in a B16 murine melanoma model (137). Our understanding of how these memory populations arise is limited (138). Suffice it to say, we used these markers as a phenotypic panel to ensure that the T cells produced by the vaccination scheme were memory cells.

Briefly, to generate memory cells, WT mice were injected with 5e6 AT OT1 cells, rested then vaccinated with 3.4mg LPS/OVA much like previous vaccination schedules. Eye bleeds were performed at 2-week intervals to evaluate the expansion. One week later, the mice were boosted (week 0) with LPS/OVA according to the previous schedule. Eye bleeds at that time revealed a CD45.2+ AT population that had expanded to 3-4% of PBL, and 12-15% of the CD8+ population in PBL. It was difficult to characterize the AT cells phenotypically by the memory markers, as they did not fit the "classic" EEC and did not express $KLRG1^{lo}$, $CD127^{lo}$ (**Figure 13A**). This fit in with what is known about activated and expanding T cells and their heterogeneous expression of memory markers (139). Two weeks after the boost (week 2), another eye

www.manaraa.com

bleed was performed which showed some contraction of the CD45.2+ AT population to 2-2.5% of PBL. Phenotypically, cells showed more EEC phenotype, as seen by downregulated expression of CD127 and KLRG (**Figure 13B**). Additionally, a majority had shed CD62L. CD44 expression was not increased (data not shown). On week 4, mice were bled again and the CD45.2+ AT population had further contracted to 0.5-1% of PBL. Phenotypic expression was similar to week 2 (**Figure 13C**). On week 7, the experiment was terminated and PBL, SPL, and LN cells obtained (**Figure 13D**). LN were purified by CD45.2 negative selection, whereas SPL were purified by sequential CD45.2 then CD8 negative selection. PBL were left unpurified. Phenotypic analysis revealed that PBL OT1 cells had become MPEC ($CD127^{hi}$ $KLRG1^{lo}$) and SLEC ($CD127^{lo}$ $KLRG1^{hi}$) cells, whereas OT1 splenocytes and lymph node cells remained EEC ($CD127^{lo}$ $KLRG1^{lo}$). We were somewhat surprised by this result in LN, as we expected secondary lymphoid tissues to exhibit preferential localization of MPECs over the spleen, an observation reported by others (140). Functional analysis of the different compartments showed that ACF could only be detected in the PBL, and not in any of the EEC cells from the SPL or LN (**Figure 13E**). Indeed, quite surprisingly, calcium flux in splenocytes pulsed with EIINFEKL-loaded (nonspecific peptide) DC was *higher* than the SIINFEKL-loaded (specific peptide) group. It's possible that activation-induced cell death underlies these findings (141), but this experiment clearly must be repeated before any conclusions are drawn. In addition, we unfortunately did not have enough splenocytes to stimulate the splenocytes with anti-CD3 antibody as a positive control.

DISCUSSION

In the first part of this project, we developed a model for expanding freshly isolated naïve human T cells using 3 different APC, and in the case of PPM and UM, without the addition of artificial cytokines. We observed a high degree of variability in this system, which was similar to that reported by others (131, 142). However, our study is unique in two aspects. Firstly, we have demonstrated for the first time that PPM are non-inferior by functional analysis to FastDC and PBMC. Others have used macrophages (143) and B cells (144) in MART-1 specific immune responses, but to our knowledge, no study has shown PPM capable of expanding naïve human T cells.

www.manaraa.com

Secondly, unlike the most recent MART expansion study by Wolfl and Greenberg (131), we used the MART-1 25 amino-acid long peptide, and not the $MART1_{26-35}$ SP used in their expansions. We felt the LP was advantageous for our purposes in two major respects: 1) the 25-amino acid peptide requires internalization, processing, and presentation by APC, thereby making it more physiologic; and, 2) the LP contained binding sequences for presentation by both MHC class I and II, allowing the study of both CD8 and CD4 cells. However, MART LP may have been taken up and processed variably between duplicates and between donors. Another explanation for why variability exists may be that certain donors may be HLA-A*0201 homozygous or may have a polymorphism with enhanced MART-1 epitope binding capability, as suggested by Wolfl and Greenberg (131).

Previous expansions with MART-1 LP have been reported but the coefficients of variance in these experiments were not disclosed (80). In Faure et al.'s study, the authors showed that long-peptide (LP)-loaded DC required longer co-culture periods to expand naïve T cells as compared with short peptide (SP). Curiously, these authors report that while mature DC present SP more efficiently than immature DC, the results appeared reversed when LP was used. We also observed similar differences in our own experiments (results not shown). Results like these give one pause and serve as a reminder that a peptide or whole protein does not substitute for a whole tumor cell being phagocytosed. In other words, some observations from experiments using peptides as sources of antigen may not make inherent biological sense. As such, it is important to evolve from peptide experiments to using whole tumors. Our laboratory is currently initiating such experiments.

Comparing the average expansion in our hands using the LP with Chauvin et al. (in which authors use LP), we had arrived at average expansions of 8-10% compared with 2% on d13 in their experiments (86). However our COV, which was approximately 40%, was higher than the 10% reported by Wolfl and Greenberg (131) and might be due to our use of the long peptide contributing to a greater complexity in our experimental set-up. In fact, we calculated the COV among the LP expansions reported by Chauvin et al. (86), which was 65% by d13 of their expansion, compared to approximately 40% in our hands. Our study therefore was the first of its kind to elaborate significant expansions using PPM, the LP, and introduce the lowest reported COV in the system.

www.manaraa.com

Focusing on variability among our PPM, population, we considered the considerable complexities of the plate passage process itself. Since monocyte activation relies on the activation of platelets, variability among donors may be linked to the variability in *baseline* platelet activation status. We began investigating this, and showed that resting human platelets are variably activated, and respond variably to adhesion onto a polystyrene surface, similar to a flow chamber (data not shown). We also began to show that enhanced pre-activation of platelets using a platelet activator, thrombin, allowed maximal platelet activation and potentially improved the functional capability of PPM in co-culture experiments (data not shown).

The data shown in Figure 5 suggest that the presence of CD4 cells may have assisted in the expansion of CD8 cells, however, the differences did not reach statistical significance. This may be a result of the specific *in vitro* co-culture conditions (e.g. the particular ratios of APC:CD8:CD4 cells employed, but in fact, little is known about CD4 responses in cancer patients. In a trial of melanoma patients immunized with MHC Class I and II epitopes, no significant benefit was derived from immunization with Class II peptides (145). In another trial, modest Th1/Th2 responses were induced in a small number of immunized patients (146). More studies are needed to unpack the role of helper T cells in the expansion of anti-tumor CD8+ T cells.

The conclusions from this part of the study are several-fold: 1) artificial cytokines may not be necessary for the generation of functional responses; 2) different donors respond differently to co-culture studies, and results are difficult to duplicate with any precision; and, 3) the current laboratory model of ECP does not confer functional advantage to the PPM compared with UM and DC. The latter two conclusions may be related, and may be explained by the observation that, at the end of the procedure, millions of monocytes remain adherent to the ECP device even after the device is washed. We believe these adherent monocytes may, in fact, be more potent APC than their counterparts that are washed off, since they are most likely to have formed strong platelet interactions, as described in **Figure 2B**. Our group is currently pursuing strategies for removing these adherent monocytes to use in co-culture experiments. Ultimately, further optimization of the ECP conditions is needed in order to extend its applicability to cancer types that have shown response to other immunotherapies, such as melanoma and renal cell carcinoma.

www.manaraa.com

In the second part of the project, we sought to develop an assay that would track early T cell signals (via calcium flux) in an antigen-specific manner. The usefulness and broad applicability of a technique such as the one we propose is that it could potentially capture all polyclonal responses to a broad variety of known and unknown TAAs. As such, it would capture responses to neoantigens as well as overexpressed self-antigens, however rare or frequent those responses. Because of the complexity of a multi-antigen tumor model, we focused initially on a single-antigen, transgenic system from which we hope to ultimately develop a multi-antigen tumor model. Additionally, through direct comparison of TCR transgenic cells of the same number and specificity, we were able to avoid the ambiguities brought on by inconsistent precursor frequencies. Initially, we could not detect ASF in our system. We made two modifications in our system that have been reported by others. The first was to track ASC by surface labeling T cells and DC separately with anti-CD8 and anti-CD11c flourochrome-conjugated antibodies (147). The next modification was to facilitate DC/ T cell encounter by centrifuging the sample to drive T/ DC contacts and initiate T cell activation, as proposed by others (130). In doing so, we were able to detect ASC formation and within that population, we demonstrated ASF in a naïve, single-antigen, murine system (OT1) as well as a single-antigen, transduced human model (DMF5).

Next we addressed the detection limits of our system by varying the peptide-loading concentration and by diluting our responding T cells in a pool of WT, non-responding cells. By doing so, we showed that ASF disappeared, by peptide loading concentration at the order of 10^{-3}uM in OT1 and DMF5 cells, and by dilution at the order of 0.1% in OT1 cells and 1% in DMF5 cells. These conclusions were made by visual evaluation of the antigen-specific and non-specific calcium flux curves. We are also currently testing a Random Forest in order to describe an algorithm that would utilize the parameters of the calcium flux curves and predict whether ASF is present or not.

Lastly, we were interested in the activation ability of antigen-experienced and memory cells compared with naïve cells. We observed lower calcium flux intensity in *in vitro* pre-activated T cells in both OT1 and DMF5 systems. However, we also recognized that *in vitro* models were different from *in vivo* counterparts. For instance, it has been shown that *in vitro* produced memory T cells do not require co-stimulatory signals to initiate activation and recall expansion (148, 149), whereas *in vivo* memory cells do (150, 151). Therefore, we next turned to an *in vivo* antigen-experienced model. We showed that even

www.manaraa.com

within the first week of an expansion, both AT and WT endogenous antigen-specific T cells had expanded and displayed activation markers such as increase in CD44 expression and shedding of CD62L. We were surprised to see that activation in the endogenous population in Vax WT was higher than in the AT population in Vax+AT WT. This suggested a difference between a transgenic T cell and a naturally occurring endogenous counterpart. Alternatively, this observation is consistent with the possibility that the number of the starting population of responding cells influenced the response. In fact, others have shown that the number of transgenic T cells used in adoptive transfer studies can affect phenotype and kinetics of responding cells (70, 152, 153). These authors showed that higher transfer numbers resulted in reduced expansion following vaccination. We were not able to test this hypothesis, as it was outside the scope of this work.

The second surprising result was that OT1 mice were relatively anergic to direct immunization. We had expected that since OT1 mice are antigen-naïve, they would respond classically to a primary antigen encounter by becoming activated, rather than appearing anergic. It is possible that since *all* CD8 T cells in an OT1 mouse were capable of responding to antigen, this resulted in competition over costimulatory molecules and cytokines. Competition has been proposed to act as a deterrent for immune activation. This is based on experiments in the OT1 system in which lymphopenic hosts developed autoimmune, inflammatory responses, whereas lymphocompetent hosts developed anergy (154). Perhaps the OT1 mouse was overwhelmed by "competition" over peptide-MHC and this resulted in anergy towards the OVA antigen.

Because of the inability to generate functional effector cells in a naïve, transgenic animal, we then turned our focus to studying the memory population that forms after a primary expansion in a wild-type mouse. We chose the Vax+AT WT model over the Vax WT model because of the higher starting numbers of responding cells. By transferring a starting population, we would increase the absolute number of cells in the contraction phase, thereby affording enough cell numbers to proceed with the experiment. Tracking of the PBL population by phenotype assured that we obtained an expansion and that AT cells contracted within 2 weeks following the boost. Surprisingly, although purified SPL, purified LN, and unpurified PBL were 36%, 6% and 1% CD45.2+ positive, we could only detect ASF in the PBL population. The caveat to our interpretation of these results is that we do not have information about the SPL and LN expansion and

www.manaraa.com

contraction phases prior to week 7. Future experiments will address this. These results are not, however, surprising as others have shown that memory T cells have *reduced* activation capability following antigen-specific stimulation from BMDC (155), as well as other APC sources (156), possibly due to decreased surface TCR expression or increased protein tyrosine phosphatases as compared with their naïve counterparts.

Ultimately, we hope to apply this concept of early T cell signaling as a method for tracking antigen-specific T cell responses using nanodevices, such as nano-wires that are able to sense changes in proton flux (157). Proton flux is a well-recognized early event in the signaling of a T cell (158), and our collaborating laboratory (Dr. Tarek Fahmy) has shown that nano-wires can be used to track the signals produced by OT1 cells when they contact antigen-specific peptide-MHC dimmers (159). Additionally, proton flux and calcium flux in activated T cells have been correlated by others by others (160, 161). We hope to use our DC/T cell conjugate assay to detect T cell proton flux when T cells make antigen-specific contacts with DC. To arrive at T/DC conjugates, we aim to use label-free separation techniques based on conjugate size using existing technology known as dielectrophoretic field-flow fractionation, which we are in the midst of developing (162).

Although our measurement of early T cell activation responses to date have been applied only to defined single antigens, its advantage lies in its potential to monitor T cell stimulation of polyclonal populations responding to undefined antigens from complex sources, such as tumors. Currently available T cell monitoring reagents, particularly multimeric MHC/peptide complexes such as tetramers or dextramers, are limited in quantitating T cell responses against single disease-associated antigen (per reaction), and only after relevant MHC class I- and/or class II-restricted epitopes have been characterized. This makes these reagents expensive and restricts T cell monitoring to a limited group of epitopes currently associated with a particular infectious or disease state.

Additionally, in disease states where the antigen pool is potentially vast and unknown, including cancer and autoimmune diseases, the “ultimate” device could be used to identify panels of potential antigens tailored to the T cell repertoire of the patient. For instance, if no tumor material was available to provide a “personalized” set of tumor-associated protein from a patient, panels of known tumor-associated proteins could be fed to autologous APC (and exposed to autologous T cell populations) as an alternative

www.manaraa.com

antigen source. Utilizing the nanosensors as a direct readout of activation of existing anti-tumor T cell precursors already present in patient blood, individualized antigen groups most likely to initiate potent T cell responses following vaccination could be identified prior to the initiation of therapy.

Lastly, the sensor could also be applied to multiple host/donor-specific antigens potentially targeted by recipient or donor T cells following organ transplant or bone marrow allograft of foreign tissue. It could be used to calculate pre-transplant probability of organ rejection and could be incorporated into the matching algorithm used by the United Network for Organ Sharing (UNOS). The device would also be useful to make quantitative determinations of the progress of treatments initiated to down-regulate T cell responses, in organ transplant settings, but also in the case of autoimmune diseases. These include cell-based therapies, such as DC therapy with "tolerogenic" DC as well as the systemic use of tolerogenic drugs or other agents. Patient-derived T cell populations could be removed during such therapies and T cell responses evaluated in vitro or ex vivo and compared as a measure of treatment efficacy.

In short, this body of work hopes to have humbly contributed to an exciting field of cancer immunotherapy. Through our laboratory model of plate-passage, we have developed a functional assay for the evaluation and optimization of APC and T cells. We have also shown that it is possible to utilize early T cell signals, including-but not limited to- calcium flux, to track the evolution of the antigen-specific response.

www.manaraa.com

REFERENCES

1. Burnet FM. Immunological aspects of malignant disease. *Lancet* 1967;1(7501):1171-74.
2. Burnet FM. The concept of immunological surveillance. *Prog Exp Tumor Res* 1970;13:1-27.
3. Thomas L. On immunosurveillance in human cancer. *Yale J Biol Med*. 1982;55:329-33.
4. Virchow R. Cellular pathology as based upon physiological and pathological histology. Philadelphia: J. B. Lippincott; 1863.
5. Mellman I, Coukos G, Dranoff G. Cancer Immunotherapy comes of age. *Nature* 2014;480(7378): 480-89.
6. Matsushita H, Vesely MD, Koboldt DC, Rickert CG, Uppaluri R, et al. Cancer exome analysis reveals a T-cell-dependent mechanism of cancer immunoediting. Nature 2012;482:400-404.
7. Tran E, Turcotte S, Gros A, et al. Cancer immunotherapy based on mutation-specific CD4+ T cells in a patient with epithelial cancer. Science 2014;344:641-645
8. van Rooij N, van Buuren MM, Philips D, et al. Tumor exome analysis reveals neoantigen-specific T-cell reactivity in an ipilimumab-responsive melanoma. J Clin Oncol 2013;31:e439-e442.
9. Lennerz V, Fatho M, Gentilini C, Frye RA, Lifke A, Ferel D, et al. The response of autologous T cells to a human melanoma is dominated by mutated neoantigens. Proc Natl Acad Sci USA 2005;102:16013–8.
10. Kenter GG, Welters MJ, Valentijn AR, Lowik MJ, Berends-van der Meer DM, et al. Vaccination against HPV-16 oncoproteins for vulvar intraepithelial neoplasia. *N. Engl J Med* 2009;361:1838–1847.
11. Kantoff PW, Higano CS, Shore ND, Berger ER, Small EJ, et al. Sipuleucel-T immunotherapy for castration-resistant prostate cancer. *N Engl J Med* 2010;363:411–422.
12. Hodi FS, Butler M, Oble DA, Seiden MV, Haluska FG, et al. Immunologic andclinical effects of antibody blockade of cytotoxic T lymphocyte-associated antigen 4 in previously vaccinated cancer patients. *PNAS* 2008;105:3005–3010.
13. Rosenberg SA, Sherry RM, Morton KE, Scharfman WJ, Yang JC, et al. Tumor progression can occur despite the induction of very high levels of self/tumor antigen-specific CD8+ T cells in patients with melanoma. *J Immunol* 2005;175, 6169–6176.
14. Dudley ME, Wunderlich JR, Robbins PF, Yang JC, Hwu P, et al. Cancer regression and autoimmunity in patients after clonal repopulation with antitumor lymphocytes. *Science* 2002;298, 850–854.
15. Rosenberg RA, Restifo NP, Yang JC, Morgan RA, Dudley ME. Adoptive cell transfer: a clinical path to effective cancer immunotherapy. *Nature Rev. Cancer* 2008;8, 299–308.
16. Wrzesiniski C, Paulos CM, Gattinoni L, Palmer DC, Kaiser A, et al. Hematopoietic stem cells promote the expansion and function of adoptively transferred antitumor CD8 T cells. *J. Clin. Invest* 2007;117:492–501.
17. Kalos M, Levine BL, Porter DL, Katz S, Grupp SA, et al. T cells with chimeric antigen receptors have potent antitumor effects and can establish memory in patients with advanced leukemia. *Sci. Transl. Med* 2011;3:95ra73.
18. Kvistborg P, Philips D, Kelderman S, Hageman L, Ottensmeier C, et al. Anti-CTLA-4 therapy broadens the melanoma-reactive CD8+ T cell response. *Sci Transl Med* 2014;6:254ra128-254ra128.
19. Ku GY, Yuan J, Page DB, Schroeder SE, Panageas KS, et al. Single-institution experience with ipilimumab in advanced melanoma patients in the compassionate use setting: lymphocyte count after 2 doses correlates with survival. *Cancer* 2010;116:1767-1775.
20. Ji RR, Chasalow SD, Wang L, Hamid O, Schmidt H, et al. An immune-active tumor microenvironment favors clinical response to ipilimumab. *Cancer Immunol Immunother* 2012;61:1019-1031.
21. Gajewski TF, Louahed J, Brichard VG. Gene signature in melanoma associated with clinical activity: a potential clue to unlock cancer immunotherapy. *Cancer* 2010;16:399-403.

www.manaraa.com

22. Snyder A, Makarov V, Merghoub T, Yuan J, Zaretsky JM, et al. Genetic basis for clinical response to CTLA-4 blockade in melanoma. *N Eng J Med* 2014;371:2189-2199.
23. Topalian SL, Hodi S, Brahmer JR, Gettiner SN, Smith DC, et al. Safety, activity, and immune correlates of anti-PD-1 antibody in cancer. *N Eng J Med* 2012;366:2443-2454.
24. Ali HR, Provenzano E, Dawson SJ, Blows FM, Liu B, et al. Association between CD8+ T-cell infiltration and breast cancer survival in 12 439 patients. *Ann Oncol*. 2014: 1536-1543.
25. Loi S, Michiels S, Salgado R, Sirtaine N, Jose V, Fumagalli D, et al. Tumor infiltrating lymphocytes are prognostic in triple negative breast cancer and predictive for trastuzumab benefit in early breast cancer: results from the FinHER trial *Ann Oncol*. 2014 25:1544-1550.
26. Di Caro G, Bergomas F, Grizzi F, Doni A, Bianchi P, et al. Occurrence of Tertiary Lymphoid Tissue Is Associated with T-Cell Infiltration and Predicts Better Prognosis in Early-Stage Colorectal Cancers. *Clin. Cancer Res*. 2014;15:2147-2158.
27. Wu X, Zou Y, He X, Yuan R, Chen Y, Lan N, et al. Tumor-Infiltrating Mast Cells in Colorectal Cancer as a Poor Prognostic Factor. *Int J Surg Pathol.* 2013: 111-120.
28. Galon J, Costes A, Sanchez-Cabo F, Kirilovsky A, Mlecnik B, et al. Type, density and location of immune cells within human colorectal tumors predict clinical outcome. *Science* 2006;313(5796):1960-1964.
29. Lodge PA, Jones LA, Bader RA, Murphy GP, Salgaller ML. Dendritic cell-based immunotherapy of prostate cancer: immune monitoring of phase II clinical trial. *Cancer Res* 2000;60:829.
30. Edelson RL, Berger C, Gasparro F, Jegasothy B, Heald P, et al., Treatment of cutaneous T-cell lymphoma by extracorporeal photochemotherapy. Preliminary results. *N Eng J Med* 1987;316(6):297-303.
31. Heald P, Rok A, Perez M, Wintroub B, Knobler R, et al. Treatment of erythrodermic cutaneous T-cell lymphoma with extracorporeal photochemotherapy. *J Amer Acad Dermatol* 1992;17:427–33.
32. Lin WM, Lewis JM, Filler RB, Modi BG, Carlson KR, et al. Characterization of the DNA Copy-Number Genome in the Blood of Cutaneous T-Cell Lymphoma Patients. *J Inves Derm* 2012;132:188-197.
33. Girardi M, Heald PW. Cutaneous T-cell lymphoma and cutanesou graft-versus-host disease: two indications for photopheresis in dermatology. *Dermatologic Clinics* 2000;18(3):417-23.
34. Schechter GP, Sausville EA, Fischmann AB, Soehnlen F, Eddy J, et al. Evaluation of circulating malignant cells provides prognostic information in cutaneous T cell lymphoma. *Blood* 1987; 69:841–9.
35. Girardi M, Knobler R, Edelson RL. Selective immmunotherapy through extracorporeal photochemotherapy: yesterday, today, and tomorrow. *Hematol Oncol Clin N Am* 2003;17:1391-1403.
36. Greinix HT, Volc-Platzer B, Rabtsch W, Gmeinhart B, Guevara-Pineda C, et al. Successful use of extracorporeal photochemotherapy in the treatment of severe acute and chronic graft-versus-host disease. *Blood* 1998;92:3098–104.
37. Foss FM, DiVenuti GM, Chin K, Sprague K, Grodman H, et al. Prospective study of extracorporeal photopheresis in steroid-refractory or steroid-resistant extensive chronic graft-versus host disease: analysis of response and survival incorporating prognostic factors. *Bone Marrow Transplant.* 2005;35(12):1187-93.
38. Rook AH, Freundlich B, Jegasothy BV, Perez MI, Barr WG, Jimenez SA, et al. Treatment of systemic sclerosis with extracorporeal photochemotherapy - results of a multicenter trial. *Arch Dermatol*. 1992;128:337-e46.
39. Wolfe JT, Lessin SR, Singh AH, Rook AH. Review of immunomodulation by photopheresis: treatment of cutaneous T-cell lymphoma, autoimmune disease and allograft rejection. *Artif Organs*. 1994;18(12): 888-97.
40. Choy JC. Granzymes and perforin in solid organ transplant rejection. *Cell Death Differ*. 2010. 17(4): 567-76.
41. Stenger EO, Turnguist HR, Mapara MY, Thomson AW. Dendritic cells and regulation of graft-versus-host disease and graft-versus-leukemia activity. *Blood*. 2012. 119(22): 5088-5103.
42. Dall'Amico R, Montini G, Murer L, Andreetta B, Tursi V, et al. Benefits of photopheresis in the treatment of heart transplant patients with multiple/refractory rejection. *Transplant Proc.* 1997. 29(1-2): 609-11.

www.manaraa.com

43. Meiser BM, Kur F, Reichenspurner H, Wagner F, Boos KS, et al., Reduction of the incidence of rejection by adjunct immunosuppression with photochemotherapy after heart transplantation. *Transplantation*, 1994. 57(4):563-8.
44. Sunder-Plassman G, Druml W, Steininger R, Honigsmann H, Knobler R. Renal allograft rejection controlled by photopheresis. *Lancet*. 1995. 346(8973):506.
45. Salerno CT, Park SJ, Kreykes NS, Kulick DM, Savik K, et al., Adjuvant treatment of refractory lung transplant rejection with extracorporeal photopheresis. J *Thorac Cardiovasc Surg*. 1999. 117(6):1063-9.
46. Slovis BS, Loyd JE, King JH, Photopheresis for chronic rejection of lung allografts. *N Engl J Med*. 1995. 332(14):962.
47. Barr ML, Meiser BM, Eisen HJ, Roberts RF, Livi U, et al., Photopheresis for the prevention of rejection in cardiac transplantation. *N Engl J Med*, 1998. 339(24):1744-51.
48. Barr ML, Baker CJ, Schenkel FA, McLaughlin SN, Stouch BC, et al., Prophylactic photopheresis and chronic rejection: Effects on graft intimal hyperplasia in cardiac transplantation. *Clin Transplant*, 2000. 14(2):162-6.
49. McKenna KE, Whittaker S, Rhodes LE, Taylor P, Lloyd J, et al., Evidence-based practice of photopheresis. *Brit J Dermatol*. 2006. 154(1):7–20.
50. Shlomchik WD. Graft-versus-host disease. *Nat Rev Immunol.* 2007. 7(5):340-52.
51. Marques MB, Tuncer HH. Photopheresis in solid organ transplant rejection. *J Clin Apher*. 2006. 21(1): 72-7.
52. Marshall SR. Technology insight: ECP for the treatment of GvHD—can we offer selective immune control without generalized immunosuppression? *Nat Clin Pract Oncol*. 2006. 3(6):302-14.
53. Balagula Y, Taube JM, Wang T, Dorafshar AH, Sweren RJ. Regression of cutaneous invasive squamous cell carcinoma in a patient with graft-versus-host disease. *Dermatol Online J.* 2014;20(5):22614.
54. Durazzo TS, Tigelaar RE, Filler R, Hayday A, Girardi M, Edelson RL. Induction of monocyte-to-dendritic cell maturation by extracorporeal photochemotherapy: initiation via direct platelet signaling. *Transf and Apheresis Sc.* 2014;50(3):370-78.
55. Gonzalez AI, Berger CL, Remington J, Girardi M, Tigelaar RE, Edelson RL. Integrin-driven monocyte to dendritic cell conversion in modified extracorporeal photochemotherapy. *Clin and Exp Immunology.* 2013;175:449-457.
56. Stephen J, Emerson B, Fox KAA, Dransfield I. The uncoupling of monocyte-platelet interactions fro mthe induction of proinflammatory signaling in monocytes. *J Immunol.* 2013;191:1-7.
57. Suzuki J, Hamada E, Shodai T, Kamoshida G, Kudo S, et al. Cytokine secretion from human monocytes potentiated by P-selectin-mediated cell adhesion. *Int Archives All Immunol* 2013;160:152-60.
58. Berger C, Hoffmann K, Vasquez JG, Mane S, Lewis J, et al., Rapid generation of maturationally synchronized human dendritic cells: contribution to the clinical efficacy of extracorporeal photochemotherapy. *Blood.* 2010. 116(23):4838-47.
59. Futterleib JS, Feng H, Tigelaar RE, Choi J, Edelson RL. Activation of GILZ gene by photoactivated 8-methoxypsoralen: potential role of immunoregulatory dendritic cells in extracorporeal photochemotherapy. *Transfus Apher Sci*. 2014;50(3):379-87.
60. de Saint-Vis B, Vincent J, Vandenabeele S, Vanbervliet B, Pin JJ, Ait-Yahia S, et al. A novel lysosome-associated membrane glycoprotein, DC-LAMP, induced upon DC maturation, is transiently expressed in MHC class II compartment. *Immunity.* 1998;9:325-36.
61. Lamioni A, Parisi F, Isacchi G, Giorda E, Di CeSare S, et al., The immunological effects of extracorporeal photopheresis unraveled: Induction of tolerogenic dendritic cells in vitro and regulatory T cells in vivo. *Transplantation.* 2005. 79(7):846-50.
62. Berger CL, Xu AL, Hanlon D, Girardi M, Edelson R. Induction of human tumor-loaded dendritic cells. *Int J Cancer*. 2001;91:438– 47.
63. Banchereau J, Briere F, Caux C, Davoust J, Lebecque S, et al. Immunobiology of dendritic cells. *Annu Rev Immunol*. 2000;18(1):767-811.
64. Edelson RL. Mechanistic insights into extracorporeal photochemotherapy: efficient induction of monocyte-to-dendritic cell maturation. *Trans Apher Sci* 2014;50(3):32209.

www.manaraa.com

65. Girardi M, Schechner J, Glusac E, Berger C, Edelson R. Transimmunization and the evolution of extracorporeal photochemotherapy. *Trans Apher Sci* 2002;26:181-190.
66. Heald PW, Perez MI, Christensen I, Dobbs N, McKiernan G, Edelson R. Photopheresis therapy of cutaneous T-cell lymphoma: the Yale-New Haven Hospital Experience. *Yale J Biol Med* 1989;62:629– 38.
67. Koh HK, Davis BE, Meola T, Lim HW. Extracorporeal photopheresis for the treatment of 34 patients with cutaneous T-cell lymphoma (CTCL). *Soc Invest Dermatol.* 1994;2(4):260.
68. Vonderheid EC, Zhang Q, Lessin SR, Polansky M, Abrams JT, Bigler RD, et al. Use of serum soluble interleukin-2 receptor levels to monitor the progression of cutaneous T-cell lymphoma. *J Am Acad Dermatol* 1998;38:207– 20.
69. Rook AH, Suchin KR, Kao DM, Yoo EK, Macey WH, DeNardo BJ, et al. Photopheresis: clinical applications and mechanism of action. *J Investig Dermatol Symp Proc.* 1999;4:85– 90.
70. Badovinac V, Haring J, Harty J. Initial T cell receptor transgenic cell precursor frequency dictates critical aspects of the CD8+ T cell responses to infection. *Immunity* 2007;26(6):827-41.
71. Blattman JN, Antia R, Sourdive DJ, Wang X, Kaech SM, et al. Estimating the precursor frequency of naïve antigen-specific CD8 T cells. *J Exp Med* 2002;195(5):657-664.
72. Sllusto F, Geginat J, Lanzavecchia A. Central and memory effector memory T cell subsets: function, generation, and maintenance. *Annu Rev Immunol.* 2004;22(1):745-63.
73. Alanio C, Lemaitre F, Law HK, Hasan M, Albert ML. Enumeration of human antigen-specific naïve CD8+ T cells reveals conserved precursor frequencies. *Blood.* 2010;115(18):3718-3725.
74. Coulie PG, Brichard V, Van Pel A, Wolfel T, Schneider J, et al. A new gene coding for a differentiation antigen recognized by autologous cytolytic T lymphocytes on HLA-A2 melanomas. *J Exp Med* 1994;180:35-42.
75. Kawakami Y, Eliyahu S, Delgado CH, Robbins PF, Sakaguchi K, et al. Cloning of the gene coding for a shared human melanoma antigen recognized by autologous T cells infiltrating into tumor. *PNAS* 1994;91:3515-19.
76. Romero P, Valmoro D, Pittet MJ, Zippelius A, Rimoldi D, et al. Antigenicity and immunogenicity of Melan-A/MART-1 derived peptides as targets for tumor reactive CTL in human melanoma. *Immunol Reviews.* 2002;188:81-96.
77. De Maziere AM, Muehlethaler K, van Donselaar E, Salvi S Davoust J, et al. The melanocytic protein Melan-A/MART-1 has a subcellular localization distinct from typical melanosomal proteins. *Traffic* 2002;3:678-93.
78. Rimoldi D, Muehlethaler K, Salvi S, Valmori D, Romero P, et al. Subcellular localization of the melanoma-associated protein Melan-A/MART-1 influences the processing of its HLA-A2-restricted epitope. *J Biol Chem* 2001;276:43189-96.
79. Wolfel T, Van Pel A, Crichard V, Schneiter J, Seliger B, et al. Two tyrosinase nonapeptides recognized on HLA-A2 melanomas by autologous cytolytic T lymphocytes. *Eur J Immunol.* 1994;24:759-64.
80. Faure FA, Mantegazza C, Sadaka C, Sedlik F, Amigorena S. Long-lasting cross-presentation of tumor antigen in human DC. *Eur. J. Immunol*. 2009;39: 380–390.
81. Slingluff CL Jr, Petroni GR, Olson W, Czarkowski A, Grosh WW, et al. Helper T-cell responses and clinical activity of a melanoma vaccine with multiple peptides from MAGE and melanocytic differentiation antigens. *J Clin Oncol.* 2008;26:4973–80.
82. Schadendorf D, Ugurel S, Schuler-Thurner B, Nestle FO, Enk A, et al. DC study group of the DeCOG: Dacarbazine (DTIC) versus vaccination with autologous peptide-pulsed dendritic cells (DC) in first-line treatment of patients with metastatic melanoma: a randomized phase III trial of the DC study group of the DeCOG. *Ann Oncol* 2006;17:563–570.
83. Ribas A, Comin-Anduix B, Chmielowski B, Jalil J, de la Rocha P, et al. Dendritic cell vaccination combined with CTLA-4 blockade in patients with metastatic melanoma. *Clin Cancer Res.* 2009;15:6267–76.
84. Speiser DE, Pittet MJ, Guillaume P, Lubenow N, Hoffman E, et al. Ex vivo analysis of human antigen-specific CD8+ T-cell responses: quality assessment of fluorescent HLA-A2 multimer and interferon-gamma ELISPOT assays for patient immune monitoring. *J Immunother* 2004;27:298–308.

www.manaraa.com

85. Bijker MS, van den Eeden SJ, Franken KL, Melief CJ, van der Burg SH, et al. Superior induction of anti-tumor CTL immunity by extended peptide vaccines involves prolonged, DC-focused antigen presentation. *Eur. J. Immunol*. 2008. 38:1033–1042.
86. Chauvin JM, Larrieu P, Sarrabayrouse G, Prevost-Blondel A, Lengagne R, et al. HLA anchor optimization of the Melan-A-HLA-A2 epitope within a long peptide is required for efficient cross-priming of human tumor-reactive T cells. *J Immunol* 2012, 188:2102-2110.
87. Chen JL, Stewart-Jones G, Bossi G, Lissin NM, Wooldridge L, et al. Structural and kinetic basis for heightened immunogenicity of T cell vaccines. *J. Exp. Med*. 2005;201:1243–55.
88. Rosenberg SA, Yang JC, Restifo NP. Cancer immunotherapy: moving beyond current vaccines. *Nat. Med.* 2004;10: 909–915.
89. Bioley G, Jandus C, Tuyaerts S, Rimoldi D, Kwok WW, et al. MelanA/MART-1-specific CD4 T cells in melanoma patients: identification of new epitopes and ex vivo visualization of specific T cells by MHC class II tetramers. *J Immunol* 2006;177:6769-6779.
90. Rocha B, Tanchot C. Towards a cellular definition of CD8 T-cell memory: the role of CD4 T-cell help in CD8 T-cell responses. *Curr. Opin. Immunol*. 2004;16: 259–263.
91. Janssen EM, Lemmens EE, Wolfe T, Christen U, von Herrath MG, et al. CD4 T cells are required for secondary expansion and memory in CD8 T lymphocytes. *Nature*. 2003;421: 852–856.
92. Marzo AL, Kinnear BF, Lake RA, Frelinger JJ, Collins EJ, et al. Tumor-specific CD4 T cells have a major "post-licensing" role in CTL mediated anti-tumor immunity. *J Immunol.* 2000. 165:6047–6055.
93. Jandus C, Bioley G, Dojcinovic D, Derre L, Baitsch L, et al. Tumor antigen-specific Foxp3+ CD4 T cells identified in metastatic melanoma: peptide vaccination results in selective expansion of Th1-like counterparts. *Cancer Res.* 2009;69(20):8085-8093.
94. Ray S, Chhabra A, Chakraborty NG, Hegde U, Dorsky DI, et al. MHC-I-restricted melanoma antigen specific TCR-engineered human CD4+ T cells exhibit multifunctional effector and helper responses, in vitro. *Clin Immunol* 2010;136:338-47.
95. Dillman RO, Fogel GB, Cornforth AN, Selvan SR, Schiltz PM, et al.: Features associated with survival in metastatic melanoma patients treated with patient-specific dendritic cell vaccines. Cancer biother Radiopharm. 2011;26:407-15.
96. Fox BA, Schendel DJ, Butterfield LH, Aamdal S, Allison JP, et al. Defining the critical hurdles in cancer immunotherapy. *J Transl Med*. 2011;14;9:214.
97. Finke LH, Wentworth K, Blumenstein B, Rudolph NS, Levitsky H, et al. Lessons from randomized phase III studies with active cancer immunotherapies-outcomes from the 2006 meeting of the Cancer Vaccine Consortium (CVC). *Vaccine* 2007, 25:B97-B109.
98. Hoos A. Proposal of a clinical development paradigm for cancer immunotherapy: novel endpoints. In: *Endpoints for Immunotherapy Studies: Design and Regulatory Implications, American Society of Clinical Oncology (ASCO) Annual Meeting*; June 2, 2008; Chicago, IL.
99. Fine GD. Consequences of delayed treatment effects on analysis of time-to-event endpoints. *Drug Inf J*. 2007;41:535–539.
100. Hamid O, Urba WJ, Yellin M, Nichol GM, Weber J, et al. Kinetics of response to ipilimumab (MDX-010) in patients with stage III/IV melanoma. *J Clin Oncol* 2007;25(18):8525.
101. Weber JS, O'Day S, Urba W, Powderly J, Nichol G, et al. Phase I/II study of ipilimumab for patients with metastatic melanoma. *J Clin Oncol* 2006;26(36):5950-6.
102. Wolchok JD, Hoos A, O'Day S, Weber JS, Hamid O, et al. Guidelines for the Evaluation of Immune Therapy Activity in Solid Tumors: Immune-Related Response Criteria. *Clin Cancer Res* 2009;15(23):7412-7420.
103. Hoos A, Britten CM, Huber C, O'Donnell-Tormey. A methodological framework to enhance the clinical success of cancer immunotherapy. *Nat biotech* 2011;29(10):867-70.
104. Robert C, Long GV, Brady B, Dutriaux C, Maio M, et al. Nivolumab in Previously Untreated Melanoma without BRAF Mutation. *NEJM* 2015;372(4):320-30.
105. Keilholz U, Weber J, Finke JH, Gabrilovich DI, Kast WM, et al. Immunologic Monitoring of Cancer Vaccine Therapy: Results of a Workshop Sponsored by the Society for Biological Therapy. *J of Immunother* 2;25(2):97–138.
106. Sharma P, Wagner K, Wolchok JD, Allison JP. Novel cancer immunotherapy agents with survival benefit: recent successes and next steps. *Nature Reviews Cancer* 2011;11:805-812

www.manaraa.com

107. Iinuma T, Homma S, Noda T, Kufe D, Ohno T, et al. Prevention of gastrointestinal tumors based on adenomatous polyposis coli gene mutation by dendritic cell vaccine. *J of Clin Invest* 2004;113(9):1307–17.
108. Kaplan DH, Shankaran V, Dighe AS, Stockert E, Aquet M, et al. Demonstration of an interferon γ-dependent tumor surveillance system in immunocompetent mice. *PNAS* 1998;95(13):7556–61.
109. Dunn GP, Sheehan KC, Old L, Schreiber RD. IFN unresponsiveness in LNCaP cells due to the lack of JAK1 gene expression. *Cancer Res.* 2005;65(8):3447–3453.
110. Kirkwood JM, Lee S, Moschos SJ, Albertini MR, Michalak JC, et al. Immunogenicity and antitumor effects of vaccination with peptide vaccine +/− granulocyte-monocyte colony-stimulating factor and/or IFNα2b in advanced metastatic melanoma: Eastern Cooperative Oncology Group Phase II Trial E1696. *Clin Cancer Res*. 2009;15(4):1443–1451.
111. Britten CM, Janetzki S, van der Burg SH, Gouttefangeas C, Hoos, A. Toward the harmonization of immune monitoring in clinical trials: quo vadis? *Cancer Immunol Immunother.* 2008;57(3):285–88.
112. Janetzki S, Britten CM, Kalos M, Levitsky HI, Maecker HT, et al. "MIATA"-minimal information about T cell assays. *Immunity*. 2009;31(4):527–28.
113. Janetzki S, Cox JH, Oden N, Ferrari G. Standardization and validation issues of the ELISPOT assay. Methods Mol. Biol. 2005;302:51–86.
114. Janetzki S, Panageas KS, Ben-Porat L, Boyer J, Britten CM, et al. Results and harmonization guidelines from two large-scale international Elispot proficiency panels conducted by the Cancer Vaccine Consortium (CVC/SVI). *Cancer Immunol. Immunother*. 2008;57(3):303–315.
115. Moodie Z, Price L, Gouttefangeas C, Mander A, Janetzki S, et al. Response definition criteria for ELISPOT assays revisited. *Cancer Immunol. Immunother*. 2010;59(10):1489–1501.
116. Dustin ML. The immunological synapse. *Cancer Immunol Res* 2014;2(11):1023-1033.
117. Schmits R, Kundig TM, Baker DM, Shumaker G, Simard JJ, et al. LFA-1-deficient mice show normal CTL responses to virus but fail to reject immunogenic tumor. *J Exp Med*. 1996;183(4):1415–26.
118. Oh-hora M, Rao A. Calcium signaling in lymphocytes. *Curr Opin Immunol*. 2008;20(3):250-8.
119. Hogan PG, Chen L, Nardone J, Rao A. Transcriptional regulation by calcium, calcineurin, and NFAT. *Genes Dev* 2003;17(18):2205–32.
120. Macian F. NFAT proteins: key regulators of T-cell development and function. *Nat Rev Immunol*. 2005;5(6):472–484.
121. Le Deist F, Hivroz C, Partiseti M, Thomas C, Buc HA, et al. A primary T-cell immunodeficiency associated with defective transmembrane calcium influx. *Blood*, 1995;85(4):1053–1062.
122. Griffoen AW, Rijkers GT, Keij J, Zegers BJ. Measurement of cytoplasmic calcium in lymphocytes during flow cytometry. *J Immunol Methods* 1989;120(1):23-27.
123. Dissanayake D, Gronski MA, Lin A, Elford AR, Ohashi PS. Immunological perspective of self versus tumor antigens: insights from the RIP-gp model. *Immunol. Rev*. 2011;241(1):164–79.
124. Jensen ER, Shen H, Wettstein FO, Ahmed R, Miller JF. Recombinant *Listeria monocytogenes* as a live vaccine vehicle and a probe for studying cell-mediated immunity. *Immunol Rev.* 1997;158:147–57.
125. Ohlen C, Kalos M, Cheng LE, Shur AC, Hong DJ, et al. CD8+ T cell tolerance to a tumor-associated antigen is maintained at the level of expansion rather than effector function. *J Exp Med*. 2002;195(11):1407-18.
126. Kvistborg P, Boegh M, Pederson AW, Claesson MH, Zocca MB. Fast generation of dendritic cells. *Cell Immunol* 2009;260(1):56-62.
127. Yewdall AW, Drutman SB, Jinwala F, Bahjat KS, Bhardwaj N. CD8+ T cell priming by dendritic cell vaccines requires antigen transfer to endogenous antigen presenting cells. *PLOS One* 2010;5(6):1-10.
128. Johnson LA, Heemskerk B, Powell DJ Jr, Cohen CJ, Morgan RA, et al. Gene transfer of tumor-reactive TCR confers both high avidity and tumor reactivity to nonreactive peripheral blood mononuclear cells and tumor-infiltrating lymphocytes. *J Immunol*. 2006;177(9):6548-59.
129. Stipdonk MJB, Lemmens EE, Schoenberger SP. Naïve CTLs require a single, brief period of antigenic stimulation for clonal expansion and differentiation. *Nature Immunol.* 2001;2(5):423-29.
130. Irving M, Zoete V, Hebeisen M, Schmid D, Baumgartner P, et al. Interplay between T Cell Receptor Binding Kinetics and the Level of Cognate Peptide Presented by Major

www.manaraa.com

Histocompatibility Complexes Governs CD8 + T Cell Responsiveness. *J Biol Chem* 2012;287(27):23068-78.
131. Wolfl M, Greenberg PD. Antigen-specific activation and cytokine-facilitated expansion of naïve human CD8+ T cells. *Nature Protocols* 2014;9(4):950-66.
132. Joshi NS, Cui W, Chandele A, Lee HK, Urso DR, et al. Inflammation directs memory precursor and short-lived effector CD81 T cell fates via the graded expression of T-bet transcription factor. *Immunity* 2007; 27(2):281–95.
133. Kaech SM, Tan JT, Wherry EJ, Konieczny BT, Surh CD, et al. Selective expression of the interleukin 7 receptor identifies effector CD8 T cells that give rise to long-lived memory cells. *Nat Immunol* 2003;4(12): 1191–98.
134. Sarkar S, Kalia V, Haining WN, Konieczny BT, Subramaniam S, et al. Functional and genomic profiling of effector CD8 T cell subsets with distinct memory fates. *J Exp Med* 2008;205(3):625–640.
135. Sallusto F, Lenig D, Forster R, Lipp M, Lanzavecchia A. Two subsets of memory T lymphocytes with distinct homing potentials and effector functions. *Nature*. 1999;401(6754):708-12.
136. Schlub TE, Badovinac VP, Sabel JT, Harty JT, Davenport MP. Predicting CD62L expression during the CD8 T-cell response in vivo. *Immunol and Cell Biol* 2010;88(2):157-64.
137. Klebanoff CA, Gattinoni L, Torabi-Parizi P, Kerstann K, Cardones AR, et al. Central memory self/tumor-reactive CD8+ T cells confer superior antitumor immunity compared with effector memory T cells. *PNAS* 2005;102(27):9571-6.
138. Jenkins MR, Kedzierska K, Doherty PC, Turner SJ. Heterogeneity of effector phenotype for acute phase and memory influenza A virus-specific CTL. *J Immunol* 2007; 179(1):64–70.
139. Huster KM, Busch V, Schiemann M, Linkemann K, Kerksiek KM, Wagner H et al. Selective expression of IL-7 receptor on memory T cells identifies early CD40L-dependent generation of distinct CD81 memory T cell subsets. *PNAS* 2004;101(15):5610–15.
140. Yuzefpolskiy Y, Baumann FM, Kalia V, Sarkar S. Early CD8 T-cell memory precursors and terminal effectors exhibit equipotent in vivo degranulation. *Cell Mol Immunol* 2014 [ahead of print]. Doi: 10.1038/cmi.2014.48.
141. Arakaki R, Yamada A, Kudo Y, Hayashi Y, Ishimaru N. Mechanism of activation-induced cell death of T cells and regulation of FasL expression. *Crit Rev Immunol*. 2014;34(4):301-14.
142. Xu S, Koski GK, Faries M, Bedrosian I, Mick R, et al. Rapid high efficiency sensitization of CD8+ T cells to tumor antigens by dendritic cells leads to enhanced functional avidity and direct tumor recognition through an IL-12-dependent mechanism. *J. Immunol.* 2003;171(5):2251–61.
143. Barrio MM, Abes R, Colombo M, Pizzurro G, Boix C, et al. Human macrophages and dendritic cells can equally present MART-1 antigen to CD8+ T cells after phagocytosis of gamma-irradiated melanoma cells. *PLoS One* 2012;7(7):1-11.
144. von Bergwelt-Baildon MS, Vonderheide RH, Maecker B, Hirano N, Anderson KS, et al. Human primary and memory cytotoxic T lymphocyte responses are efficiently induced by means of CD40-activated B cells as antigen-presenting cells: potential for clinical application. *Blood* 2002;99(9):3319–25.
145. Phan GQ, Touloukian CE, Yang JC, et al. Immunization of patients with metastatic melanoma using both class I- and class II-restricted peptides from melanom-aassociated antigens. *J Immunother* 2003;26(4):349–56.
146. Wong R, Lau R, Chang J, Kuus-Reichel T, Brichard V, et al. Immune responses to a class II helper peptide epitope in patients with stage III/IV resected melanoma. *Clin Cancer Res* 2004;10(15):5004–13.
147. Yachi PP, Ampudia J, Zal T, Gascoigne NRJ. Altered peptide ligands induce delayed CD8-T cell receptor interaction–a role for CD8 in distinguishing antigen quality. *Immunity* 2006;25(2):203-11.
148. Flynn K, Mullbacher A. Memory alloreactive cytotoxic T cells do not require costimulation for activation in vitro. *Immunol. Cell Biol.* 1996;74(5):413–20.
149. Bachmann MF, Gallimore A, Linkert S, Cerundolo V, Lanzavecchia A, et al. Developmental regulation of Lck targeting to the CD8 coreceptor controls signaling in naive and memory T cells. *J. Exp. Med.* 1999;189(10):1521–30.
150. Boesteanu AC, Katsikis PD. Memory T cells need CD28 costimulation to remember. *Semin. Immunol.* 2009;21(2):69–77.

www.manaraa.com

151. Borowski AB, Boesteanu AC, Mueller YM, Carafides C, Topham DJ, et al. Memory CD8+ T cells require CD28 costimulation. *J. Immunol.* 2007;179(10):6494–6503.
152. Kemp RA, Powell TJ, Dwyer DW, Dutton RW. Cutting edge: regulation of CD8+ T cell effector population size. *J Immunol* 2004; 173(5): 2923–27.
153. Stock AT, Mueller SN, Kleinert LM, Heath WR, Carbone FR, et al. Optimization of TCR transgenic T cells for in vivo tracking of immune responses. *Immunol Cell Biol* 2007; 85(5):394–96.
154. Katzman SD, O'Gorman WE, Villarino AV, Gallo E, Friedman RS, et al. Duration of antigen receptor signaling determines T-cell tolerance or activation. *PNAS* 2010;107(42):18085-90.
155. Wakim LM, Bevan MJ. Cross-dressed dendritic cells drive memory CD8+ T-cell activation after viral infection. *Nature*. 2011;471(7340):629–32.
156. Mehlhop-Williams ER, Bevan MJ. Memory CD8+ T cells exhibit increased antigen threshold requirements for recall proliferation. *J Exp Med.* 2014;211(2):345-56.
157. Stern E, Klemic JF, Routenberg DA, Wyrembak PN, Turner-Evans DB. Label-free immunodetection with CMOS-compatible semiconducting nanowires. *Nature Letters.* 2007;445(7127):519-22.
158. Beeson C, Rabinowitz J, Tate K, Gutgemann I, Chien Y, et al. Early biochemical signals arise from low affinity TCR-ligand reactions at the cell-cell interface. *J Exp Med.* 1996;184(2):777-82.
159. Stern E, Steenbock ER, Reed MA, Fahmy TM. Label-free electronic detection of the antigen-specific T-cell immune response. *Nanoletters.* 2008;8(10):3310-14.
160. Wülfing C, Rabinowitz JD, Beeson C, Sjaastad MD, McConnell HM, et al. Kinetics and Extent of T Cell Activation as Measured with the Calcium Signal. *JEM*. 1997;185(10):1815–1825.
161. Rabinowitz JD, Beeson C, Wülfing C, Tate K, Allen PM, et al. Altered T Cell Receptor Ligands Trigger a Subset of Early T Cell Signals. *Immunity*, 1996;5(2):125–135.
162. Wang XB, Yang J, Huang Y, Vykoukal J, Becker FF et al. Cell Separation by Dielectrophoretic Field-flow-fractionation. *Anal Chem.* 2000;72(4):832-39.

www.manaraa.com

FIGURES AND LEGENDS

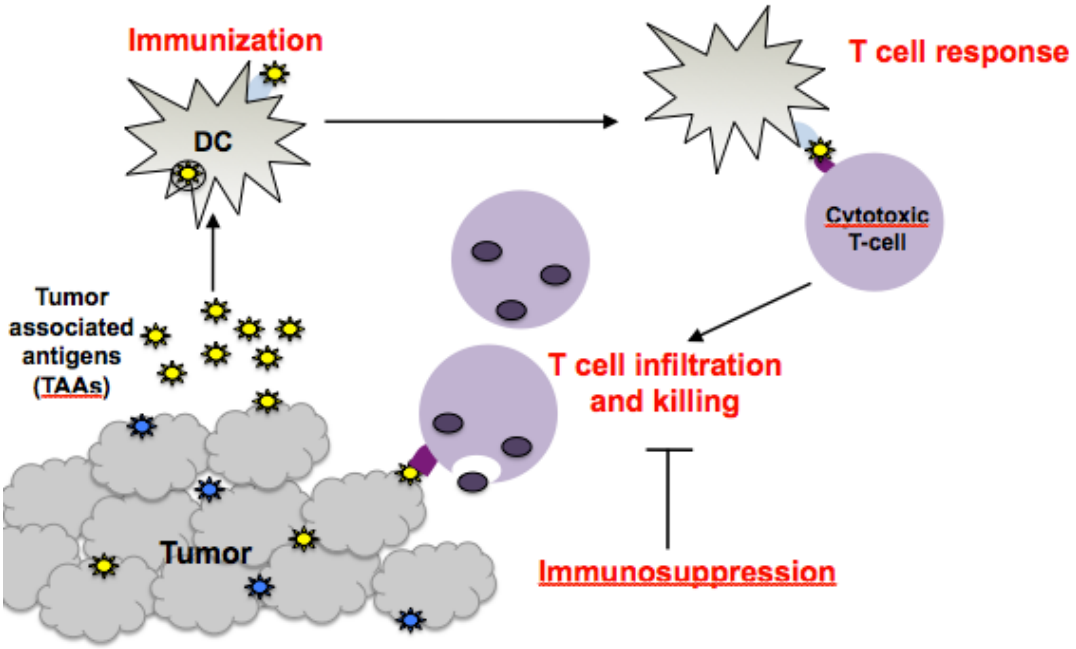

Figure 1: The immune system is shown to combat cancer.
In a classical immune response against cancer, the tumor microenvironment expresses a number of tumor associated antigens (TAAs) that act as a source of antigen for the immune system's potent antigen presenting cell, the dendritic cell (DC). DC take up antigen in one of several mechanisms, process, and present antigen onto their MHC Class I or II, in a process known as immunization. Immunized DC then traffic to the regional lymph node where they make contact with T cells whose surface T cell receptor can recognize cognate peptide-MHC on the DC, in a process known as cross presentation. Following this, a T cell response is initiated whereby T cells clonally expand, are able to exit the lymph node, infiltrate the tumor bed and result in tumor cell killing. The tumor often produces a host of immunossuppressive defense mechanisms that may prevent tumor shrinkage. For immunotherapy to be successful, it must initiate T cell responses in the tumor bed. Adapted from Mellman I, et al. *Nature.* 2011.

www.manaraa.com

A

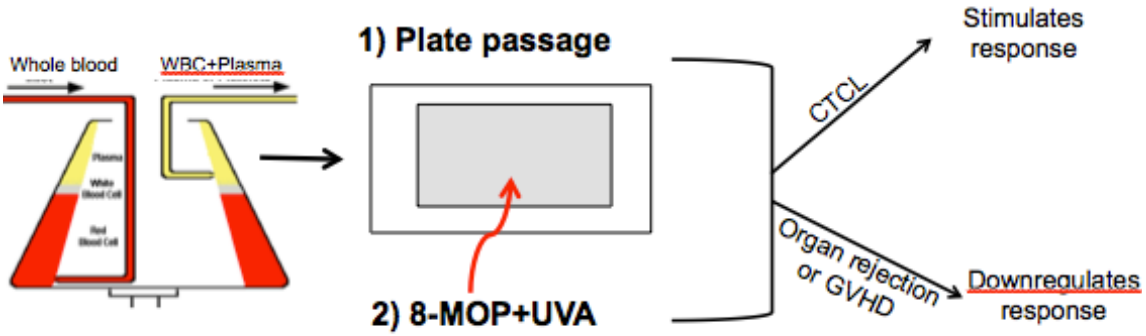

Figure 2A: Extracorporeal photopheresis has two paradoxical applications.
In an ECP procedure, a patient's blood is apheresed, or taken out of his body and spun to obtain three layers: a red blood cell, white blood cell (WBC) and platelet-rich plasma layers. The WBC and plasma are then run over a plate, which constitutes the first part of the treatment labeled 1) plate passage. For some part of the plate passage, the WBC are exposed to a photoactivatable DNA alkylating agent known as 8-methoxypsoralen (8-MOP) and ultraviolet light type A (UVA), labeled as 2) 8-MOP+UVA. At the end of the procedure, the WBC and plasma are reinfused back into the patient. In the case of CTCL, the effect is to stimulate immune responses, and in SOTR and GVHD the responses are downregulatory.

B

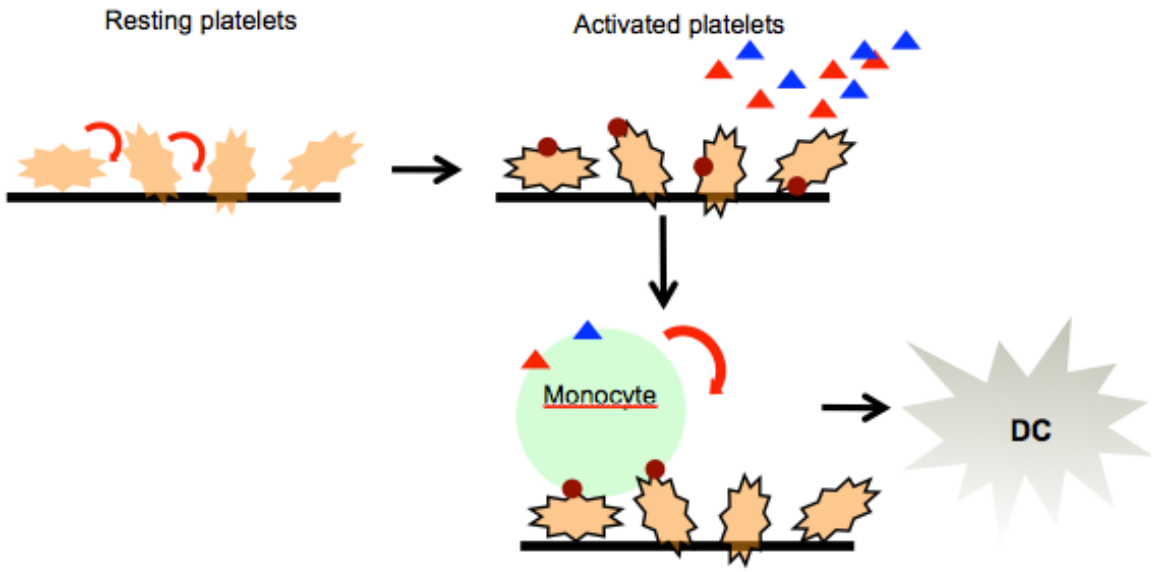

Figure 2B: The plate-passage procedure relies on monocyte-platelet interactions.
Plate passage exposes resting platelets to shear stress rates which activates them. When activated, platelets express surface markers, such as P-selectin, (marked in brown circles) and release soluble factors (marked in triangles). Monocytes rolling on the plate then transiently bind platelets as well as platelet-derived soluble factors and differentiate along the DC pathway.

www.manaraa.com

A

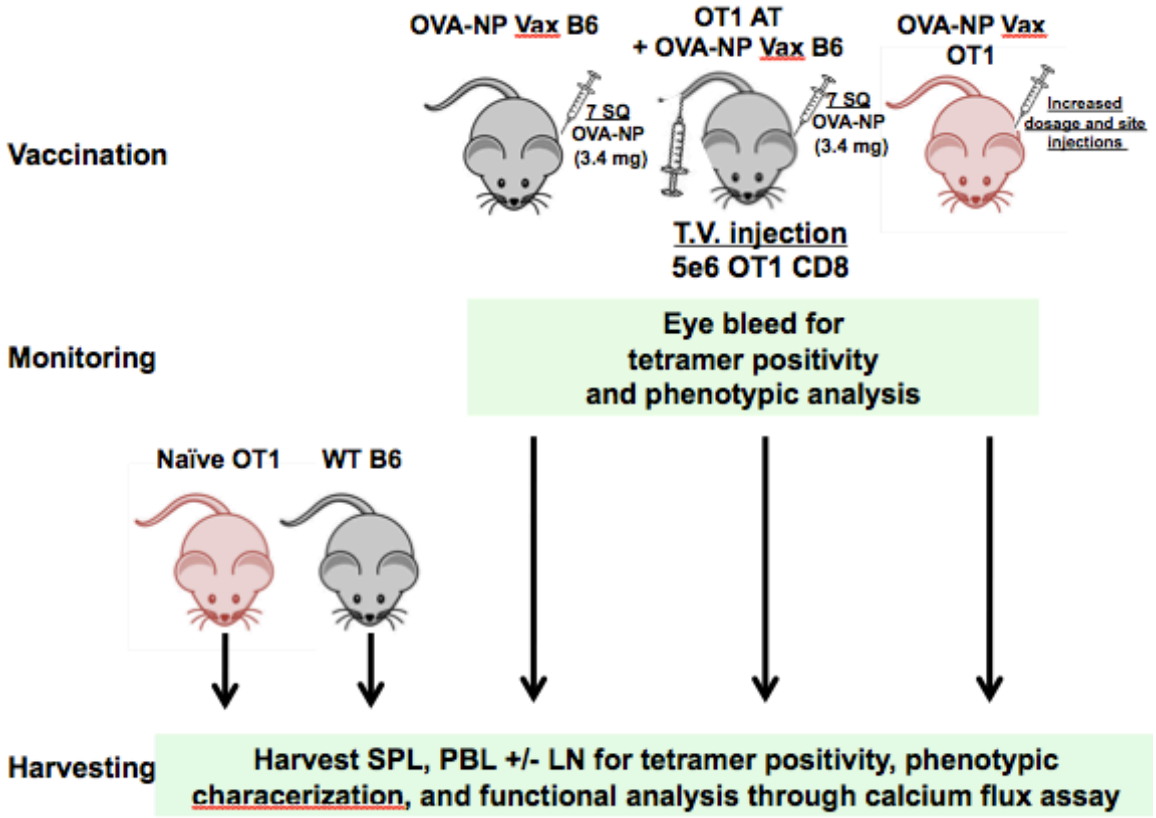

Figure 3A: Vaccinations and in vivo experimental are set up produce antigen experienced or memory T cells.
Each experiment utilized at least one of the groups in this figure. For vaccinations, OVA/LPS NP were administered at a maximum of 7 site. For primary expansion experiments, experiments were terminated and organs harvested one week from vaccination. For memory experiments, animals were boosted at the same schedule as primary vaccination one week after vaccination. When applicable eye bleeds were performed for tetramer positivity and phenotypic analysis.

www.manaraa.com

B

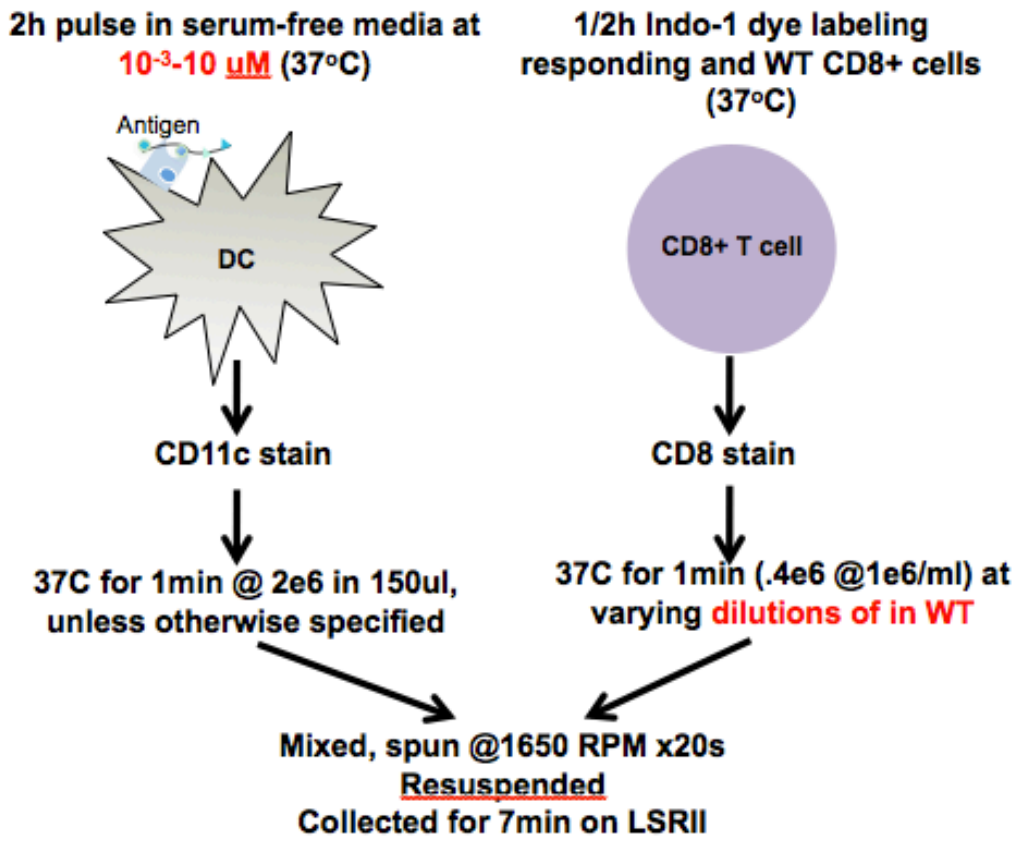

Figure 3B: In the calcium flux assay, murine or human T cells and DC are brought in contact. Whether murine or human, DC are pulsed for 2 hours with a specific peptide (SIINFEKL or MART-1) or non-specific peptide (EIINFEKL or gp100) at varying concentrations (10^{-3}-10uM) and in serum-free media. Meanwhile, responding T cells (OT1 or DMF5) as well as non-responding T cells (B6 or naïve, unstimulated human CD8+ cells) are loaded separately for 30min with 1uM Indo-1 AM at 37°C. Following loading step, DC and T cells are washed and stained with anti-CD11c-FITC and anti-CD8-PerCPCy5.5 antibody respectively. DC are concentrated at 2e6 in 150ul (for a DC:T cell ratio of 5:1) and T cells at 1e6/ml (with 0.4e6 in 400ul). When relevant, the proportion of responding T cells (OT1 or DMF5) is varied against WT, non-responding cells, keeping total cell number fixed at 0.4e6. DC are mixed with T cells, pelleted, and resuspended. Sample conjugates and calcium flux are collected for 7 minutes by flow cytometry.

www.manaraa.com

A

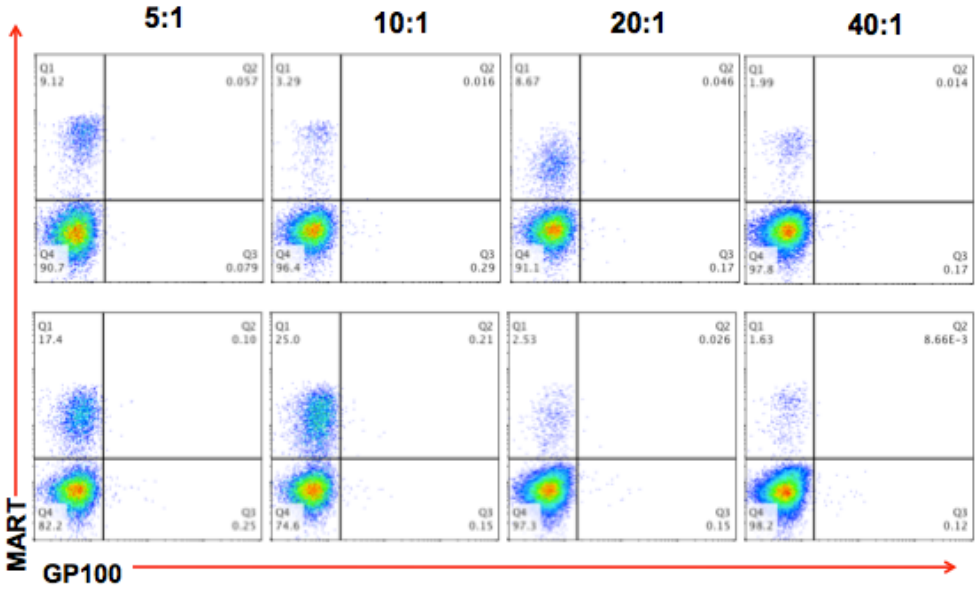

Figure 4A: Functional analysis of APC following T cell expansion.
Co-cultures were set up between APC and T cells at 4 different T:APC ratio (5:1, 10:1, 20:1, and 40:1). 13 days following co-culture, non-adherent T cells were collected and stained for tetramer positivity. Gp100 was used as a negative control tetramer. CD8+ were gated on, then the fluorescent plots of gp100 versus MART tetramer were plotted, as shown in the figure.

B

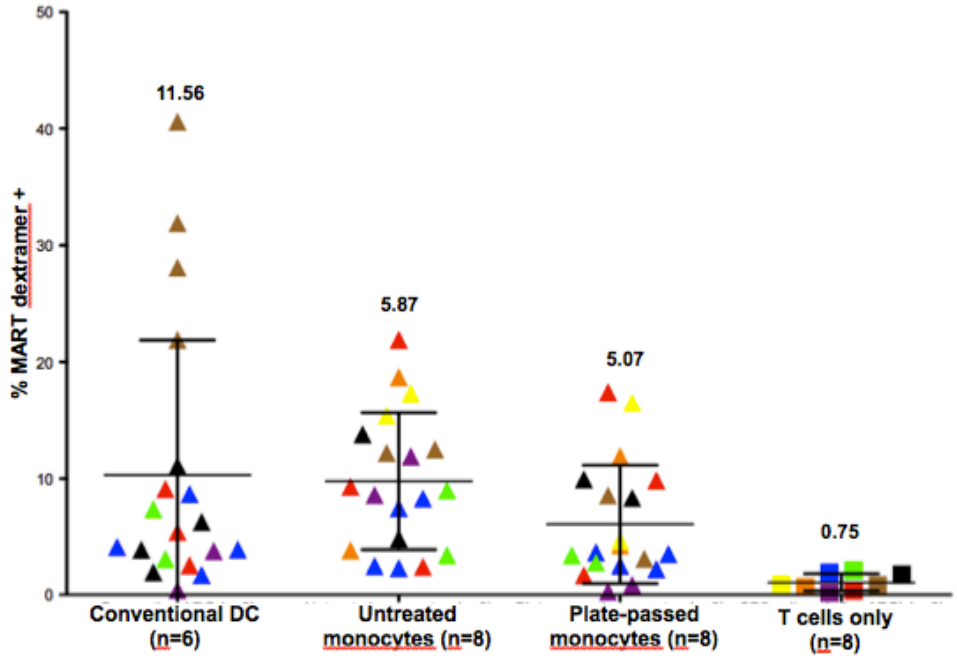

Figure 4B: PPM are non-inferior to UM and DC and donor variability is high.
The average tetramer+ expansion of CD8 cells co-cultured with each of the three myeloid cell types was the following: 10.86 % from DC (range=1.73-40.6, SD=11.56, n=6), 9.78% from UM (range=2.32-21.9, SD=5.87, n=8), and 7.3 % from PPM (range=1.71-17.4, SD=5.07, n=8). Differences were not significantly different. Negative controls were also plated using autologous CD8 cells only average 1.1% (range=0.16-2.12; SD=0.75, n=8). Dot plots are color-coded by donor, and results from all T:DC ratios are concatenated and matched equally among the different APC groups.

www.manaraa.com

C

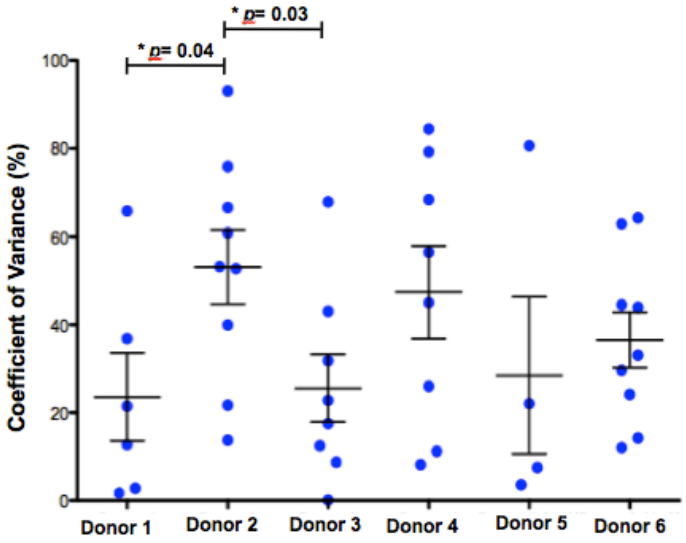

Figure 4C: The experimental design has a high coefficient of variance.
Duplicates of some samples were plated for each of the donors. The coefficient of variance (COV) was high (which has been reported by others previously). COV ranged from 23.5 to 53%. Donor variability in COV was significant by two tailed pair test.

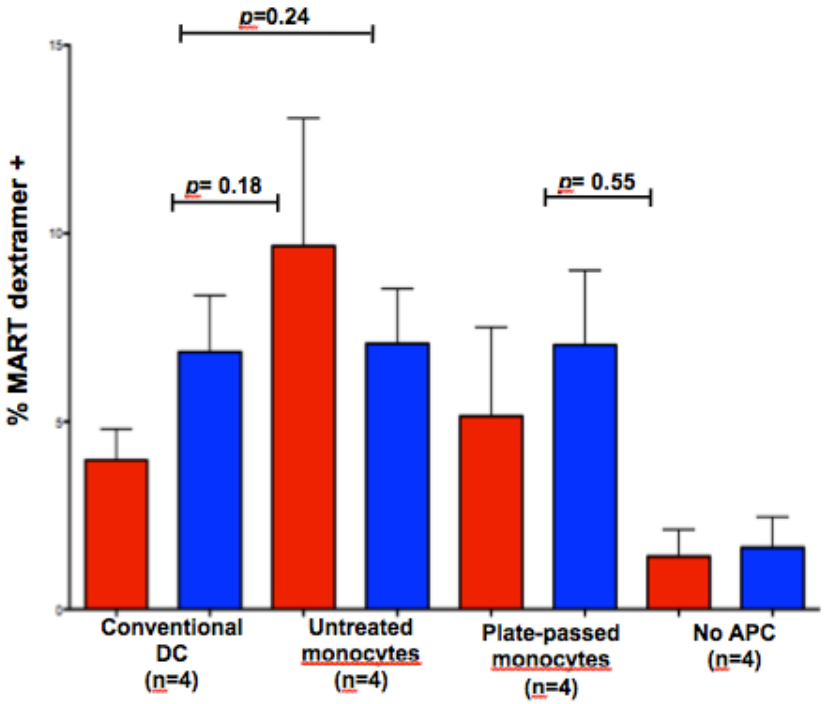

Figure 5: CD4 cells may assist in the expansion of CD8 cells.
With the addition of CD4 cells into the co-culture (blue bars), CD8 expansions tended to increase, but the differences were not significant: for conventional DC, 3.9%, SD 1.64, with CD4 addition, 6.9%, SD 3.7; for UM, 9.7%, SD 6.8, with CD4 addition, 7%, SD 3.6; for PPM, 5%, SD 4.7, with CD4 addition, 7%, SD 4.8. Negative controls, CD8 only, 1.4%, SD 1.4, with CD4 addition, 1.6%, SD 1.61. Red bars represent standard co-cultures with CD8 and APC only, except for negative control (no APC). Blue bars represent co-cultures with CD4 added to standard co-culture, except for negative control (no APC).

www.manaraa.com

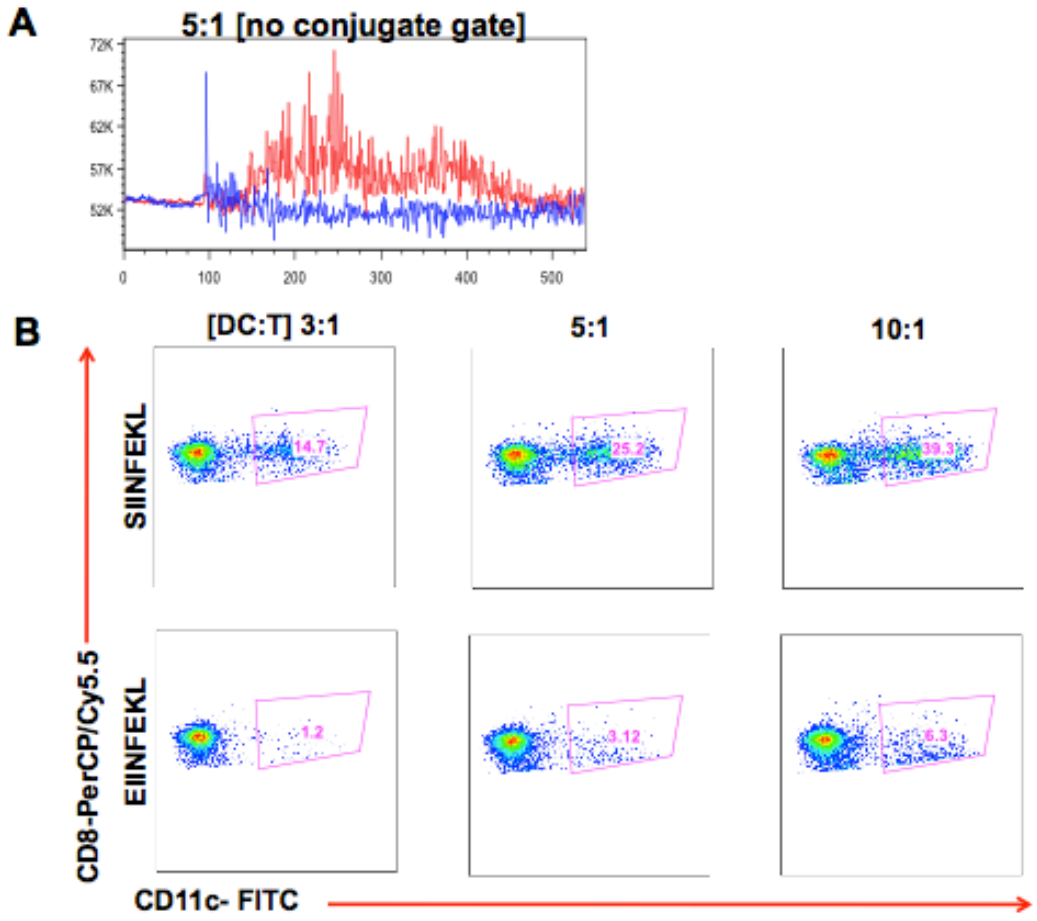

Figure 6A, B: As the DC:T cell ratio increases, antigen-specific conjugates increase in OT1 system.
A: Different DC:T cell ratios were tested. The assay developed is a delicate one for two reasons: when the sample was pelleted, but a CD11c+CD8+ gate was *not* drawn, no ASF could be detected (left).
B: In this sample gating strategy, the population of interest was defined as all CD11c+ CD8+ events. The top and bottom rows depict antigen-specific conjugates (ASC) and non-specific conjugates (NSC). The ratios 3:1, 5:1, and 10:1 represent the DC:T cell ratio in which the absolute DC number and concentration are increased, keeping the volume (150ul) fixed. These results show that as the DC:T cell ratio increases, both ASC and NSC increase, but the ASC increase far outweighs NSC.

www.manaraa.com

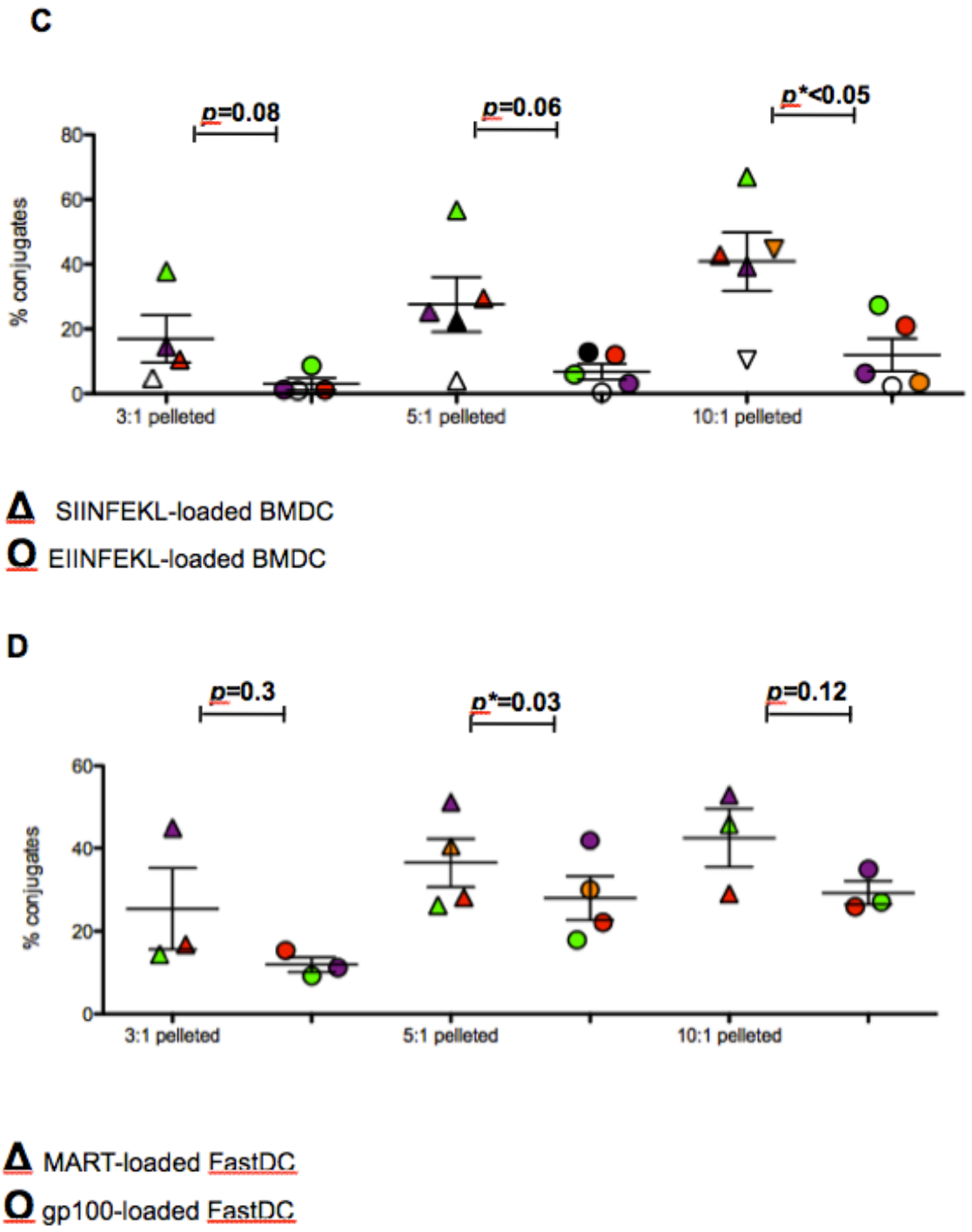

Figure 6C,D:
C: Pelleting experiment was repeated, n=4 to confirm positive correlation between ASC and DC:T cell ratio. Each color represents an experiment. Results are significant by Student *T*-test at 10:1 ratio.
D: Pelleting experiment was repeated, n=4 (6 right-most plots) to confirm positive correlation between ASC and DC:T cell ratio. Each color represents an experiment; notably, red and green-colored dots were experiments in which an old batch of DMF5 was used- ASC is lower in those as compared with purple and orange plots. Results are significant by Student *T*-test at 5:1 ratio.

www.manaraa.com

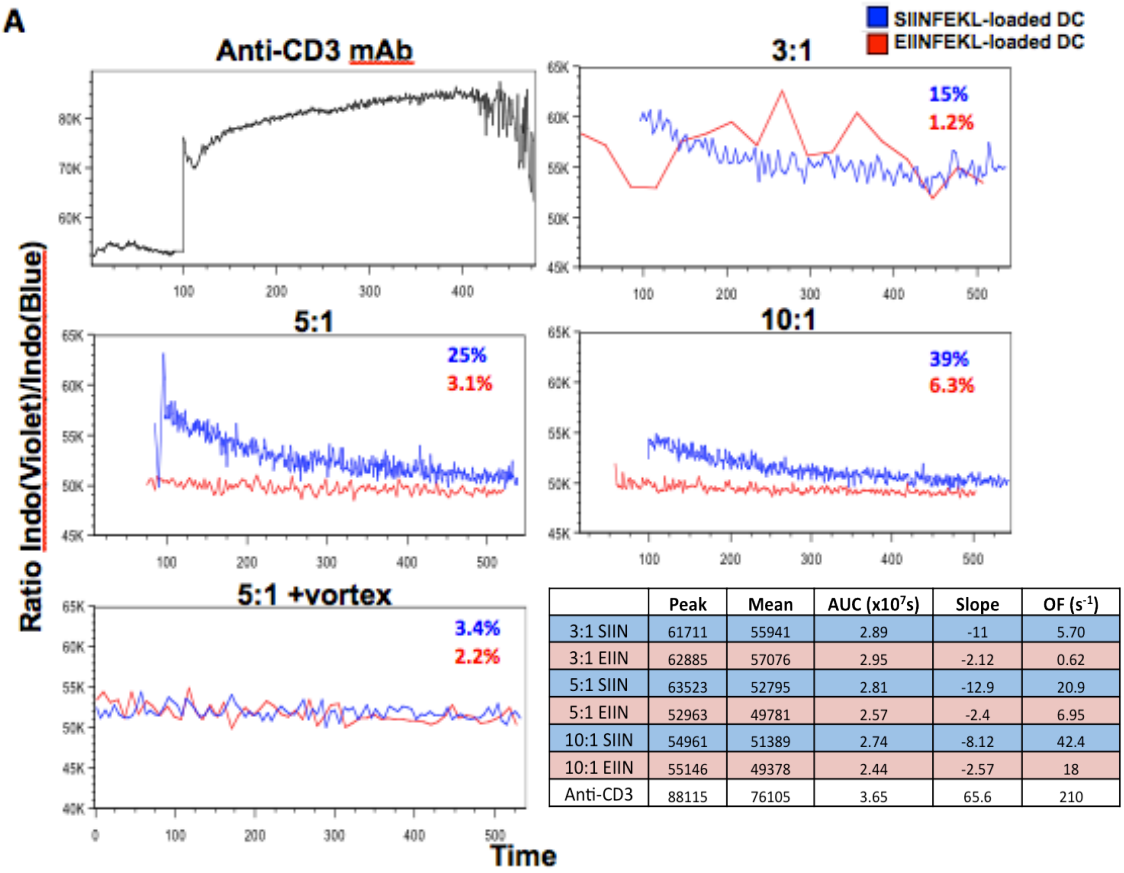

	Peak	Mean	AUC (x10^{7}s)	Slope	OF (s^{-1})
3:1 SIIN	61711	55941	2.89	-11	5.70
3:1 EIIN	62885	57076	2.95	-2.12	0.62
5:1 SIIN	63523	52795	2.81	-12.9	20.9
5:1 EIIN	52963	49781	2.57	-2.4	6.95
10:1 SIIN	54961	51389	2.74	-8.12	42.4
10:1 EIIN	55146	49378	2.44	-2.57	18
Anti-CD3	88115	76105	3.65	65.6	210

Figure 7A: Greater ASC translates to higher antigen-specific calcium flux in the OT1 system. By gating on CD11c+CD8+ conjugates, we were able to plot calcium flux curves for the T cells that had made contact with DC. The data collected for Indo-1 can be plotted as Ratio of calcium-bound-Indo (Violet)/ calcium-free-Indo (Blue). Parameters for each of the curves are displayed in the bottom right table. Blue and red curves represent T cell stimulation by antigen-specific and non-specific DC, respectively. The top plot represents maximal T cell stimulation using anti-CD3 antibody. As the ratio of DC:T cell increases from 3:1, 5:1 to 10:1, the difference between antigen-specific flux (ASF) and non-specific flux (NSF) increases. This is reflected both visually in the curves as well as with the various parameters displayed in the table. When the CD11c+ CD8+ gate was drawn, but the mixture was vortexed "vigorously" (right), no ASC formed, and no ASF was detected.

www.manaraa.com

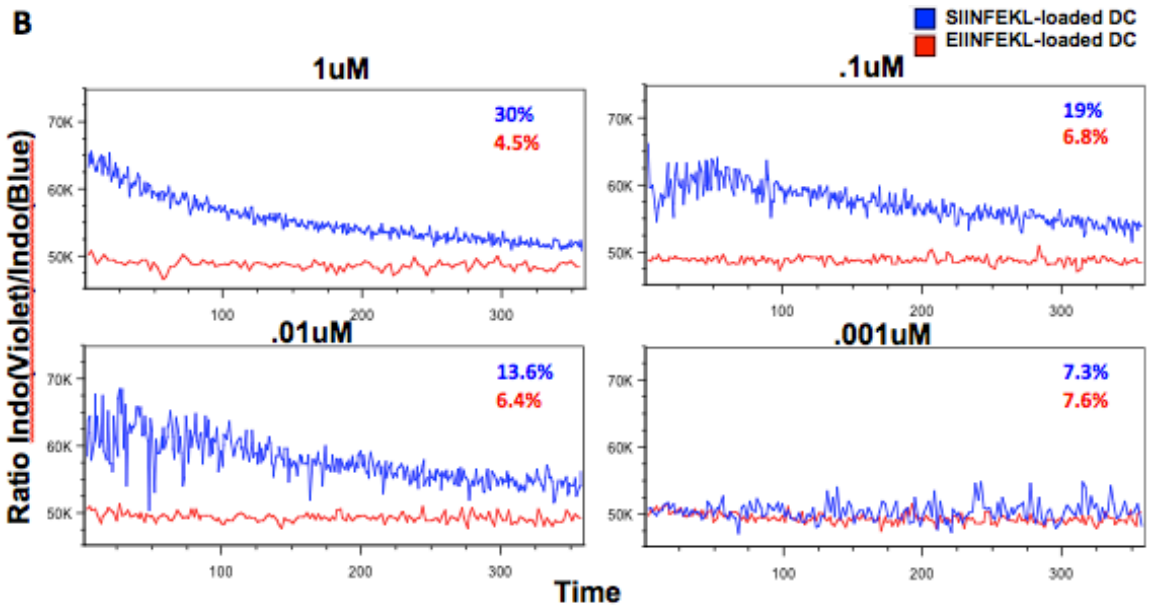

	Peak	Mean	AUC (x10^{7}s)	Slope	OF (s^{-1})
1uM SIIN	65876	55389	1.99	-31.1	43.5
1uM EIIN	50574	48505	1.74	-1.98	8.60
0.1uM SIIN	66590	57339	2.06	-22	30.3
0.1uM EIIN	50866	48635	1.75	-0.633	12.9
0.01uM SIIN	688871	57863	2.08	-26.4	21.4
0.01uM EIIN	51161	49198	1.77	-1.7	10.8
10e-3 SIIN	54776	50351	1.81	-0.95	11.3
10e-3 EIIN	51512	49275	1.77	-3.28	11.8

Figure 7B: ASC and ASF disappear at 10^{-3}uM in the OT1 system.
As the peptide loading concentration was decreased by a logarithm from 1uM to 10^{-3}uM, the difference between antigen-specific flux (ASF) and non-specific flux (NSF) decreased. This is reflected both visually in the curves as well as with the various parameters displayed in the table. At 10^{-3}uM the difference between ASF and NSF is difficult to make, and there is no difference in ASC.

www.manaraa.com

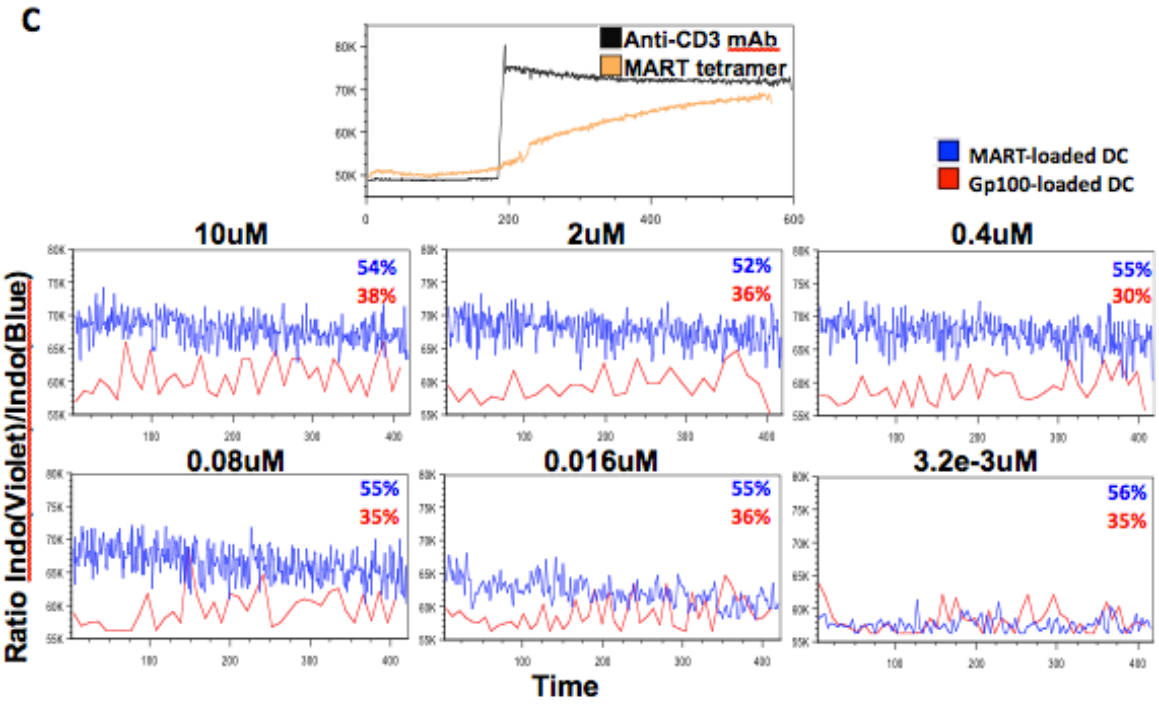

	Peak	Mean	AUC (x10^{7}s)	Slope	OF (s^{-1})
10uM MART	74669	68145	2.42	-7.66	30.1
10uM gp100	66143	60740	2.16	-6.37	2.40
2uM MART	73670	68043	2.42	-6.56	27.8
2uM gp100	64820	59620	2.11	-11.5	1.83
0.4uM MART	72684	67791	2.41	-7	27.6
0.4uM gp100	63523	59365	2.11	-10.2	2.38
8e-2uM MART	72439	66711	2.39	-11.9	24.6
8e-2uM gp100	68871	59466	2.11	-8.62	2.28
1.6e-2uM MART	68277	62301	2.23	-11.5	18.4
1.6e-2uM gp100	64820	58928	2.09	-7.69	3.24
3.2e-3uM MART	61317	57596	2.05	-0.187	7.64
3.2e-3uM gp100	63874	58247	2.06	-0.679	3.29

Figure 7C: ASC and ASF disappear on the order of 10^{-3}uM in the DMF5 system.
The top curve represents positive controls in the DMF5 system: in black are DMF5 cells stimulated non-specifically with anti-CD3 antibody. In orange are DMF5 cells stimulated with a MART tetramer. Similar to the OT1 system, as the peptide loading concentration was decreased by a half-logarithm from 10uM to $3.2x10^{-3}$uM, the difference between antigen-specific flux (ASF) and non-specific flux (NSF) decreased. This is reflected both visually in the curves as well as with the various parameters displayed in the table. At $3.2x10^{-3}$uM the difference between ASF and NSF is difficult to make, but, surprisingly, the difference between ASC and NSC was preserved.

www.manaraa.com

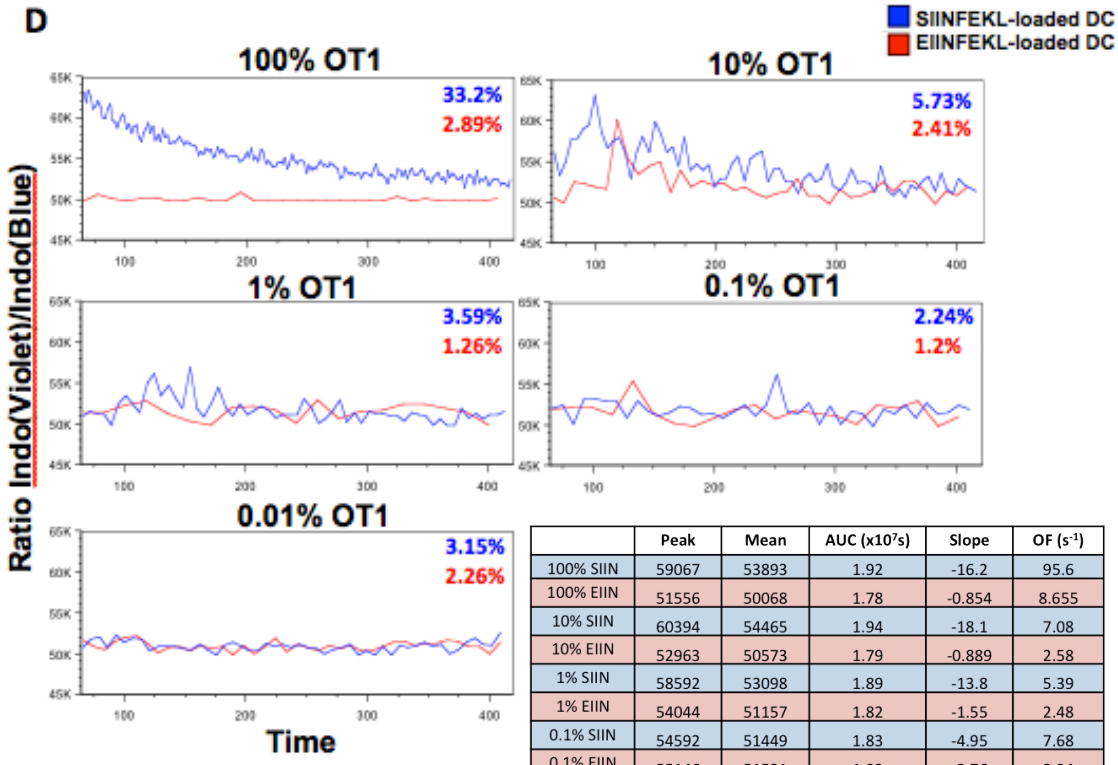

	Peak	Mean	AUC (x10^{7}s)	Slope	OF (s^{-1})
100% SIIN	59067	53893	1.92	-16.2	95.6
100% EIIN	51556	50068	1.78	-0.854	8.655
10% SIIN	60394	54465	1.94	-18.1	7.08
10% EIIN	52963	50573	1.79	-0.889	2.58
1% SIIN	58592	53098	1.89	-13.8	5.39
1% EIIN	54044	51157	1.82	-1.55	2.48
0.1% SIIN	54592	51449	1.83	-4.95	7.68
0.1% EIIN	55146	51531	1.83	-3.76	2.24
0.01% SIIN	56272	52978	1.85	-6.78	0.86
0.01% EIIN	54409	50991	1.81	-3.64	2.26

Figure 7D: ASC and ASF disappear at 0.1% dilution in the OT1 system.
As OT1 cells are increasingly diluted by a logarithm in a pool of wildtype (WT), non responding cells, the difference between ASF and NSF decreases. This is reflected both visually in the curves as well as with the various parameters displayed in the table. At 0.1% OT1, the difference between ASF and NSF is difficult to make, and there is no difference in ASC.

www.manaraa.com

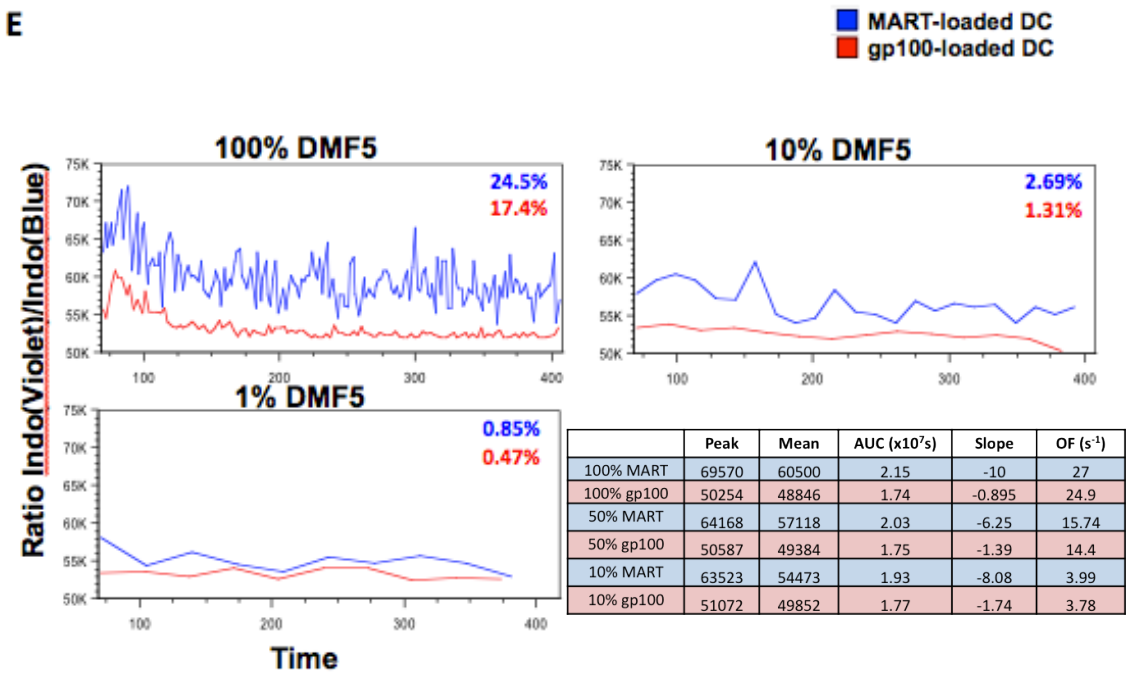

	Peak	Mean	AUC (x10^{7}s)	Slope	OF (s^{-1})
100% MART	69570	60500	2.15	-10	27
100% gp100	50254	48846	1.74	-0.895	24.9
50% MART	64168	57118	2.03	-6.25	15.74
50% gp100	50587	49384	1.75	-1.39	14.4
10% MART	63523	54473	1.93	-8.08	3.99
10% gp100	51072	49852	1.77	-1.74	3.78

Figure 7E: ASC and ASF disappear at 1% dilution in the DMF5 system.
As DMF5 cells are increasingly diluted by a logarithm in a pool of wildtype (WT), non responding cells, the difference between ASF and NSF decreases. This is reflected both visually in the curves as well as with the various parameters displayed in the table. At 1% DMF5, the difference between ASF and NSF is difficult to make, and there is no difference in ASC.

www.manaraa.com

A

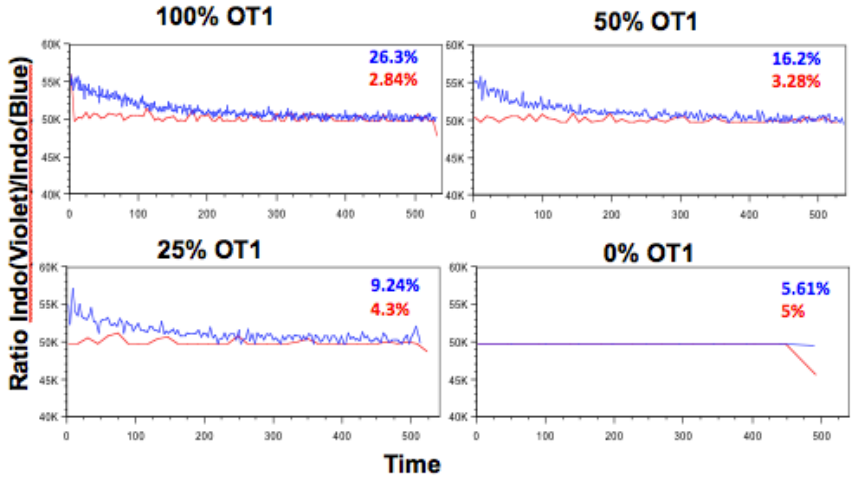

	Peak	Mean	AUC (x10^{7}s)	Slope	OF (s^{-1})
100% SIIN	56272	51339	2.44	-7.76	53.9
100% EIIN	56272	50337	2.42	-1.88	4.92
50% SIIN	56158	51297	2.44	-7.46	18.3
50% EIIN	51124	50164	2.38	-1.88	2.56
25% SIIN	57420	51342	2.34	-6.83	7.63
25% EIIN	51383	50060	2.37	-0.816	1.59
0% SIIN	49849	49849	2.36	-1.1	0.5
0% EIIN	49849	49849	2.36	-1	0.542

B

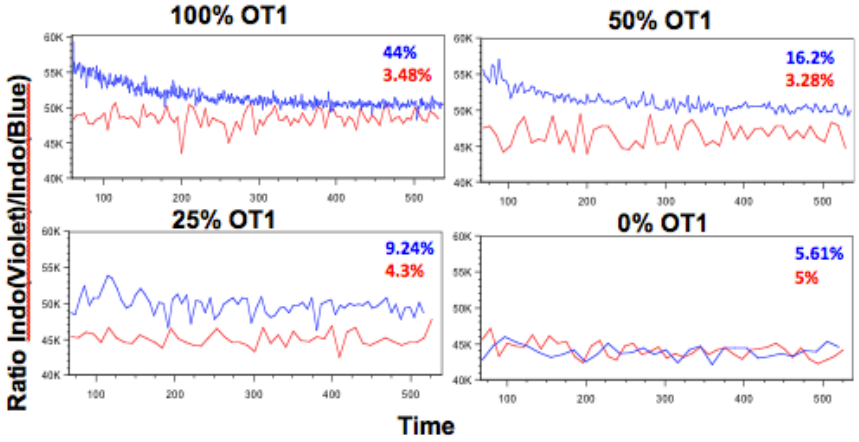

	Peak	Mean	AUC (x10^{7}s)	Slope	OF (s^{-1})
100% SIIN	56272	51339	2.44	-7.76	53.9
100% EIIN	56272	50337	2.42	-1.88	4.92
50% SIIN	56158	51297	2.44	-7.46	18.3
50% EIIN	51124	50164	2.38	-1.88	2.56
25% SIIN	57420	51342	2.34	-6.83	7.63
25% EIIN	51383	50060	2.37	-0.816	1.59
0% SIIN	49849	49849	2.36	-1.1	0.5
0% EIIN	49849	49849	2.36	-1	0.542

Figure 8A, B: When diluted among WT cells, *in vitro* pre-activated OT1 cells have lower ASF than naïve OT1.

Both naïve and pre-activated OT1 demonstrated decreased ASF as dilution in WT increases. However, at each % tested, pre-activated OT1 consistently had lower ASF, suggesting a reduced ability to activate calcium flux.

www.manaraa.com

C

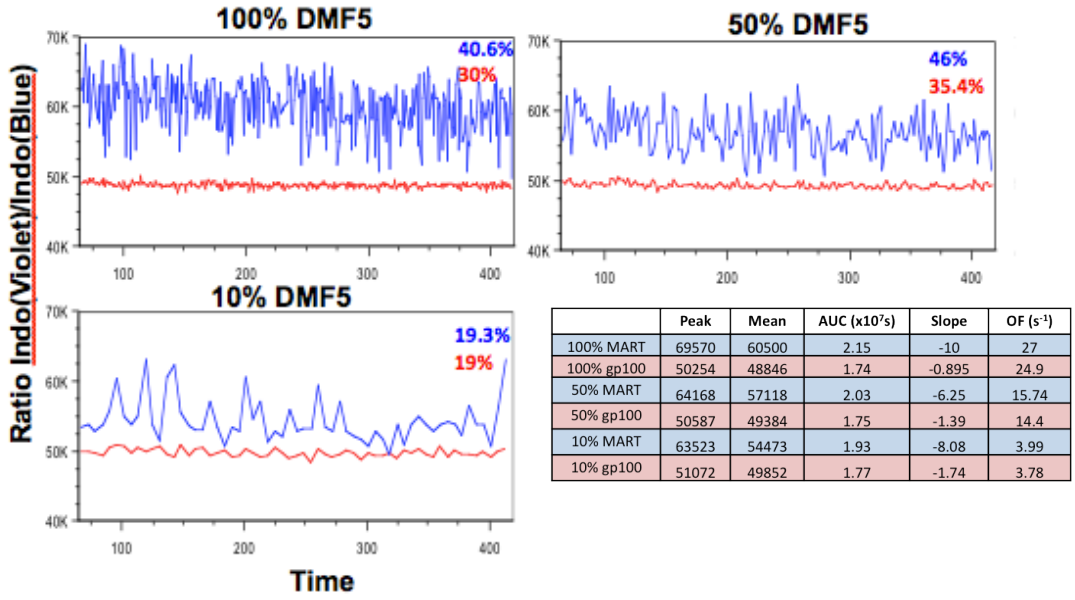

	Peak	Mean	AUC (x10⁷s)	Slope	OF (s⁻¹)
100% MART	69570	60500	2.15	-10	27
100% gp100	50254	48846	1.74	-0.895	24.9
50% MART	64168	57118	2.03	-6.25	15.74
50% gp100	50587	49384	1.75	-1.39	14.4
10% MART	63523	54473	1.93	-8.08	3.99
10% gp100	51072	49852	1.77	-1.74	3.78

D

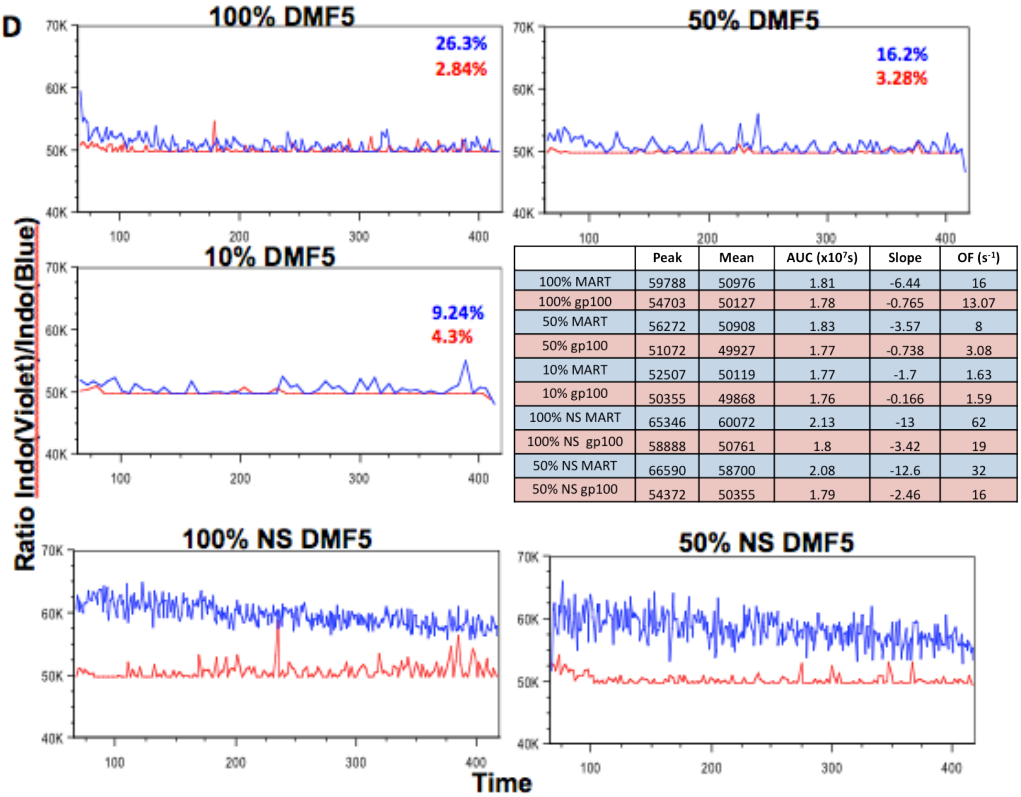

	Peak	Mean	AUC (x10⁷s)	Slope	OF (s⁻¹)
100% MART	59788	50976	1.81	-6.44	16
100% gp100	54703	50127	1.78	-0.765	13.07
50% MART	56272	50908	1.83	-3.57	8
50% gp100	51072	49927	1.77	-0.738	3.08
10% MART	52507	50119	1.77	-1.7	1.63
10% gp100	50355	49868	1.76	-0.166	1.59
100% NS MART	65346	60072	2.13	-13	62
100% NS gp100	58888	50761	1.8	-3.42	19
50% NS MART	66590	58700	2.08	-12.6	32
50% NS gp100	54372	50355	1.79	-2.46	16

Figure 8C,D: When diluted among WT cells, *in vitro* pre-activated DMF5 cells have lower ASF than untreated DMF5.

Both untreated and pre-activated DMF5 demonstrated decreased ASF as dilution in WT increases. However, at each % tested, pre-activated DMF5 consistently form fewer ASC and the difference between ASF and NSF is smaller, suggesting a reduced ability to activate calcium flux. D, bottom 2 plots: Intriguingly, when DMF5 were pre-activated using gp100 (a non-specific source of peptide), the ability to flux calcium was restored to levels comparable to untreated DMF5 from 7E.

www.manaraa.com

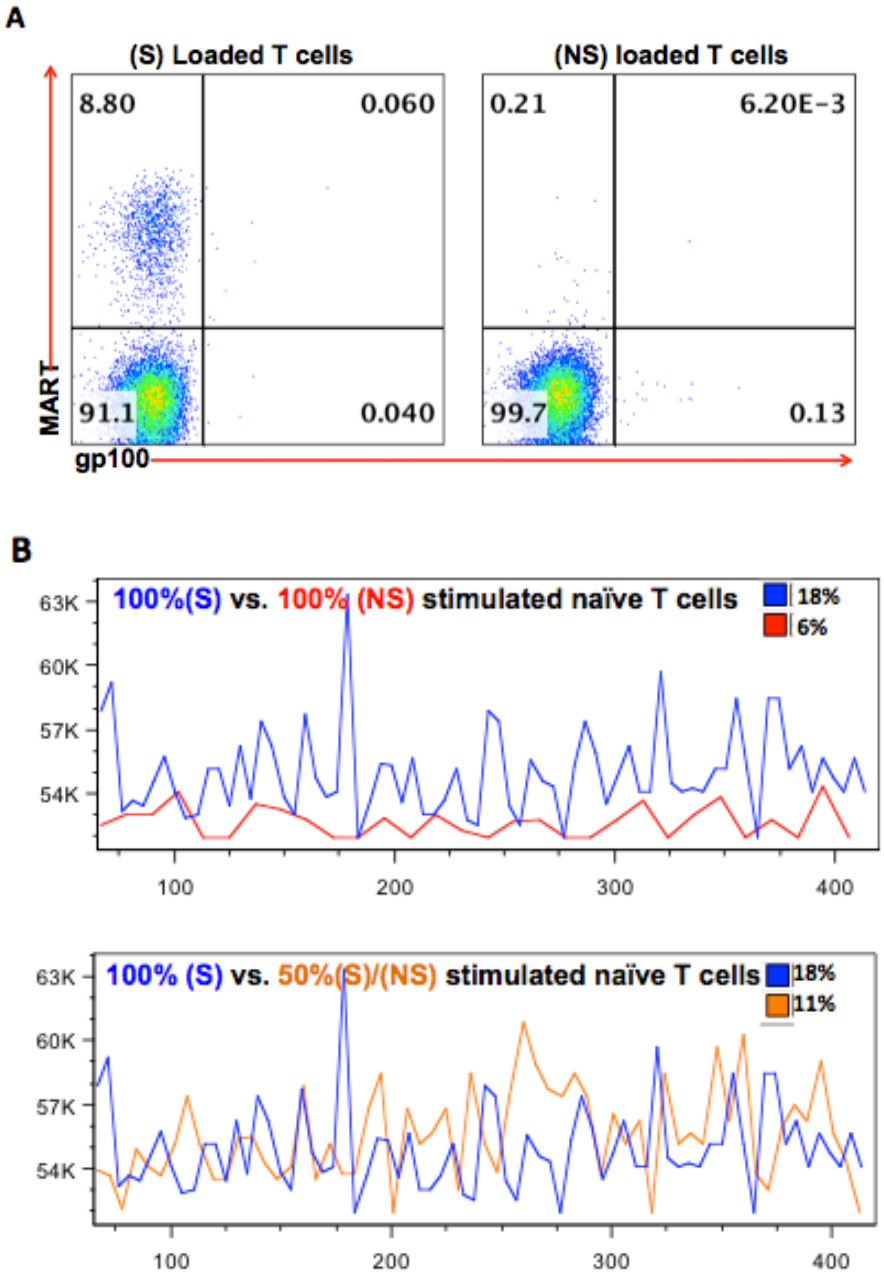

Figure 9A,B: T cells from HLA-A2 donor expanded specifically in response to MART-1, and (S) T cells demonstrated ASF, whereas (NS) T cells did not.
A: 7 day co-cultures were set up with HLA-A2+ donor FastDC and autologous naïve cells in the presence of IL2 and IL7. T cells in the co-culture were stimulated either specifically (S) with MART-1 SP-loaded DC or non-specifically (NS) with gp100 SP-loaded DC. On day 7, cells were harvested and tetramer stained. (S) T cells expanded to approximately 9% of the CD8 pool, whereas (NS) T cells did not.
B: (S) T cells demonstrate ASC formation and ASF compared with (NS) T cells. Intriguingly, when (S) T cells are diluted with (NS) T cells at a 50% dilution rate, ASC and ASF are not significantly altered.

www.manaraa.com

A

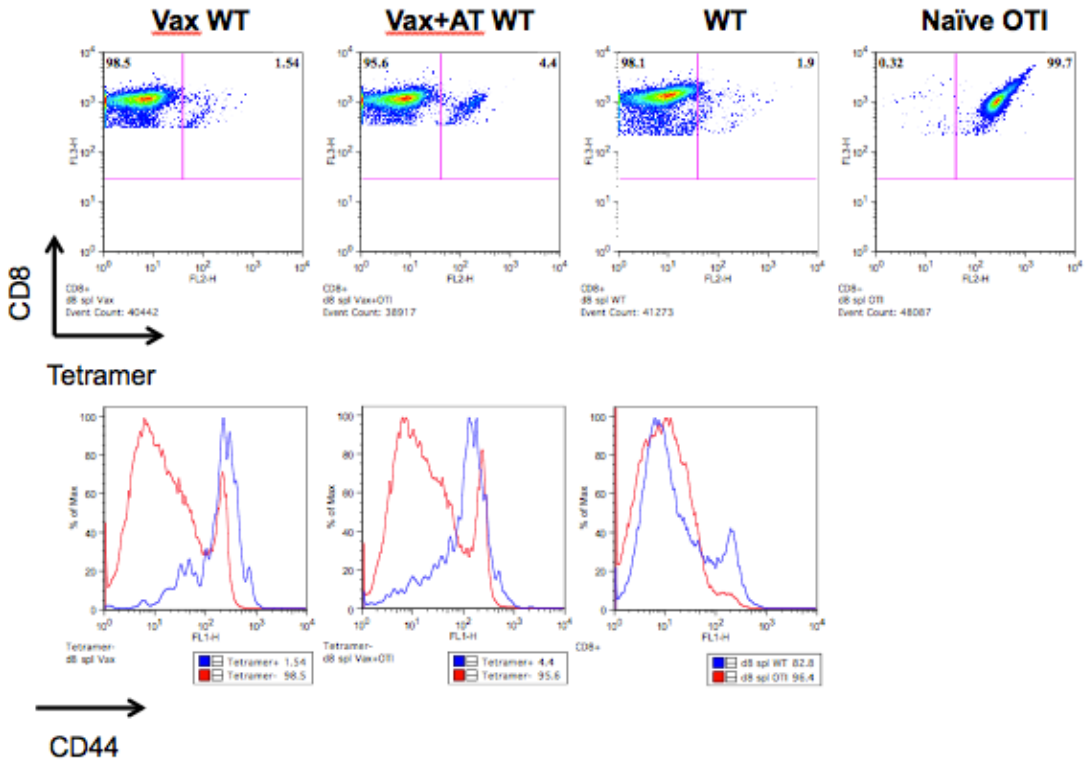

Figure 10A: Phenotypically, 1-week old antigen-experienced T cells are expanded and activated *in vivo*.
In this experiment, 2 WT B6 mice were vaccinated with LPS/OVA (Vax) and one was also adoptively transferred 5e6 OT1 cells (Vax+AT WT). One week later after vaccination, splenic SIINFEKL-tetramer positive cells had expanded to 1.5% in the Vax WT mouse and to 4.4% in the Vax+AT WT mouse from the total CD8+ population. For controls, WT and naïve OT1 CD8+ splenocytes were 0% and 100% SIINFEKL tetramer positive, respectively. Bottom panels: CD44 expression was used to evaluate activation status with naïve OT1 cells as negative control. We compared CD44 intensity in the tetramer+ and tetramer- populations in Vax and Vax+AT mice. CD44 activation was high in the tetramer+ population in the vaccinated mice, but not the tetramer- population, and relatively low the naïve OT1 mouse.

www.manaraa.com

B

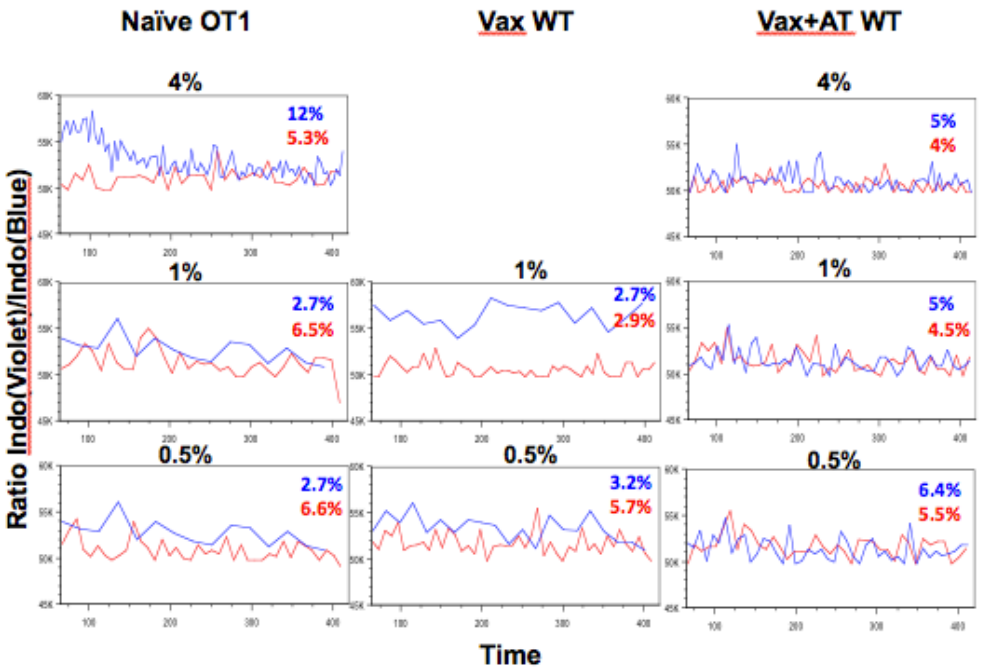

		Peak	Mean	AUC (x10^{7}s)	Slope	OF (s^{-1})
Naïve OT1	4% SIIN	58592	53098	1.89	-13.8	5.39
	4% EIIN	54044	51157	1.82	-1.55	2.48
	1% SIIN	54592	51449	1.83	-4.95	7.68
	1% EIIN	55146	51531	1.83	-3.76	2.24
	0.5% SIIN	56272	52978	1.85	-6.78	0.862
	0.5% EIIN	54409	50991	1.81	-3.64	2.25
Vax WT	1% SIIN	58592	56661	2.00	-0.197	0.99
	1% EIIN	52963	50625	1.80	-1.6	2.87
	0.5% SIIN	56272	53578	1.91	-5.32	1.27
	0.5% EIIN	55706	51831	1.84	-1.58	2.61
Vax+AT WT	4% SIIN	55146	51131	1.82	-2.35	4.60
	4% EIIN	52963	50654	1.80	-0.886	3.68
	1% SIIN	55519	51478	1.83	-2.55	3.04
	1% EIIN	55146	51463	1.83	-4.89	2.74
	0.5% SIIN	54869	51454	1.83	-3.59	2.58
	0.5% EIIN	55706	51782	1.83	-2.78	2.40

Figure 10B: Depending on the host, 1-week-antigen experienced T cells have distinct activation ability. 1 week post-vaccination, purified CD8+ splenocytes were diluted or run undiluted, and when possible at 4%,1%, and 0.5% in order to compare ASF among three different hosts: naïve OT1, Vax WT, and Vax+AT WT. Functionally, splenic ASC had lower activation ability in the Vax+AT WT group at all 3 dilutions tested. Surprisingly, Vax WT had higher ASF at 1% than both naïve and Vax+AT mice, and at 0.5% ASF was comparable to naïve OT1.

www.manaraa.com

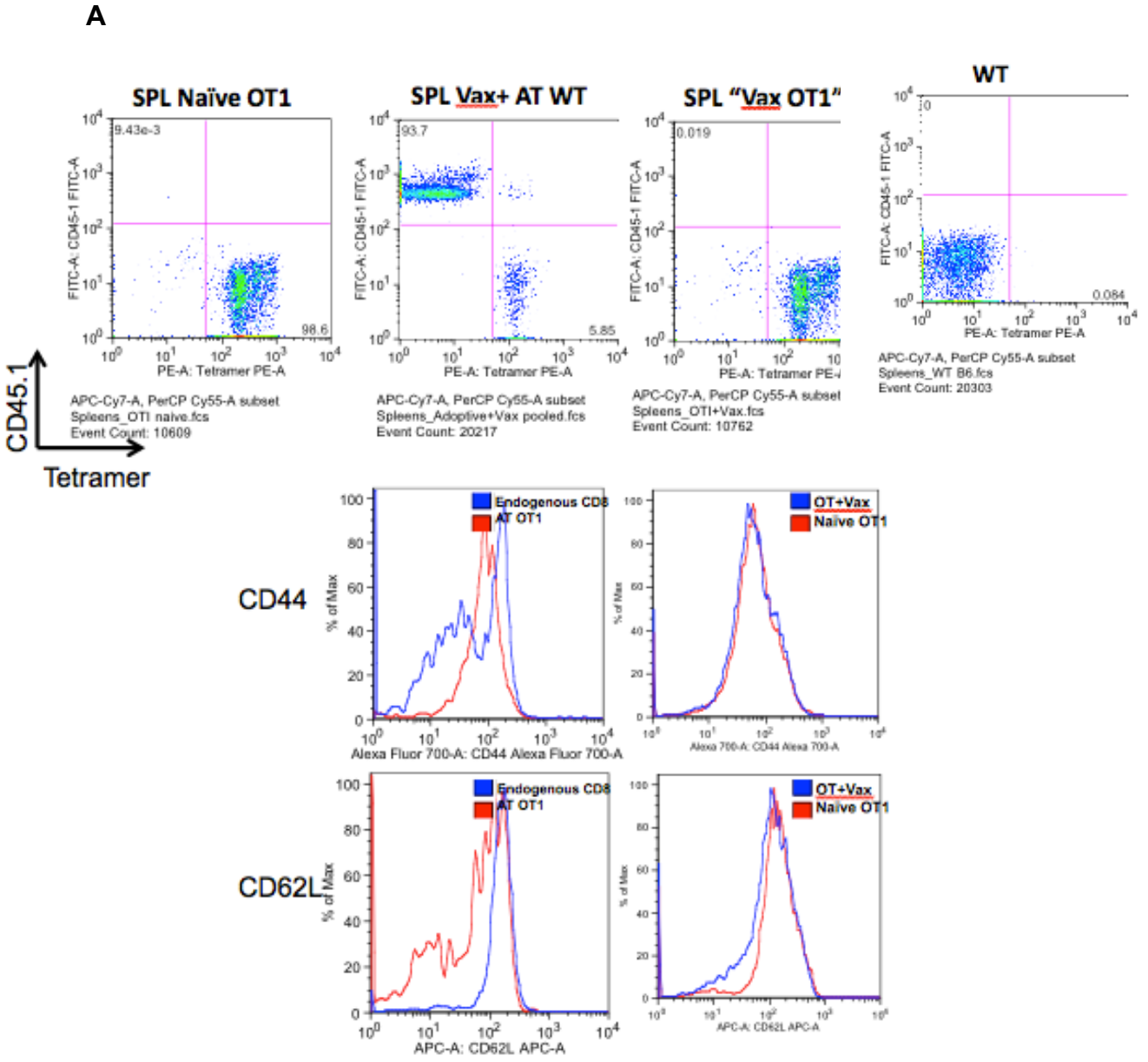

Figure 11A: Directly vaccinated OT1 cells are less activated than AT cells.
In this experiment, an OT1 mouse was directly vaccinated with increasing doses of LPS/OVA. Naïve OT1 and Vax+AT WT were used for controls. CD45.1 was used as a marker of the endogenous WT population. One week later after vaccination, splenic CD45.1- tetramer+ (AT) cells had expanded to 6% in the Vax+AT WT mouse, and predictably, all cells in the naïve and Vax OT1 mice were tetramer+CD45.1-. Bottom panels: CD44 and CD62L expression were used to evaluate activation status with naïve OT1 cells as negative control. In the Vax+AT mice (plots representative of 2 mice), CD44 expression was high and CD62L low in the tetramer+ population, compared with the endogenous, tetramer- population. In Vax OT1, no significant difference in CD44 activation was noted compared with naïve OT1, but there may have been some shedding of CD62L.

www.manaraa.com

B

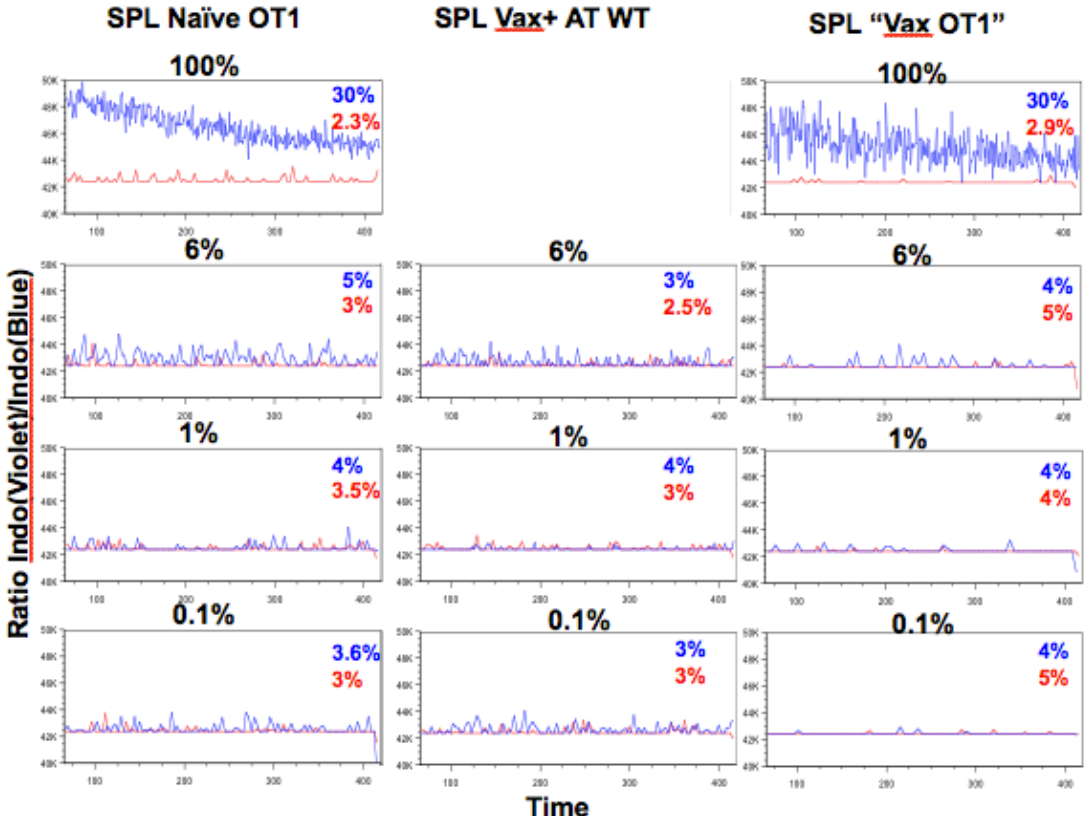

		Peak	Mean	AUC (x10^{7}s)	Slope	OF (s^{-1})
Naïve OT1	100% SIIN	50186	46602	1.64	-10.7	61.7
	100% EIIN	43571	42526	1.50	-0.205	6.75
	6% SIIN	44880	43012	1.51	-0.9	9.34
	6% EIIN	44161	42493	1.50	-0.317	8.95
	1% SIIN	44161	42549	1.50	-0.0202	8.01
	1% EIIN	43279	42509	1.49	-0.0722	8.01
	0.1% SIIN	43865	42613	1.50	-0.0118	6.91
	0.1% EIIN	43806	42465	1.50	-0.292	9.36
Vax OT1	100% SIIN	48730	45098	1.59	-6.41	21.9
	100% EIIN	42916	42439	1.49	-0.0445	6.3
	6% SIIN	44161	42544	1.5	-0.117	5.24
	6% EIIN	42930	42434	1.49	-0.127	6.90
	1% SIIN	43279	42483	1.5	-0.271	4.39
	1% EIIN	42844	42427	1.5	-0.0722	7.89
	0.1% SIIN	42592	42433	1.49	-0.053	4.22
	0.1% EIIN	42757	42429	1.49	-0.0662	6.55
Vax+AT WT	6% SIIN	44289	42705	1.51	-0.725	12.8
	6% EIIN	43498	42488	1.50	-0.202	13.5
	1% SIIN	42952	42444	1.49	-0.0164	13.1
	1% EIIN	43498	42505	1.50	-0.171	8.63
	0.1% SIIN	44161	42683	1.50	-0.155	6.88
	0.1% EIIN	43438	42502	1.50	-0.089	8.44

Figure 11B: Directly vaccinated OT1 have reduced ASF compared with naïve OT1 and AT cells. 1 week post-vaccination, purified CD8+ splenocytes were diluted or run undiluted, and when possible at 100%, 6%, 1%, and 0.1% in order to compare ASF among three different hosts: naïve OT1, Vax+AT WT, and Vax OT1. Functionally, splenic ASC had lower activation ability in the Vax OT1 group at all 4 dilutions tested, compared with both naïve OT1 and Vax+AT mice. Comparing Vax+ AT WT to naïve OT1, Vax+AT may have lower ASF, but the differences were not obvious.

www.manaraa.com

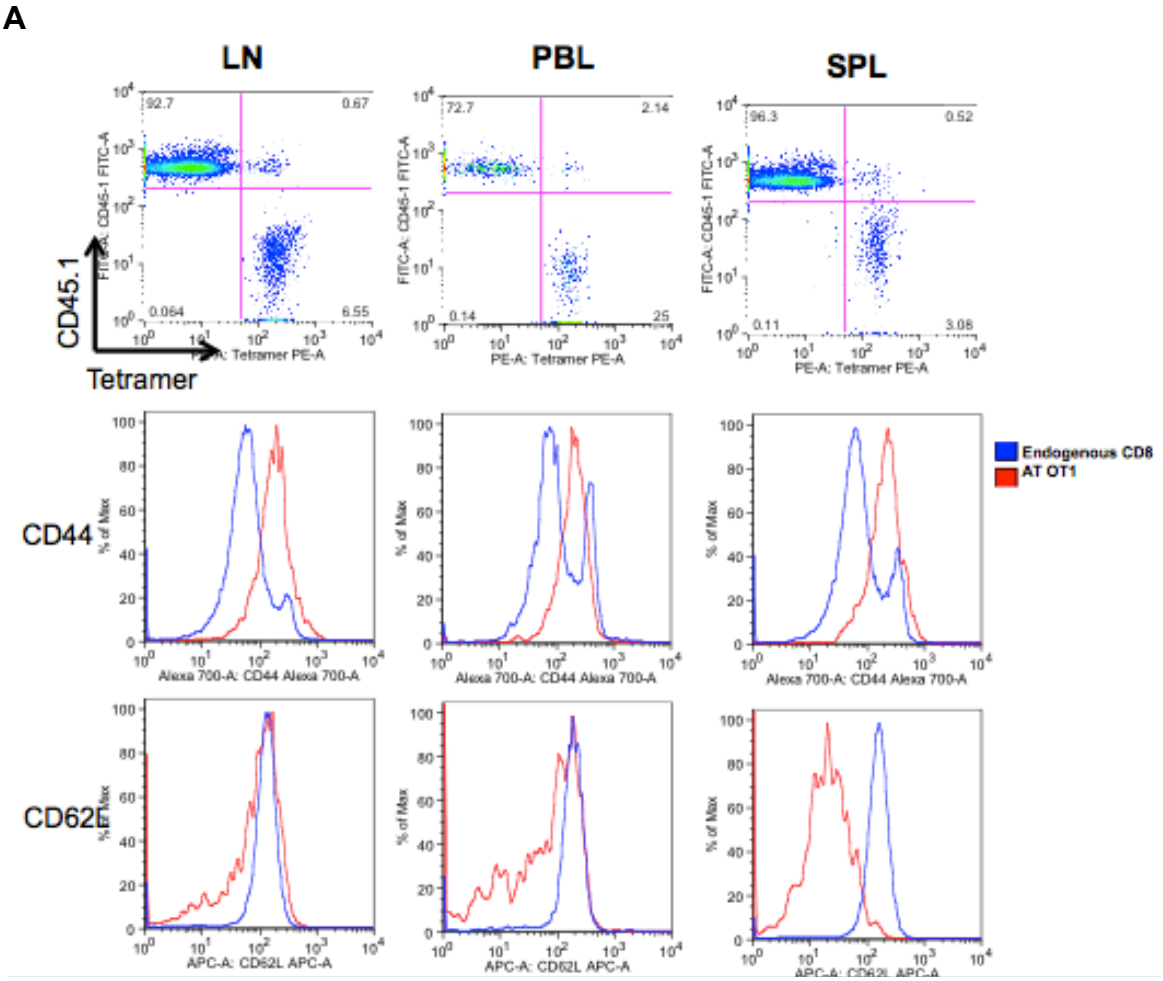

Figure 12A: Compared with lymph node and spleen CD8+ cells, peripheral blood cells were the most expanded.
In this experiment, 3 WT B6 mice were vaccinated with LPS/OVA (Vax) and adoptively transferred 5e6 OT1 cells (Vax+AT WT). One week later after vaccination, lymph nodes (LN), peripheral blood (PBL) and spleens (SPL) were harvested and found to be expanded to 7, 25, and 3%, respectively. **Bottom panels:** CD44 and CD62L expression were used to evaluate activation status comparing endogenous . CD44 expression was high in the AT cells in all 3 compartments, but CD62L was shed most effectively in the AT splenocytes.

www.manaraa.com

B

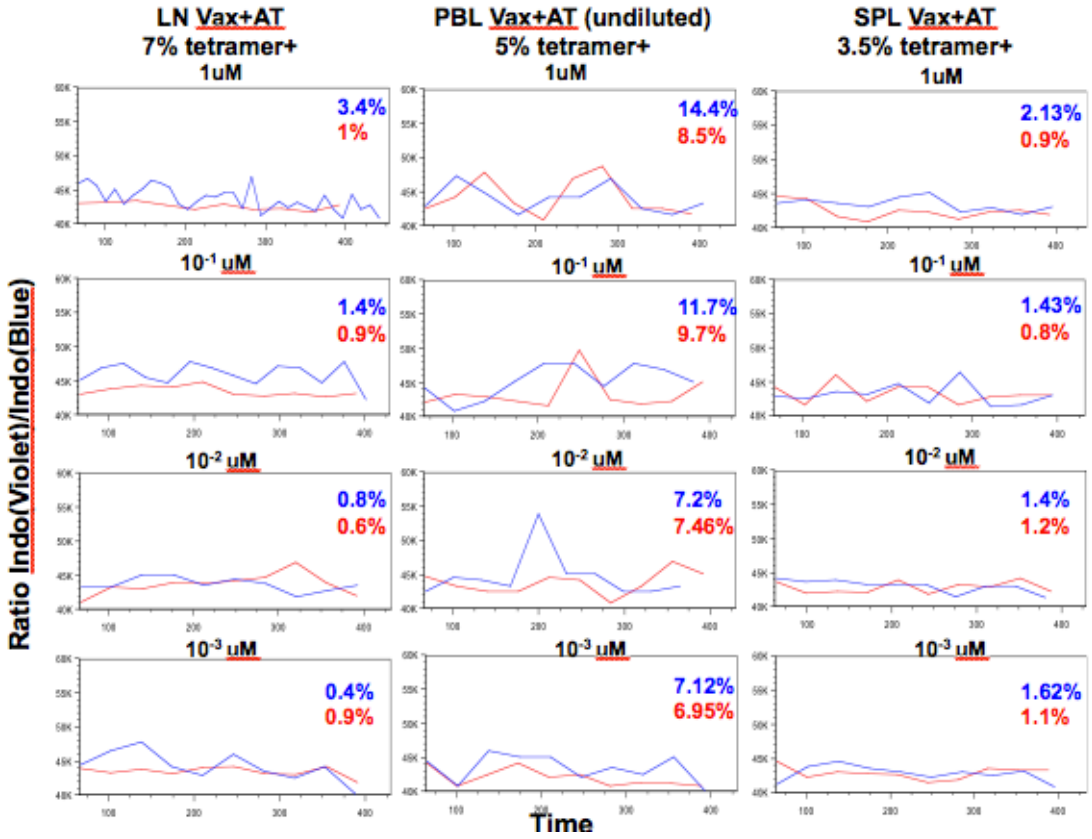

		Peak	Mean	AUC (x10^{7}s)	Slope	OF (s^{-1})
LN	1uM SIIN	46919	4.37E+04	1.59	-9.37	1.89
	1uM EIIN	43358	42553	1.45	-5.06	0.601
	0.1uM SIIN	47876	46289	1.63	-1.32	0.821
	0.1uM EIIN	44803	43487	1.53	-3.77	0.538
	10e-2uM SIIN	45062	43648	1.52	-4.72	0.407
	10e-2uM EIIN	46919	43841	1.53	-12.5	0.279
	10e-3 uM SIIN	47876	44675	1.57	-9.52	0.191
	10e-3uM EIIN	44161	43612	1.54	-0.0192	0.504
PBL	1uM SIIN	47395	43959	1.56	-5.95	0.293
	1uM EIIN	48853	44340	1.5	-0.172	0.186
	0.1uM SIIN	47876	45245	1.54	-18.9	0.249
	0.1uM EIIN	49849	43110	1.52	-1.18	0.243
	10e-2uM SIIN	54044	44829	1.43	-1.56	0.178
	10e-2uM EIIN	46919	43619	1.52	-3.35	0.198
	10e-3 uM SIIN	45981	43798	1.53	-0.138	0.2
	10e-3uM EIIN	44161	42116	1.46	-7.38	0.2
SPL	1uM SIIN	45062	43368	1.51	-5.43	0.496
	1uM EIIN	44609	42367	1.45	-6.82	0.28
	0.1uM SIIN	46448	43079	1.51	-1.96	0.423
	0.1uM EIIN	45981	43252	1.51	-3.78	0.231
	10e-2uM SIIN	44161	43204	1.47	-5.74	0.368
	10e-2uM EIIN	44161	42859	1.49	-3.34	0.32
	10e-3 uM SIIN	44609	42965	1.51	-0.339	0.469
	10e-3uM EIIN	44519	42775	1.47	-2.3	0.297

Figure 12B: ASF could only be detected in the lymph node AT cells and down to 10^{-2}uM.
1 week post-vaccination, purified CD8+ SPL and LN were stimulated with DC loaded at different peptide concentrations. PBL were run undiluted to maintain high enough numbers for a comparison. ASF was detected in the LN AT cells at 1uM and 10^{-1}uM. Neither ASC nor ASF could be detected in PBL and SPL.

www.manaraa.com

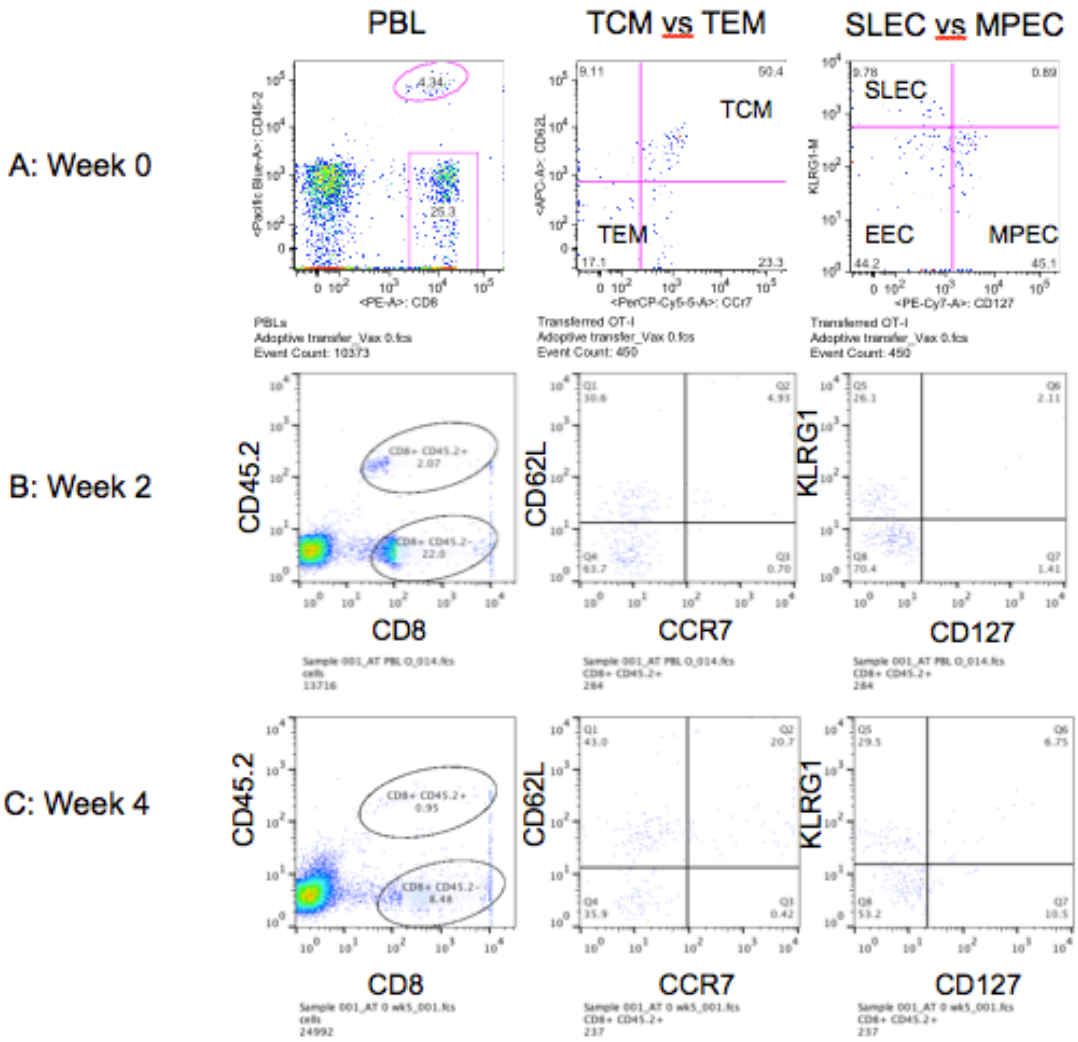

Figure 13A, B, C, D:
A: In this experiment, 2 WT B6 mice were vaccinated with LPS/OVA (Vax) and adoptively transferred 5e6 OT1 cells (Vax+AT WT) on week -1. One week later after vaccination (week 0), mice were boosted with LPS/OVA at the same schedule. Eye bleeds on week 0 revealed significant expansion of the AT cells to 3-4% (representative plots shown). Phenotypic analysis of CCR7, CD62L, CD127, and KLRG1 revealed no distinct population, consistent with the phenotype of primary expanding T cells, as these are markers that define memory populations. **B:** On week 2, eye bleeds revealed significant contraction of the AT cells to 2.5%. Phenotypic analysis of CCR7, CD62L, CD127, and KLRG1 markers revealed an expression profile consistent with T_{CM}, EEC, and SLEC (representative plot). **C:** On week 4, eye bleeds revealed persistent contraction of the AT cells to 1%. Phenotypic analysis showed T_{CM}, EEC, and SLEC were relatively unchanged from week 2.
T_{CM}: central memory T cells; T_{EM}: effector memory cells; SLEC: short-lived effector cells; MPEC: memory progenitor cells; EEC: early effector cells.

www.manaraa.com

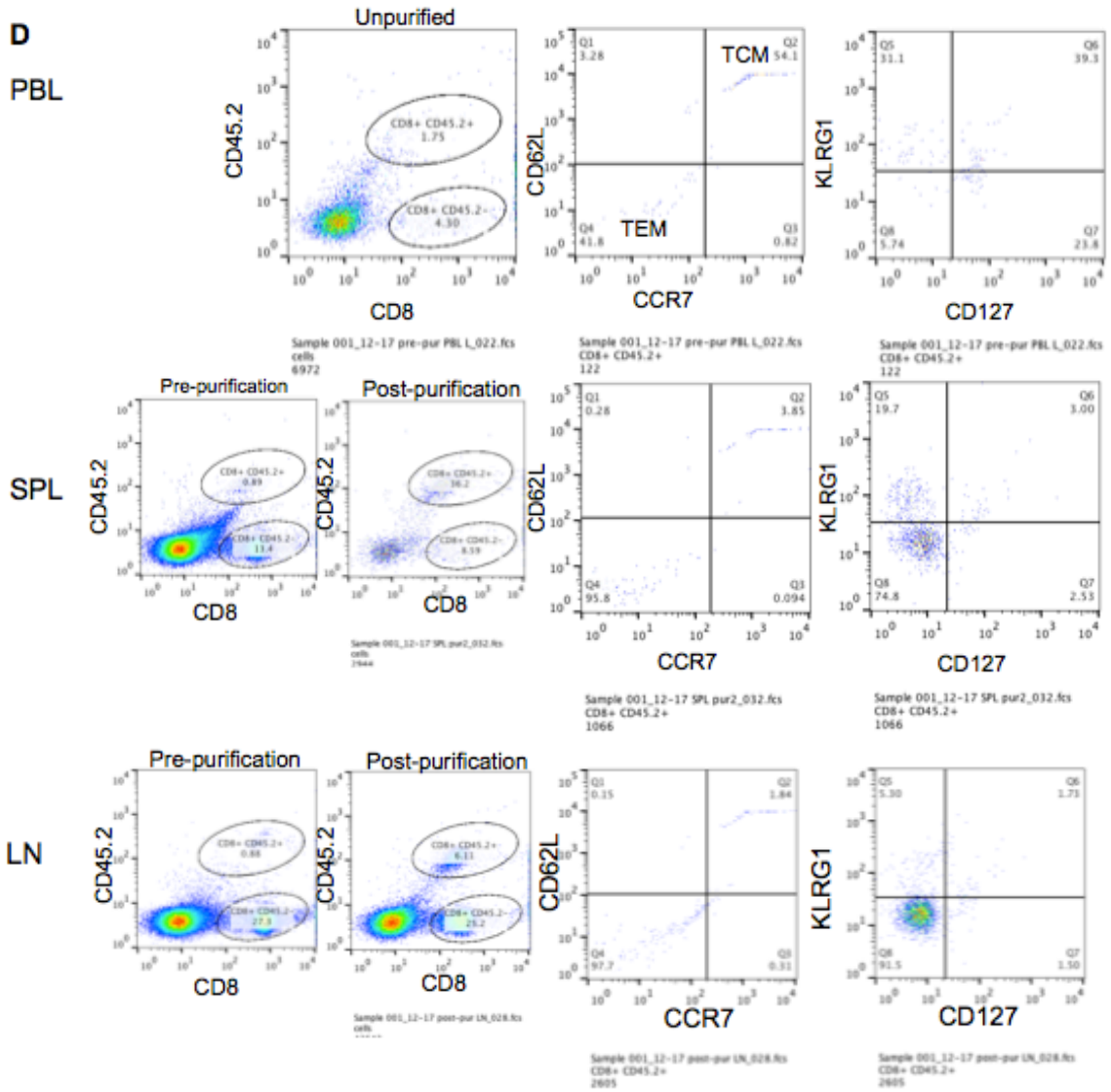

Figure 13D: At week 7, the three compartments displayed markedly different phenotypes.
7 weeks from the boost, the experiment was terminated. PBL, SPL, and LN were harvested, and stained for evaluation of the AT population. AT cells represented 1.75, 0.9, and 0.9% of PBL, SPL and LN cells respectively. Because of low-absolute numbers, PBL were used unpurified in functional experiments. AT SPL and LN cells were encriched to 36 and 6% of the total population. Phenotypic analysis of CCR7, CD62L, CD127, and KLRG1 revealed, in the PBL, cells were both T_{CM} and T_{EM} and had differentiated into both MPEC ad SLEC. By contrast, SPL and LN cells displayed increased preference towards T_{EM} and produced almost exclusively EEC. SPL produced some SLEC but at a lower rate than in PBL.

www.manaraa.com

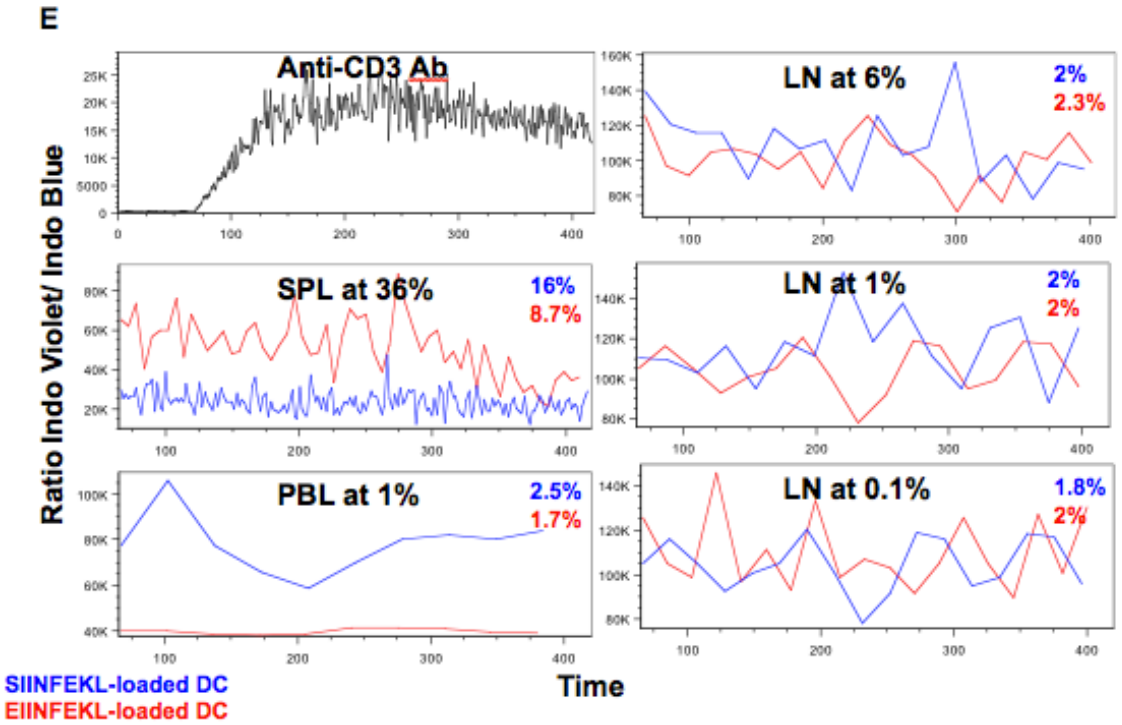

Figure 13E: Only PBL AT cells demonstrated ASF, but SPL were able to form ASC.
Enriched AT cells from the SPL and LN and unpurified PBL were evaluated by calcium flux. Anti-CD3 antibody was used as a positive control to stimulate WT SPL. Surprisingly, while 36% enriched AT from SPL demonstrated ASC formation (16% ASC compared with 8.7% NSC), calcium flux was *higher* in the non-specific group! By contrast, 1% AT from PBL demonstrated ASF. No such flux could be obtained from the LN at any of the three dilutions tested (6%, 1%, 0.1%). Of note, the overall curves in LN cells are *higher* than in PBL and SPL.

www.manaraa.com